The Tahorakuri Formation: Investigating the early evolution of the Taupo Volcanic Zone in buried volcanic rocks at Ngatamariki and Rotokawa geothermal fields

A thesis submitted in partial fulfilment of the requirements for the degree of

Master of Science in Geology

at the

Department of Geological Sciences

University of Canterbury

By

Alan A. Eastwood

UNIVERSITY OF CANTERBURY
Te Whare Wānanga o Waitaha
CHRISTCHURCH NEW ZEALAND

2013

Frontispiece

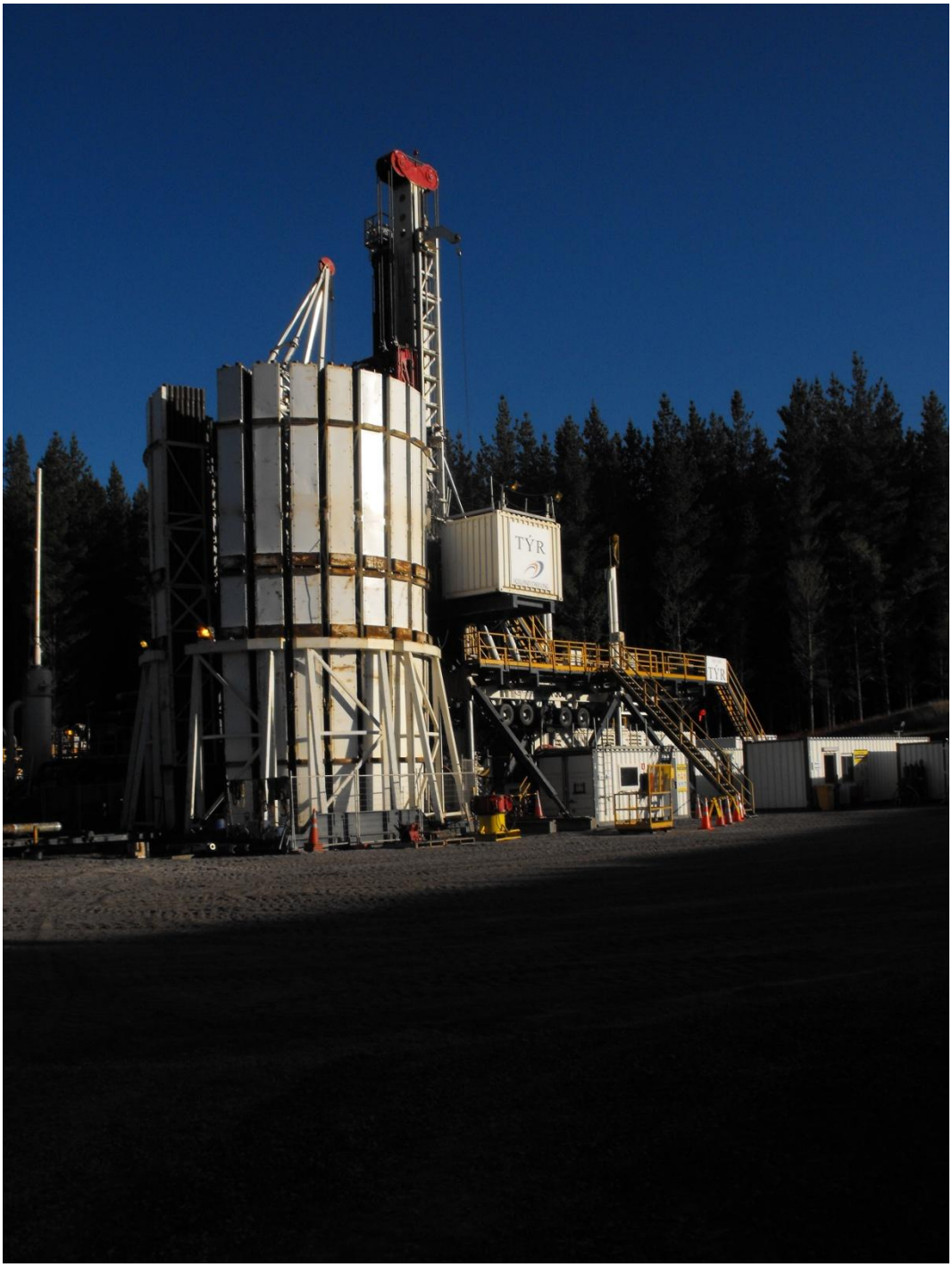

The drilling rig at Ngatamariki – where this all starts...

Abstract

The Tahorakuri Formation was introduced as a stratigraphic term to simplify the sometimes complex and inconsistent naming conventions in subsurface deposits within the geothermal fields of the central Taupo Volcanic Zone (TVZ). It consists of all volcaniclastic and sedimentary deposits between the ~350 ka Whakamaru-group ignimbrites and the greywacke basement that cannot be correlated with known ignimbrites. As such, it represents a long period in which relatively little is known about the volcano-tectonic history of the TVZ. The thesis focuses on the Tahorakuri Formation at Ngatamariki and Rotokawa geothermal fields and the implications for the volcano-tectonic evolution of the TVZ. Drill cuttings from wells NM5 and NM6 are re-examined, and new U-Pb zircon dates from the Tahorakuri Formation are presented and implications discussed.

Potassium feldspars identified in the drill cuttings from NM5 were examined by Raman spectroscopy and electron microprobe (EMP) analysis. Although petrographically many of the feldspars appear similar to sanidine, a primary volcanic mineral phase, this showed them to be adularia which formed during hydrothermal alteration. Raman spectroscopy was found to be ideal for analysing a large number of grains quickly, with the spectral peak at ~140 cm^{-1} being particularly useful for identifying adularia as it is absent in sanidine. EMP analysis was found to be somewhat slower, but definitively identified the feldspars as adularia, with typical potassium-rich compositions of Or_{94}-Or_{99}.

U-Pb dating shows that the Tahorakuri Formation formed over a very long time, with pyroclastic deposits ranging from 1.89 – 0.70 Ma. This was followed by a period with little or no explosive volcanism until ~0.35 Ma during which sediments were deposited at Ngatamariki. The periods at ~1.9 Ma and ~0.9 Ma were particularly active phases of pyroclastic deposition, with the second phase likely correlating with the Akatarewa ignimbrite. The oldest deposits overlie a large andesitic composite cone volcano. Significant subsidence of the andesite must have preceded emplacement of the silicic deposits, indicating that rifting within the central TVZ may have started earlier than previously thought. While the origin of the deposits is uncertain, the distribution of the oldest deposits outcropping at the surface, as well as the likely early initiation of rifting, would suggest a source within the TVZ is likely.

Acknowledgements

First and foremost I would like to thank my supervisors for all of their support and guidance. To Dr. Darren Gravley, how you manage to get anything done with everything on your plate is beyond me, but you've always been there to help when I really needed it, and for that I am very grateful. Thanks for your expertise and great ideas which have made this such an interesting topic, and for your encouragement which kept me going. To Prof. Jim Cole, your enthusiasm is legendary. You made my decision to return to university an easy one, and also helped make it an enjoyable experience (for the most part anyway!). Thanks for fostering my interest in geology and for making time to help me out no matter what. To Dr. Christopher Oze, what an inspired choice to have you on the team! Your fantastic ideas have contributed so much to making this thesis what it is, but what I am most grateful for is your support and encouragement when I needed it most. To Tom Powell, thanks for developing my interest in this particular topic when it was first conceived, and for your great advice along the way. To Dr. Isabelle Chambefort; a late addition to the team, but thanks for your help and advice – and for giving a different perspective. Thanks also to my other co-authors for your expertise and reviews: Sara Fraser, Prof. Keith Gordon, Prof. Colin Wilson and Prof. Trevor Ireland.

I am grateful for all of the sources of funding, including the Ministry of Business, Innovation, and Employment's TechNZ scholarship which was sponsored by Mighty River Power Ltd., as well as the Master's Scholarship from the University of Canterbury, Source to Surface programme, and the Mason Trust Fund.

To all of the staff and students in the geology department at the University of Canterbury, thanks for making it such a great environment – in particular the Source to Surfacers and my office mates. Thanks to the technical staff, in particular, Rob Spiers, Chris Grimshaw, Sacha Baldwin-Cunningham and Kerry Swanson for sample preparation and technical assistance. And of course to Pat Roberts and Janet Warburton for keeping things running smoothly! I am also extremely grateful to David Shelley for his help in trying to decipher the nightmare that was the fine-grained drill cuttings. Thanks also to Bryce Williamson from the Chemistry department for advice on Raman spectroscopy.

A big thanks to Mighty River Power Ltd. for providing access to core sheds and relevant samples and reports, and to the staff for all of their help and advice, in particular Catherine Coutts and Jeremy O'Brien. Thanks to Dr. Michael Palin, Matt Sager, and Andreas Auer from

the Department of Geology at Otago for their help with zircon separations and the use of the electron microprobe respectively. Thanks also to Simon Barker from Victoria University of Wellington for help with zircon separations. Thanks to Dr. Rose Turnbull for her excellent advice regarding all things zircon related, and to the staff at GNS Wairakei and Dunedin for discussions, advice and the use of their equipment. I am also very grateful to Assoc. Prof. Pat Browne for his excellent and timely advice and to Dr. Neville Hudson and the School of Environment at Auckland for providing access to core samples.

To my friends, thanks for all the good times. About time for a drink I reckon?

Most importantly, to my family, thanks for making me who I am. Abi and Mike, thanks for the good memories and for being awesome people that any younger brother would be proud of. To my little bro Greg – gone but never forgotten. To my parents, your unconditional love and support means so much to me. Finally, to my fiancée Janine, I couldn't have done this without you, thanks so much for putting up with me. I love you all.

Table of Contents

List of Tables

List of Figures

Prologue

The Tahorakuri Formation is one of the major units encountered within the geothermal wells of the central Taupo Volcanic Zone (TVZ). At Ngatamariki Geothermal Field it reaches thicknesses of >1 km, although at nearby Rotokawa Geothermal Field it is significantly thinner. It primarily consists of fine-grained, silicic volcaniclastic deposits, but at Ngatamariki it also consists of lacustrine sediments. As it was emplaced prior to ~350 ka, it represents a time in which relatively little is known about the volcano-tectonic evolution of the TVZ. Rocks of this age rarely outcrop at the surface within the TVZ, so the rock cores and cuttings recovered during drilling within the geothermal fields are of significant value in helping unravel the evolution of the TVZ. In addition to this, the Tahorakuri Formation is also important as a geothermal reservoir rock at Ngatamariki. Successful geothermal production and management requires a detailed understanding of the subsurface stratigraphy and tectonic structures. The aim of this thesis is to further investigate the Tahorakuri Formation in order to help constrain the deep stratigraphy in this part of the TVZ, and to examine how this may help unravel the early evolution of the TVZ. Although the main focus of this thesis is on the Tahorakuri Formation at Ngatamariki, the differences in the deep stratigraphy between the two fields provide a unique opportunity to examine the early history of the TVZ.

Specific objectives outlined at the beginning of this study were:

- Determine if the Tahorakuri Formation consists of multiple smaller units emplaced over a period of time, or if it represents one large intracaldera fill deposit.
- Determine if the Tahorakuri Formation is a primary deposit or if there is any evidence of reworking of the pyroclastic eruptives.
- Examine what differences, if any, exist between the silicic deposits found at Ngatamariki and Rotokawa.
- If possible, place constraints on the source and timing of the silicic volcanism that is represented by the Tahorakuri Formation.

In order to achieve these objectives, a detailed re-examination of the Tahorakuri Formation drill cuttings from NM5 and NM6 was first conducted. This involved examination of the cuttings under both an optical and a petrographic microscope. In addition, core samples from other wells at Ngatamariki and Rotokawa were also examined. A number of issues became apparent during this stage of the study. One issue related to the presence of potassium

feldspars in the drill cuttings, which may have been one of either two polymorphs; adularia relating to hydrothermal alteration, or primary volcanic sanidine. However, this could not be confidently determined by optical observations alone, and one or both of these polymorphs may have been present. This became the basis for Chapter 1 of this thesis, in which this question is resolved.

The main issues were related to the nature of the cuttings themselves. They are generally extremely fine-grained, such that the lithology could often not be determined confidently. In addition, hydrothermal alteration is typically intense, resulting in the destruction of both primary minerals and textures. Any conclusions are therefore limited, as the correlation of units is uncertain. It quickly became apparent that U-Pb dating of zircons provided the best method for overcoming this. This was viewed as the best way of achieving the objectives, and became the basis for Chapter 2.

This thesis consists of two chapters, written as manuscripts that have or will be submitted for publication, along with appendices containing supporting data. It is arranged as follows:

- **Chapter 1:** involves distinguishing between adularia and sanidine in fine-grained drill cuttings using a combined approach of both Raman spectroscopy and electron microprobe analysis. This manuscript has already been submitted to *Geothermics.*
- **Chapter 2:** utilises Secondary Ion Mass Spectrometry (SIMS) U-Pb dating to constrain the timing of deposition of the Tahorakuri Formation, and discusses implications for the volcano-tectonic evolution of the TVZ. This will be submitted to *Journal of Geophysical Research* in the near future pending minor changes.
- **Conclusions:** summarises the findings presented in this thesis.
- **Appendix 1:** contains all hand sample and thin section descriptions for samples looked at in this study.
- **Appendix 2**: contains a summary of the stratigraphy in wells NM5 and NM6 as revealed by a detailed examination of the drill cuttings.
- **Appendix 3:** presents the full electron microprobe data.
- **Appendix 4:** presents the full SIMS data.
- **Appendix 5:** lists all samples examined during this study.

Chapter 1

Distinguishing between adularia and sanidine in hydrothermally altered volcanic rocks using Raman spectroscopy: An example from Ngatamariki Geothermal Field, New Zealand

Alan Eastwood[a]*, Christopher Oze[a], Sara Fraser[b], Jim Cole[a], Darren Gravley[a], Isabelle Chambefort[c], and Keith Gordon[b]

[a]Department of Geological Sciences, University of Canterbury, Private Bag 4800, Christchurch 8140, New Zealand

[b]Department of Chemistry and MacDiarmid Institute for Advanced Materials and Nanotechnology, University of Otago, PO Box 56, Dunedin 9054, New Zealand

[c]GNS Science, Wairakei Research Centre, Taupo 3384, New Zealand

*Email: alan.eastwood@pg.canterbury.ac.nz

Contributions:

Alan Eastwood conducted the literature review, undertook the petrographic analysis, assisted with taking Raman spectroscopy measurements, undertook and interpreted the electron microprobe analysis, and wrote the manuscript. Dr. Oze conceived the study and reviewed the manuscript. Sara Fraser undertook and interpreted the Raman spectroscopic analysis. Prof. Cole, Dr. Gravley, and Dr. Chambefort reviewed the manuscript and provided help and advice, particularly in regards to the petrographic interpretations. Prof. Gordon provided the equipment for the Raman analysis, and assisted in the interpretation of the data.

1.1 Abstract

Low temperature adularia and high temperature sanidine are polymorphs of potassium feldspar commonly found in volcanic rocks such as those of the Taupo Volcanic Zone (TVZ), New Zealand. Being able to differentiate between these polymorphs is important as they are commonly used to distinguish different geological units or to evaluate the processes of hydrothermal alteration. For example, sanidine is present in certain members of the ~350 ka Whakamaru-group ignimbrites; however, it is extremely rare in older units. Hydrothermal alteration of volcanic units in the TVZ commonly results in adularia formation, which can be difficult to petrographically distinguish from sanidine, particularly in fine-grained drill cuttings. Here Raman spectroscopy and electron microprobe (EMP) analysis are utilised to definitively identify the potassium feldspars, helping differentiate the geological units and the alteration history of the Ngatamariki Geothermal Field, New Zealand. Raman spectroscopy was found to be useful for analysing a large number of grains quickly, and no sample preparation was necessary. The Raman spectral peak at ~140 cm^{-1}, which is absent in sanidine, was useful for identifying adularia, but peaks at 172-176 cm^{-1} and 513-514 cm^{-1} may also be used for identification purposes. EMP analysis was found to be slower and required more sample preparation compared to Raman spectroscopy. All the potassium feldspars from Ngatamariki analysed via Raman spectroscopy and EMP were found to be adularia, with typical compositions of Or_{94}-Or_{99}. By combining Raman and chemical analysis, we provide a robust method for the differentiation of adularia and sanidine in hydrothermally altered silicic volcanic rocks that can be utilised within geothermal fields worldwide.

1.2 Introduction

Understanding the nature of a geothermal reservoir is an important aspect in the successful development and management of a geothermal resource. It is therefore beneficial to accurately map and characterise the different geological units that make up the geothermal reservoir. Rock cores recovered during drilling can provide detailed information about the subsurface stratigraphy, but the added expense of obtaining core samples mean they are rarely drilled. Much of the knowledge of the subsurface stratigraphy therefore comes from rock cuttings recovered during drilling. However, recognition and correlation of units can be difficult when dealing with fine-grained cuttings, particularly when trying to distinguish

between units with similar lithologies. Within the Taupo Volcanic Zone (TVZ) of New Zealand for example, it can be difficult to distinguish between different siliciclastic units which make up much of the upper 3 km of the crust (*Bibby et al.,* 1995; *Harrison and White,* 2006). An additional complication in the TVZ is the presence of large regional-scale depressions (calderas and graben structures) that cause over-thickening of siliciclastic deposits of both primary and secondary origin (e.g. *Wilson et al.,* 2008).

In some cases, the mineralogy can be useful in identifying different units. For example, sanidine is a high temperature polymorph of potassium feldspar often found in highly evolved volcanic rocks, but due to its rare occurrence in the TVZ it can be used to help determine major geological units. While it is present in certain members of the ~350 ka Whakamaru-group ignimbrites (*Martin,* 1961; *Brown et al.,* 1998; *Leonard et al.,* 2010), it appears to be absent, or at least extremely rare, in older ignimbrites (>350 ka). *Blank* (1965) reports trace amounts of sanidine in the 1.00 Ma Rocky Hill ignimbrite (*Houghton et al.,* 1995), and the Waipari ignimbrite, considered by *Wilson* (1986) to be part of the 1.21 Ma Ongatiti ignimbrite (*Houghton et al.,* 1995). However, studies prior and subsequent to this have not reported sanidine in any pre-Whakamaru ignimbrites (*Martin,* 1961; *Murphy and Seward,* 1981; *Ritchie,* 1996; *Hildyard et al.,* 2000; *Schipper,* 2004). Therefore, sanidine is a diagnostic mineral in the TVZ, and would not be expected to be present in significant quantities in the rocks below the Whakamaru-group ignimbrites.

Hydrothermal alteration within geothermal fields further complicates the identification and correlation of units, with the destruction of primary minerals and formation of secondary minerals. Adularia is a low temperature polymorph of potassium feldspar, with a distinctive morphology and genesis. The structure and optical properties can vary between samples, and even in a single crystal, with very fine scale twinning being typical (*Deer et al.,* 1992). Adularia commonly forms in active geothermal systems, with three modes of formation: 1) replacement of primary feldspars, 2) as minute, diamond-shaped crystals in the groundmass, 3) as euhedral crystals lining fractures and cavities (*Browne and Ellis,* 1970; *Steiner,* 1970). It is found in many of the geothermal fields in the TVZ, including at Ngatamariki Geothermal Field. In many cases distinguishing between adularia and sanidine optically is possible due to the distinctive twinning in adularia. However, this fine twinning is not always apparent and the two minerals can be difficult to distinguish in hydrothermally altered volcanic rocks,

particularly within fine-grained drill cuttings. It is therefore possible that in some cases sanidine may have been misidentified as adularia.

Petrographic analysis of drill cuttings from the >350 ka Tahorakuri Formation at Ngatamariki, shows that some intervals contain common potassium feldspars. The fine-grained nature of the cuttings makes identification of the feldspars difficult, and only rarely can adularia be identified where it replaces primary phenocrysts or by its distinctive fine, uneven twinning. Optically, many appear similar to sanidine, suggesting that both adularia and sanidine may be present. As they form under different conditions it is important to be able to distinguish between them as it will contribute significantly to the overall interpretation of the rocks.

This study aims to distinguish between adularia and sanidine using Raman spectroscopy. This method utilises the differences in their crystal structures in order to distinguish between them. Samples of adularia and sanidine from elsewhere in the TVZ are analysed so they can be used as standard reference spectra. Differences between the adularia and sanidine standards are then used to identify the unknown potassium feldspars from Ngatamariki. In order to confirm the identification of adularia or sanidine, a smaller sample set of the crystals are analysed by electron microprobe (EMP).

1.3 Geological setting

The Ngatamariki Geothermal Field, located ~17 km NE of Taupo (Figure 1.1), lies just outside the Whakamaru Caldera as proposed by *Wilson et al.* (1986), and is currently being developed for geothermal production. Two volcanic formations ubiquitous in geothermal drillholes across most of the central part of the TVZ are the Whakamaru-group ignimbrites and the Tahorakuri Formation (Figure 1.2). The Whakamaru-group ignimbrites are a series of widespread ignimbrites erupted at ~350 ka, marking the most active period in the history of the TVZ (*Wilson et al.,* 1986; *Houghton et al.,* 1995; *Leonard et al.,* 2010). Of broadly similar petrographic characteristics, the Whakamaru-group ignimbrites outcrop over a large area in the central North Island, although they are buried beneath younger deposits within much of the active TVZ (*Brown et al.,* 1998). Within the geothermal drillholes of the southern part of the central TVZ, the units correlated with the Whakamaru-group ignimbrites

have been termed the Wairakei ignimbrites (*Grindley*, 1965a). However, it is uncertain where in the Whakamaru sequence the Wairakei ignimbrites fit. The Tahorakuri Formation is defined as all un-named volcaniclastic and sedimentary deposits below the Whakamaru-group ignimbrites within the geothermal drillholes of the TVZ (*Gravley et al.*, 2006).

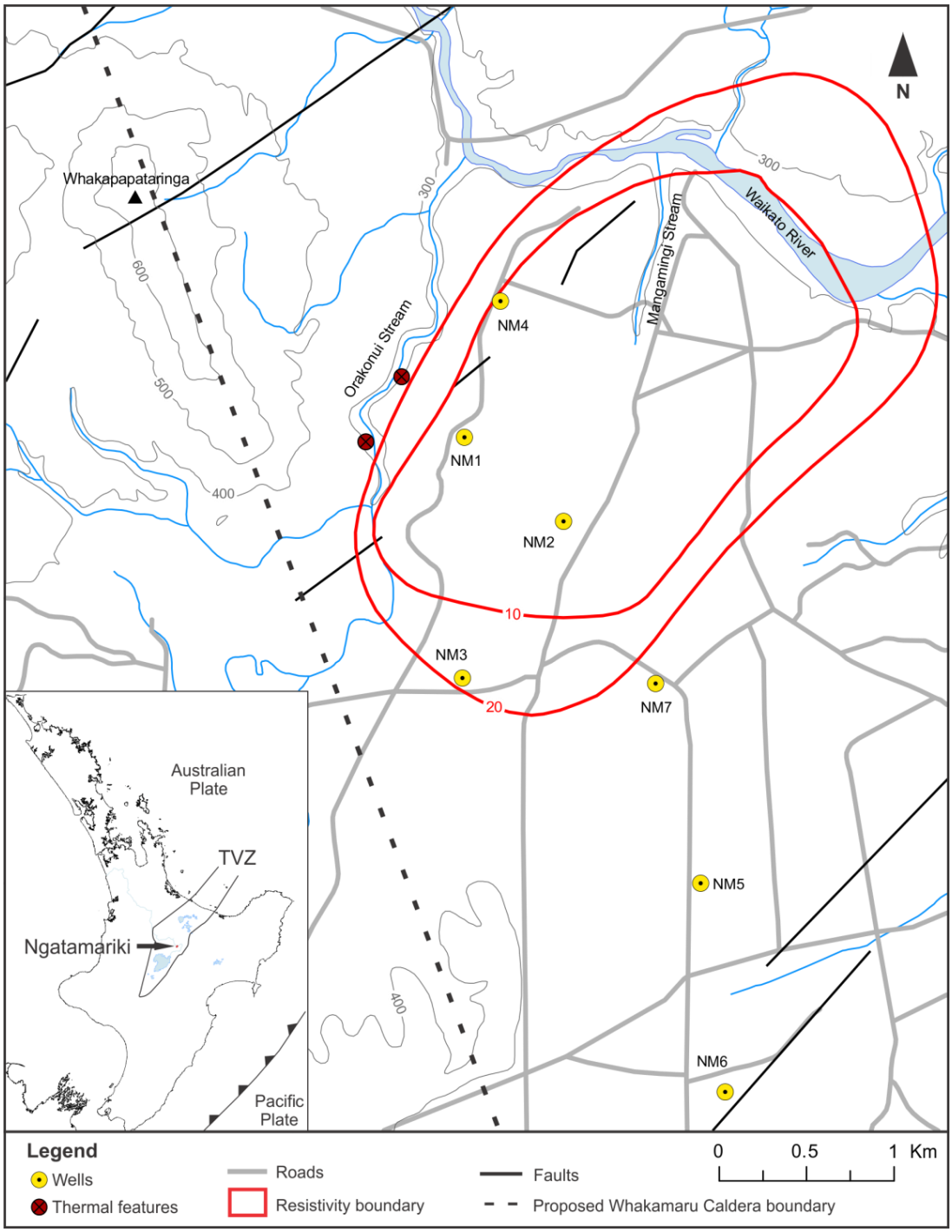

Figure 1.1: Map showing Ngatamariki Geothermal Field, with wells NM5 and NM6 in the south of the field. The approximate near surface (~500 m) extent of the hydrothermal system is marked by the 10 and 20 ohm resistivity contours (from *Stagpoole et al.*, 1985). Mapped faults are from *Leonard et al.* (2010), and the Whakamaru Caldera boundary is that proposed by *Wilson et al.* (1986).

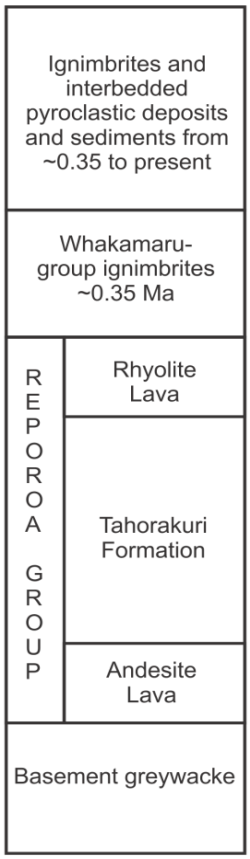

Figure 1.2: Simplified stratigraphic column showing the subsurface stratigraphy encountered in wells NM5 and NM6 at Ngatamariki. The stratigraphy reported by *Ramirez and Rae* (2009) and *Rae et al.* (2009a) is simplified following the naming conventions of *Gravley et al.* (2006), in which the Tahorakuri Formation and any locally named ignimbrites or interbedded lava bodies form the Reporoa Group. Age data has been modified after *Leonard et al.* (2010).

NM5 and NM6 are located in the southern part of Ngatamariki, with the Tahorakuri Formation reaching thicknesses of over 1 km in these wells. A detailed re-examination of the Tahorakuri Formation cuttings from these wells reveals that potassium feldspars are common at some depth intervals, particularly in NM5 (Appendix 1). The cuttings are very fine-grained and extensively altered, with quartz and feldspar the only remaining primary mineral phases. While plagioclase remains unaltered in places, it can also be seen altering to albite and rarely adularia. The secondary assemblage is characterised by quartz, illite, calcite, and chlorite. Adularia has previously been reported within the Tahorakuri Formation (*Wood*, 1985a, 1985b, 1986a; *Ramirez and Rae*, 2009; *Rae et al.*, 2009a; *Chambefort and Bignall*, 2011), and while it is clear that adularia accounts for some of the observed potassium feldspars in these wells, some of the grains appear more similar to sanidine than adularia.

As sanidine is rare in the TVZ, it was considered important to be able to confidently identify the potassium feldspars in these wells. If the feldspars are all adularia, it does not provide much information about the original rock, but it does provide information on the nature of the geothermal system. Sanidine would be more unexpected within the Tahorakuri Formation as it has not previously been reported in anything other than trace abundances in

rocks of this age. A positive identification of sanidine would therefore suggest this part of the Tahorakuri Formation might either be related to the Whakamaru-group ignimbrites, or has a primary mineralogy distinct from units of the same age that outcrop at the surface.

1.4 Methods

1.4.1 Raman spectroscopy

Potassium feldspars identified in polished thin sections were analysed using Raman spectroscopy at the University of Otago. A total of 70 grains from 14 samples were analysed from NM5, corresponding to depths in metres below the drilling rig floor (mRF) of 1125, 1175, 1225, 1300, 1350, 1400, 1450, 1500, 1550, 1600, 1650, 1700, 1750, and 1800. The number of grains measured per sample ranged from 3 to 7, with more grains measured in the interval from 1400-1700 m where the concentration of potassium feldspar was greatest. In order to compare with the unknown samples, sanidine and adularia natural standards were also analysed. An uncovered thin section of sample SB-2028 (*Brown*, 1994) from the Whakamaru-group ignimbrites was used as a standard for sanidine, while a thin section of FB11-OD8, a sample of the hydrothermally altered Ohakuri ignimbrite from near Ohakuri Dam was used as a standard for adularia.

Measurements were made using a Senterra Infinity 1 Raman microscope by Bruker Optics. Incident light at 532 nm was used at 50 mW power, with each spectrum a composite of 20 three second acquisitions. A 20x objective with 50 µm aperture was used, with the spectral region from 50-1500 cm^{-1} measured at the high resolution setting of 3-5 cm^{-1} as this region contained the major differences between sanidine and adularia.

Standards for adularia and sanidine were measured at least six times in different parts of each of the four crystals measured. Unknown samples were measured between one and six times, but usually two or three times per crystal. Some crystals also contained a signal from the epoxy resin used to mount the cuttings. A small number of the unknown grains measured were not adularia or sanidine, so grains of quartz and calcite, two of the major components of the cuttings, were also measured for comparison. This was mainly due to the difficulty in identifying the very fine, rounded grains when taking measurements. While care was taken to

measure the cleanest parts of the crystal, the inhomogeneous nature of some of the altered grains increased the chance of minerals other than potassium feldspar being included in the measurements. Unknown samples were identified using principle component analysis (PCA) and spectral peak positions. Peak positions were identified for the average spectrum of each crystal using the peak picking feature of GRAMS/AI 8.0 software.

1.4.2 Electron microprobe analysis

Elemental compositions were measured using the JEOL JXA-8600 Superprobe with wavelength dispersive detection system at the University of Otago. Analyses were performed using a 15 kV accelerating voltage and a 20 nA beam current, with a spot size of 20 µm. The instrument was calibrated using the Smithsonian standards for labradorite and microcline, and natural adularia from St Gotthard, Switzerland. Samples were first imaged using back-scattered electrons (BSE), and were analysed for SiO_2, Al_2O_3, FeO, MgO, CaO, Na_2O, K_2O, and BaO. The four adularia crystals from FB11-OD8 and the four sanidine crystals from SB-2028 were analysed, along with the samples from NM5 at 1125, 1300, 1450, 1500, 1600, and 1700 mRF depths. These samples were chosen to give a representative sample of depth intervals.

1.5 Results and discussion

1.5.1 Raman spectroscopy

Raman spectra with the major peak positions for epoxy, adularia, sanidine, and quartz are shown in Figure 1.3. As the spectral region below 620 cm^{-1} contained the major differences between adularia and sanidine but little or no epoxy signal, this region is the main focus of this study. Figure 1.4 shows the averaged Raman spectra for the adularia and sanidine standards over the spectral region 100-620 cm^{-1}. The spectra are similar, with generally only small differences in peak positions. The most obvious difference is the peak at ~138 cm^{-1} for the adularia standards, which is absent in the sanidine standards. The peak at ~457 cm^{-1} is also much more distinct in adularia than sanidine.

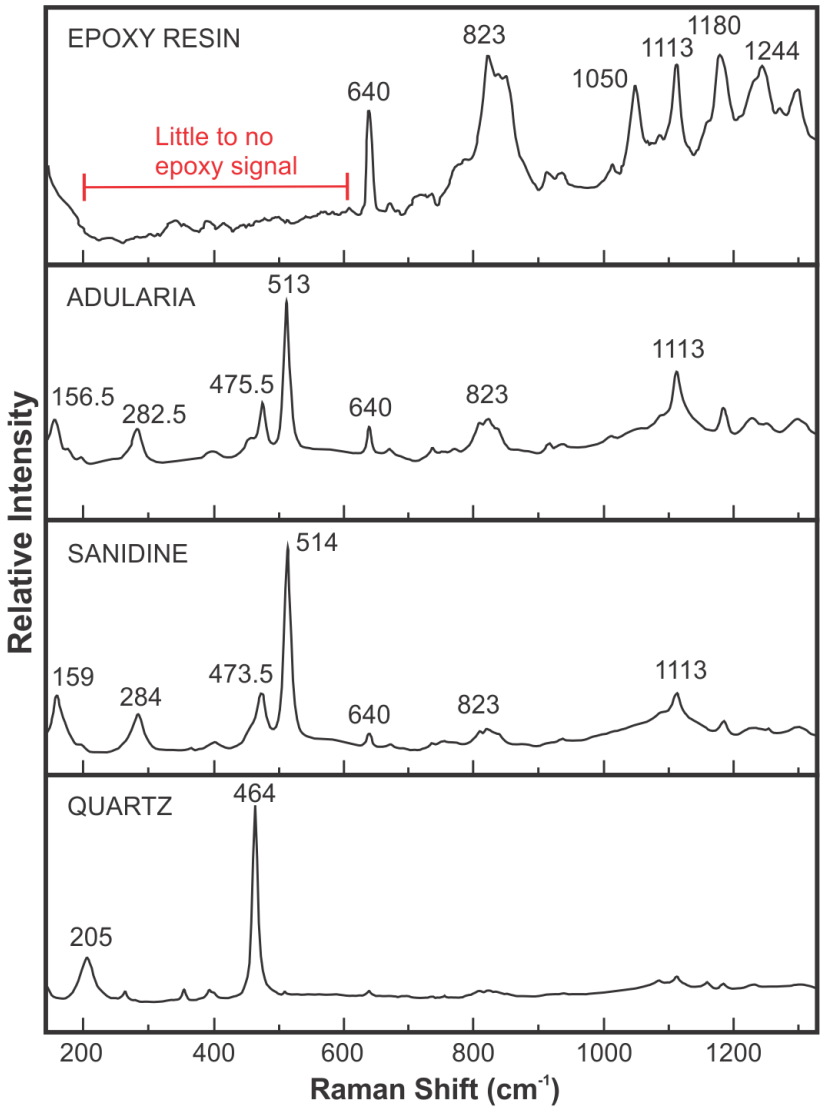

Figure 1.3: Representative spectra showing major peak positions for epoxy resin, adularia (FB11-OD8), sanidine (SB-2028), and quartz.

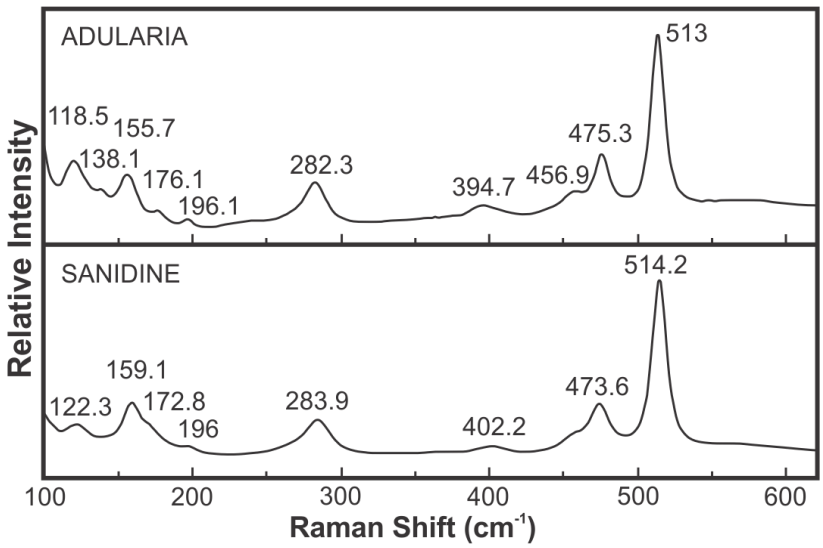

Figure 1.4: Averaged Raman spectra for all adularia and sanidine standards showing major peak positions in the 100-620 cm^{-1} spectral region.

PCA was performed in order to separate samples based on their similarities and differences, allowing a visual representation of the data. This is a commonly used statistical technique for simplifying large, complex data sets such as the Raman spectra presented here. Each spectrum plots as a single point in PC space, with similar samples plotting close together. Pre-processing was required in order to remove baseline and scale effects, allowing all spectra to be overlaid at approximately the same scale. The scores plot for all samples is shown in Figure 1.5, with PC-1 accounting for 51% of the total variance between the samples, and PC-2 accounting for a further 17% of the total variance. A small number of crystals plot in the quartz field, and are confidently classified as quartz. Three sample outliers measured in a dark area within an adularia crystal plot close to epoxy, and due to the strong epoxy signal are not considered further. The remainder of the grains plot in a feldspar field that includes both the adularia and sanidine standards.

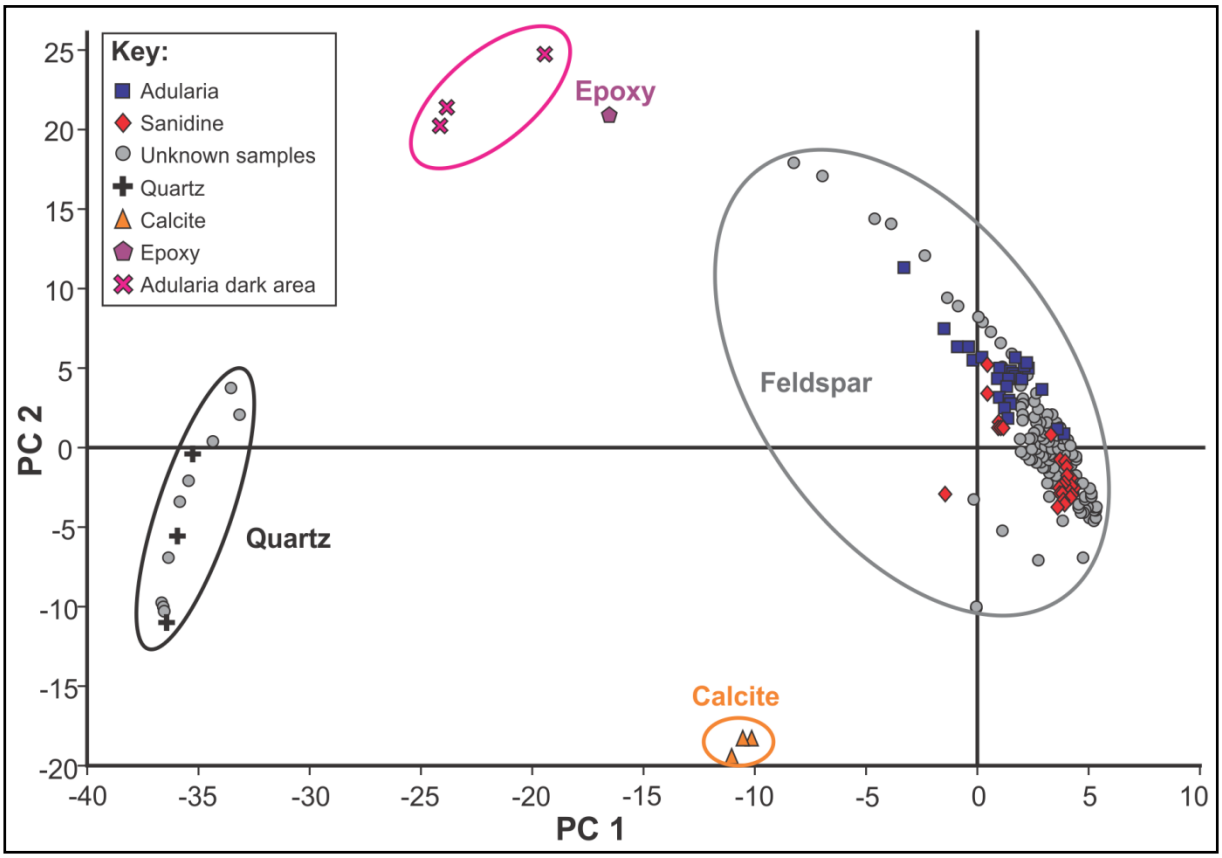

Figure 1.5: Scores plot showing all samples after PCA. The unknown samples from NM5 plotting in a field containing adularia and sanidine were analysed further, those outside this field all plot in the quartz field.

To differentiate between adularia and sanidine, PCA was recalculated using just the samples within the feldspar field (Figure 1.6). Maximum separation was found when plotting PC-4, accounting for 9% of the total variance, against PC-5, accounting for 6% of the total variance between samples. The adularia and sanidine standards form separate fields, with the unknown samples from NM5 plotting in and around the adularia field. The samples within this field are assumed to be adularia. These PCs can be confirmed to contain information based on spectral differences in the adularia and sanidine samples being reflected in the loadings plots of PCs 4 and 5 (Figure 1.7). Peaks in the loadings plots correspond to peaks in the spectra of adularia and sanidine, or are associated with slight differences in peak positions between adularia and sanidine. Negative PC-4 peaks are associated with sanidine, while in PC-5 the positive peaks correlate to sanidine, thus the sanidine samples plot in the top left quadrant in Figure 1.6. No unknown samples plot within the sanidine field, but some lie close to it. Those samples outside the adularia field, as well as some from within it, were also analysed using peak positions in order to confirm their identification.

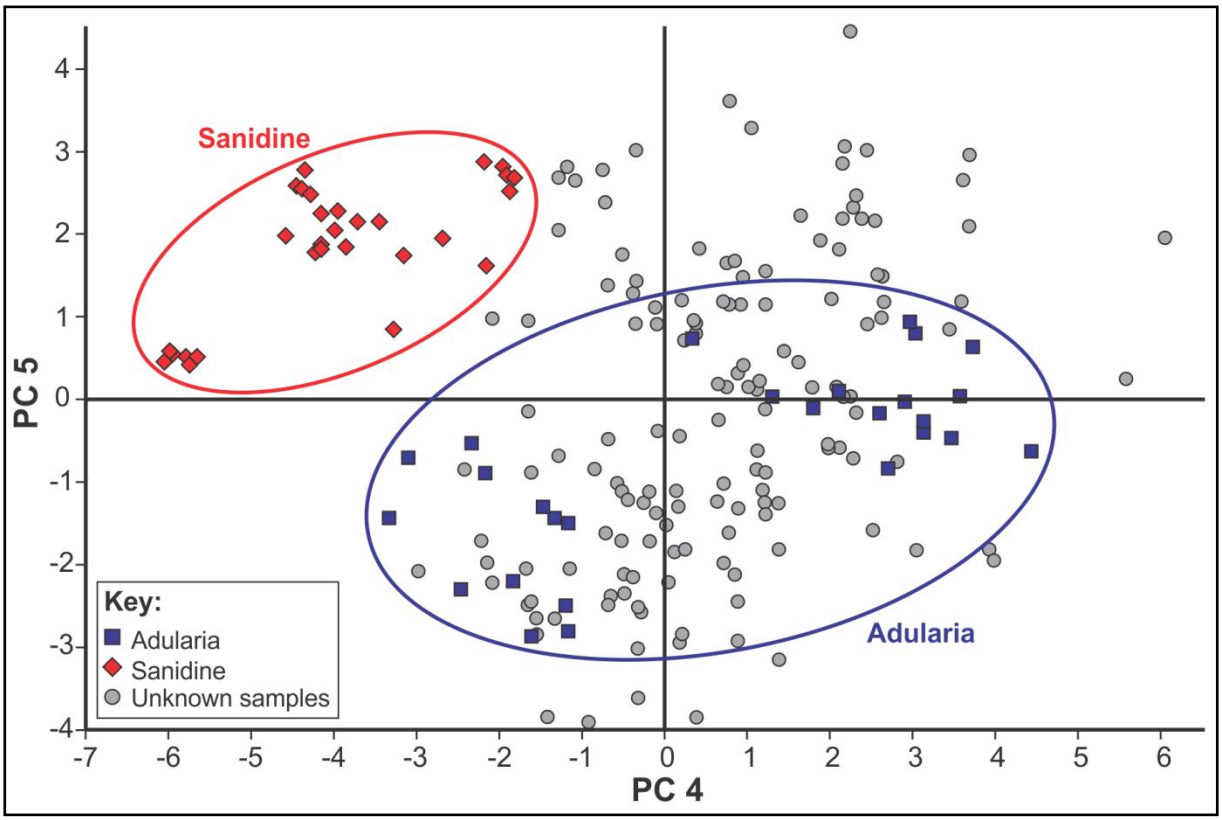

Figure 1.6: Scores plot showing PC-4 against PC-5 for the feldspar samples shown in Figure 1.5. Adularia standards are shown in blue, and the sanidine standards in red, with the unknown samples, shown in grey, plotting in and around the adularia field. The NM5 samples within the blue field are assumed to be adularia, while those samples outside this field were analysed further using peak positions.

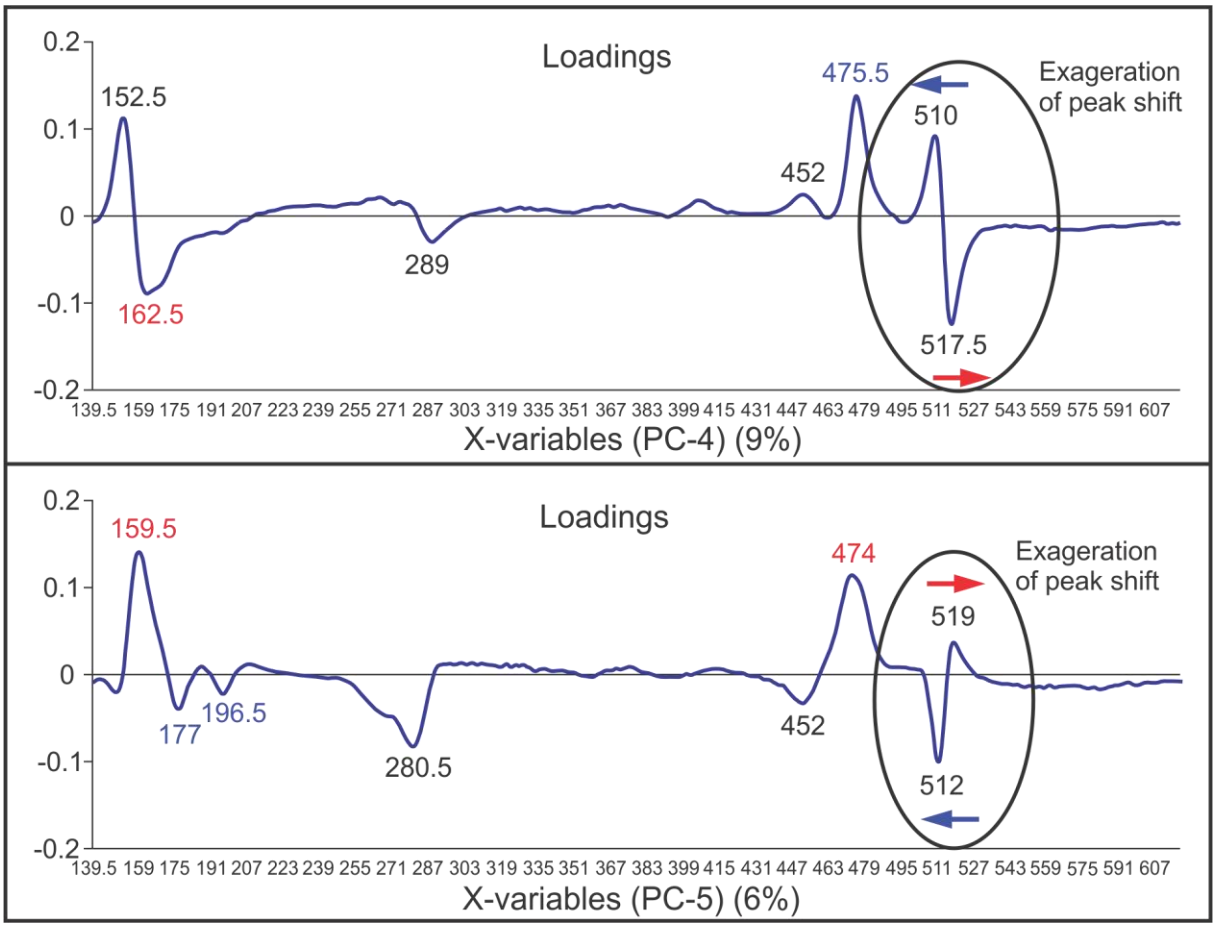

Figure 1.7: Loadings plots of PCs 4 and 5. Peaks associated with adularia spectral features are given in blue and those associated with sanidine are given in red.

Peak positions for the unknown grains are shown in Table 1.1 along with peak positions previously reported for sanidine (*Mernagh*, 1991; *Freeman et al.*, 2008) and orthoclase, which has previously been found to have Raman spectra identical to adularia (*Mernagh*, 1991). Although the spectra have been reported as being identical, it is considered very unlikely that orthoclase is present in any of the samples. It is typically found in plutonic rocks and would not be expected in the volcanic rocks of the TVZ, where it has never been reported. While it can also form in high-temperature hydrothermal settings, it is not consistent with the lower temperature alteration assemblage observed in NM5. Peak positions reported here are shifted slightly from peaks previously reported. It is unclear whether this is due to the nature of the samples or to instrumental variation, and peaks reported by *Freeman et al.* (2008) do not exactly match those reported by *Mernagh* (1991). Unknown samples are, therefore, compared with the adularia and sanidine standards measured here, rather than matching them to those previously reported.

Table 1.1: Raman peak positions for samples outside the adularia field from PCA.

Sample	Peak positions (cm^{-1})										Classification
Sanidine†	123	**nil**	155	**162**	180	282	408	456	476	514	-
Orthoclase†	122	**141**	157	**176**	198	282	403	455	475	513	-
Sanidine*	-	**-**	160.3	**-**	-	284.7	-	456.6	474.7	512.9	-
Orthoclase*	-	**-**	156.5	**-**	-	282.1	-	454.9	477	512.7	-
SB-2028	122.3	**nil**	159.1	**172.8**	196	283.9	402.2	-	473.6	514.2	**Sanidine**
FB11-OD8	118.5	**138.1**	155.7	**176.1**	196.1	282.3	394.7	456.9	475.3	513	**Adularia**
1125a	120.1	**139.3**	156.2	**~175**	196.2	282.8	405.2	455.6	475.2	513.3	Adularia
1125b	120.5	**~140**	157.1	**~175**	196.1	282.2	406.2	455	474.7	513.3	Adularia
1125c	119.2	**-**	153.7	**175.4**	~195	281.7	405.4	~455	475.1	513.1	Adularia
1175b	119.9	**137.8**	157.2	**~173**	195.8	283.1	403	453.8	474.7	513.5	Adularia
1225a	120.7	**~138**	156	**~178**	196.2	282.2	405.2	455.1	474.9	513.1	Adularia
1225b	119.1	**139**	158.6	**~178**	196.2	282.7	405.7	~457	474.9	513	Adularia
1300a	118.2	**139.5**	156.2	**~174**	195.8	283.3	404.4	457.6	474.7	513.2	Adularia
1350a	120.5	**~140**	154.3	**~175**	~195	283	405.8	~455	475.4	512.8	Adularia
1450f	127	**-**	-	**177**	-	287	409	465	479	509	Plagioclase
1450g	121.7	**139.3**	157.6	**~172**	196.4	281.8	398.6	454.8	475.1	513.6	Adularia
1500c	119.2	**~141**	155.2	**172.8**	~195	283.2	403.9	~454	474.5	513.3	Adularia
1550e	120.4	**~137**	152.8	**176.3**	196	280.3	405	454.9	475.2	513	Adularia
1600a	120.3	**~139**	157	**175.2**	~196	286.9	406.4	455.3	477	512.7	Adularia
1600e	119.7	**~138**	153.5	**176.2**	196.4	280.7	405.7	455.2	475.2	513.1	Adularia
1600g	118.7	**138.2**	157.3	**~173**	~192	281.2	392.3	453.8	474.5	513	Adularia
1600h	119.2	**~141**	155.4	**~170**	~190	280.6	393.4	~455	475	513.2	Adularia
1650a	116.2	**~140**	155.2	**~174**	~194	282.9	404.2	~455	474.6	513.2	Adularia
1650d	111.1	**~139**	153.5	**~175**	~196	281.3	404.2	~454	473.7	512.3	Adularia
1700a	120.2	**~138**	154.6	**~173**	~195	280.5	404.8	~455	474.4	512.8	Adularia
1700b	~122	**-**	152.7	**175.7**	195.1	280.8	404.7	453.9	474.8	512.6	Adularia
1700f	119.9	**~138**	154	**174.3**	195.9	281.4	403.2	~454	474.4	513	Adularia
1700g	119.2	**~139**	155.7	**~172**	~195	282.9	403.4	454.6	474.4	513.3	Adularia
1750c	118.7	**138.3**	156.6	**174.9**	196	282.2	403.2	454.2	474.7	513	Adularia
1800c	120.9	**139.8**	156.2	**~173**	196.7	282.7	405.3	465.4	475	513.3	Adularia

Main peaks used for identification are shown in bold. Published analyses for sanidine and orthoclase, as well as sanidine and adularia standards are shown for comparison. †*Mernagh* (1991); **Freeman et al.* (2008).

The peak at 138-140 cm^{-1} was the primary peak used for identification of adularia as sanidine contains no peak in this region (Figure 1.4). This peak is small and where it was absent, or at least could not be distinguished, the peak at 162-177 cm^{-1} was used, with a peak closer to 176 cm^{-1} being considered distinctive of adularia, and a peak closer to 172 cm^{-1} or below being distinctive of sanidine. Using these two peak positions it is possible to show that all but one of the unknown crystals are adularia. Sample NM5-1450f has peak positions that are more closely matched to plagioclase feldspar, in particular andesine-labradorite (*Mernagh,* 1991; *Freeman et al.,* 2008), and is therefore regarded as unaltered plagioclase (Table 1.1). While other peaks do not appear as distinctive as the two main positions used, they are generally more similar to adularia than sanidine. For example, in the 513-514 cm^{-1} region, peaks closer to 514 cm^{-1} indicate sanidine, while peaks closer to 513 cm^{-1} indicate adularia.

1.5.2 Electron microprobe analysis

In order to confirm the identification of the unknown crystals as adularia, a smaller sample of the grains was chosen to undergo EMP chemical analysis. Adularia from geothermal fields tends to form as almost pure potassium feldspar with low sodium content and no measurable calcium (*Steiner,* 1970; *Hedenquist and Browne*, 1989). Sanidine contains a higher proportion of sodium and small (typically <1 wt %) but measurable amounts of calcium (*Deer et al.*, 1992; *Brown*, 1994).

Representative chemical analyses for the adularia and sanidine standards and the samples from NM5 are shown in Table 1.2, with full analyses shown in Figure 1.8 and in Appendix 3. The adularia standards are extremely potassium-rich, with orthoclase (Or) compositions between Or_{99} and $Or_{99.4}$. Previously published adularia compositions from within the TVZ cover a wider range, with compositions of Or_{94} to $Or_{99.5}$ reported by *Hedenquist and Browne* (1989). The sanidine standards have lower potassium contents than adularia, with compositions of between $Or_{69.4}$ and $Or_{70.2}$. This is similar to the sanidine compositions from the Whakamaru-group ignimbrites reported by *Brown* (1994), which range from $Or_{66.7}$ to $Or_{68.7}$. Calcium is present in all sanidine samples analysed here and by *Brown* (1994), generally with anorthite (An) contents of $<An_1$, but ranging up to $An_{1.5}$.

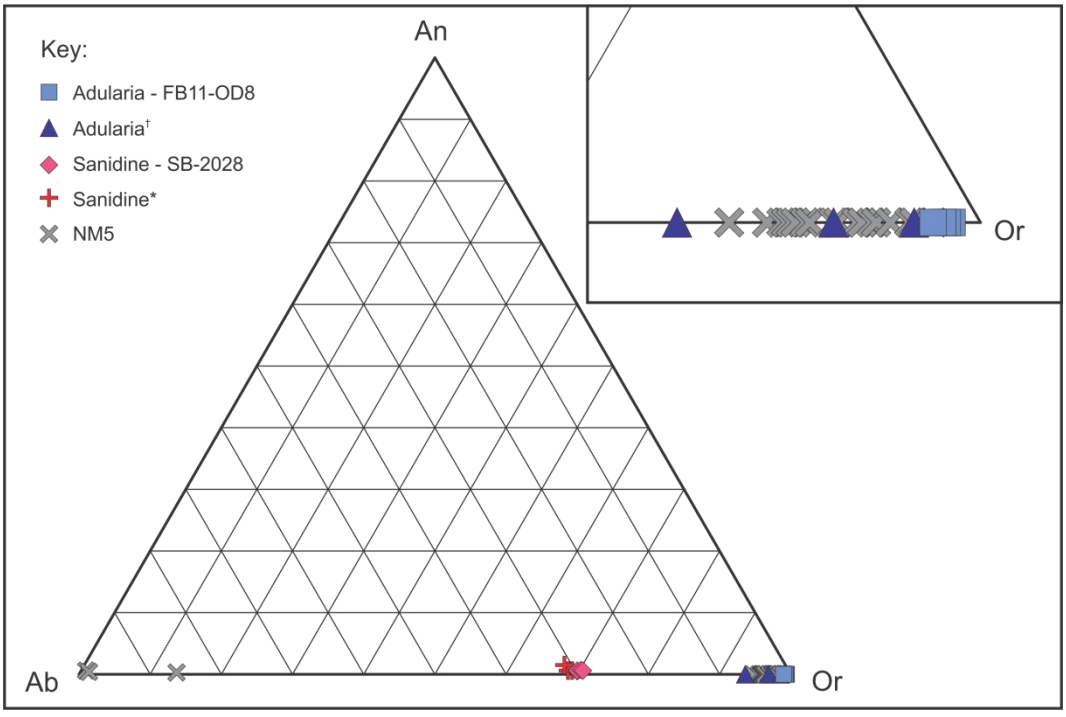

Figure 1.8: Ternary plot showing compositions for all feldspars analysed in this study, as well as sanidine and adularia from the TVZ reported elsewhere. Inset shows the orthoclase end member in a larger scale. †*Hedenquist and Browne* (1989); **Brown* (1994).

Table 1.2: Major element data for sanidine and adularia standards and representative NM5 samples.

Sample:	SB-2028a	SB-2028c	FB11-OD8b	FB11-OD8d	NM5-1125b	NM5-1300a	NM5-1450a	NM5-1500c	NM5-1700c
Type:	Sanidine	Sanidine	Adularia	Adularia	Adularia	Adularia	Adularia	Adularia	Adularia
SiO_2	64.16	63.15	64.60	64.05	64.08	64.45	64.23	63.57	63.91
Al_2O_3	18.45	18.53	18.28	18.07	18.33	18.30	18.41	17.95	18.32
FeO	0.00	0.06	0.00	0.00	0.05	0.00	0.00	0.00	0.00
MgO	0.00	0.00	0.00	0.00	0.00	0.00	0.00	0.00	0.00
CaO	0.09	0.14	0.00	0.00	0.00	0.00	0.00	0.00	0.00
Na_2O	3.25	3.15	0.08	0.11	0.16	0.28	0.28	0.47	0.41
K_2O	11.45	11.35	16.69	16.84	16.37	16.42	16.53	16.43	16.73
BaO	0.47	0.78	0.00	0.01	0.24	0.01	0.02	0.05	0.00
Total	97.87	97.16	99.65	99.08	99.23	99.46	99.47	98.47	99.37
An	0.46	0.72	0.00	0.00	0.00	0.00	0.00	0.00	0.00
Ab	30.00	29.45	0.72	0.98	1.46	2.53	2.51	4.17	3.59
Or	69.54	69.82	99.28	99.02	98.54	97.47	97.49	95.83	96.41

Table 1.3: Major element data for alteration products in NM5.

Sample:	NM5-1300b/1	NM5-1300b/2	NM5-1600b/1	NM5-1600b/2	NM5-1600f/1	NM5-1600f/2	NM5-1600g/1	NM5-1600g/2	NM5-1600g/3
Type:	Adularia	Illite?	Adularia	Albite	Adularia	Calcite?	Adularia	Albite	Ankerite?
SiO_2	64.17	51.07	64.20	67.37	63.17	0.00	62.53	66.40	1.57
Al_2O_3	18.12	30.82	18.28	19.51	18.00	0.00	17.71	18.92	1.21
FeO	0.13	1.24	0.00	0.00	0.11	1.26	0.00	0.00	15.42
MgO	0.00	1.83	0.00	0.00	0.00	0.25	0.00	0.00	8.39
CaO	0.00	0.13	0.00	0.08	0.00	54.42	0.00	0.07	29.37
Na_2O	0.11	0.07	0.41	10.98	0.35	0.00	0.45	9.78	0.00
K_2O	16.70	8.70	16.32	0.24	16.40	0.02	16.33	2.36	0.43
BaO	0.04	0.00	0.03	0.00	0.08	0.00	0.02	0.04	0.02
Total	99.27	93.86	99.24	98.18	98.11	55.95	97.04	97.57	56.41
An	0.00		0.00	0.40	0.00		0.00	0.34	
Ab	0.99		3.68	98.19	3.14		4.02	86.01	
Or	99.01		96.32	1.41	96.86		95.98	13.66	

All of the potassium feldspars analysed from NM5 have orthoclase contents greater than Or_{94}, and range up to about Or_{99}. Calcium is not present in any of these samples. These compositions confirm that they are adularia, despite many of them appearing optically similar to sanidine. The extremely potassium-rich nature of the adularia crystals is a reflection of the low temperatures of the geothermal systems they form in. While it is possible sanidine in the original rock has altered to adularia, observations made elsewhere have shown a range in compositions from Or_{67} to Or_{94} as sanidine alters to adularia (*Hedenquist and Browne*, 1989). The low Or end of this range is typical of sanidine, but increasing potassium contents occur in samples as they re-crystallise to adularia. As no NM5 analyses plot in this range it must be considered extremely unlikely sanidine was originally present in these rocks. As unaltered plagioclase is still present in NM5, it is considered likely that some unaltered sanidine would also be preserved had it originally been present in the rocks. Those crystals easily identified as adularia (FB11-OD8, NM5-1300b; Figures 1.9A and 1.9D), with variable optical properties and a generally darker colour in cross-polarised light, have slightly higher Or contents than other crystals analysed here, again possibly reflecting stages of adularia development. Three grains of albite were also measured and are shown in Figure 1.8.

1.5.3 Implications of the hydrothermal alteration

While identification of the grains as adularia provides little information on the nature of the original rock, it does provide valuable information about the geothermal system. Importantly, it is a good indicator of permeability in the formation (*Browne*, 1970). In NM5 adularia first appears in trace amounts within the Tahorakuri Formation at 1125 mRF depth and is present to at least 1800 mRF, with cuttings below this extremely fine-grained making identification difficult. From 1400 mRF the amount of adularia increases, and between 1500-1700 mRF depths it is at a maximum, indicating enhanced permeability in this zone.

Due to the fine-grained nature of the cuttings in NM5, it is often difficult to determine how the adularia was formed. While some may have crystallised in veins/cavities or in the groundmass, it is likely that most, if not all, formed by replacing plagioclase. Pseudomorphs with subhedral crystal shapes are sometimes observed, and were likely originally plagioclase. No euhedral adularia crystals were observed, suggesting vein mineralisation was not an important formation process, while adularia formed in the groundmass at Ohaaki-Broadlands Geothermal Field tend to be minute, diamond shaped crystals (*Browne and Ellis*, 1970). The

process of formation may be of interest for two reasons. Firstly, it may influence estimates of the temperature it formed at, with adularia in the groundmass reportedly forming at cooler temperatures than the adularia replacing plagioclase at Ohaaki-Broadlands (*Browne and Ellis,* 1970), while vein adularia indicates that boiling has occurred (*White and Hedenquist,* 1990). Secondly, thermo-chronological studies utilising $^{40}Ar/^{39}Ar$ dating of adularia can provide valuable information on the evolution of a hydrothermal system. However, adularia altered from plagioclase phenocrysts often also contains potassium-bearing illite, whereas, vein adularia generally does not, and is, therefore, preferable to date (*Mauk et al.,* 2011).

Some of the grains analysed here are not monomineralic, consisting of two or more mineral phases. This is particularly apparent in the BSE images, which provide more detail than the transmitted light photomicrographs (Figure 1.9). Many of these grains are primarily altered to adularia, often with only small amounts of other minerals within or surrounding the grains, but some contain large areas of various minerals within the same grain and can be internally complex. In order to better understand the process of hydrothermal alteration, a number of these grains were analysed in more than one spot, as shown in Table 1.3 and Figure 1.9. Albite is the most common mineral associated with adularia; however, illite and carbonates are also common. Albite often appears as patchy, dark brown areas (in cross polarised light) with common inclusions (Figure 1.9E), and generally only contains trace amounts of calcium and potassium (Table 1.3; Figure 1.8). The chemical analyses for illite and the carbonates are not complete as the H_2O (for illite) and CO_2 (for carbonate) contents were not measured, but the measured elemental concentrations closely match those given in *Deer et al.* (1992) and references therein. The chemistry of NM5-1600f/2 is consistent with it being calcite, a common hydrothermal mineral at Ngatamariki and worldwide. Calcite replaces plagioclase at temperatures above about 170°C (*Simmons and Christenson*, 1994).

Perhaps of more interest is NM5-1600g/3 (Figures 1.9E and 1.9F), which has a chemistry consistent with ankerite, a calcium-, iron- and magnesium-bearing carbonate. Ankerite has very rarely been recorded in the TVZ; however, it is difficult to distinguish between carbonate minerals without a full chemical analysis, and in some cases it may have been misidentified as calcite. Carbonate minerals provide information about the hydrothermal system, with studies of ore bodies showing ankerite being common in the zone closest to the ore, but calcite becoming the dominant carbonate in the outer propylitic zone (*Mueller and Groves,* 1991; *Leitch et al.,* 1991; *Dugdale et al.,* 2006). *Craw et al.* (2009) also point out that

ankeritic alteration is strongly controlled by structures that enhance permeability. While confident conclusions cannot be drawn on the basis of this one grain, the abundance of adularia also indicates high permeability at this depth. Although not the focus of this study, Raman spectroscopic analysis of the carbonate minerals would be a good method to determine the abundance of the different carbonates, and may provide valuable information about the nature of the hydrothermal system.

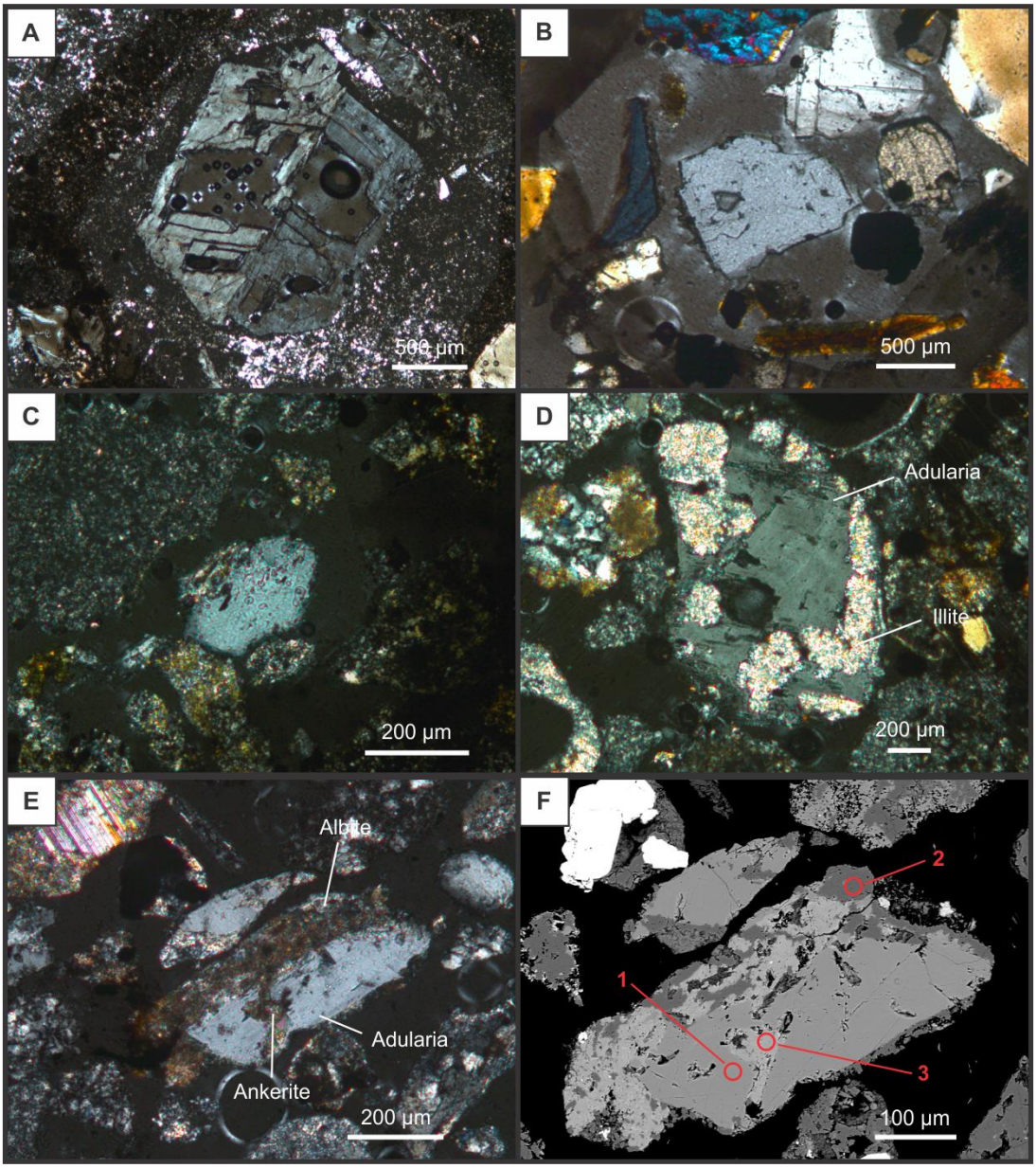

Figure 1.9: Cross-polarised light photomicrographs and BSE image of potassium feldspars and alteration products. (A) adularia from Ohakuri Dam (FB11-OD8a) used as a standard; (B) sanidine from the Whakamaru-group ignimbrites (SB-2028a) used as a standard; (C) typical potassium feldspar observed in the cuttings of NM5 with no obvious twinning; (D) pseudomorphs of adularia with fine twinning associated with alteration products such as illite are sometimes observed in NM5; (E) photomicrograph and (F) BSE image of a crystal (sample NM5-1600g) partially altered to adularia (medium grey in BSE image), albite (dark grey), and carbonate (light grey). The circles show the region the EMP measurements were taken and analysis numbers correspond to those in Table 1.3.

1.6 Conclusions

Raman spectroscopy and EMP analysis are able to independently differentiate between adularia and sanidine in hydrothermally altered volcanic rocks. Therefore, it is considered unnecessary for future studies to use a combined approach when identifying these minerals and either method could be used depending on the circumstances and equipment available. Major advantages of Raman spectroscopy are the ability to analyse a large number of grains quickly and that no sample preparation is necessary. Additionally, Raman spectroscopy is ideal for distinguishing between mineral polymorphs such as adularia and sanidine, or even carbonates that are often difficult to petrographically identify. Raman measurements should be compared to known mineral standards, but the spectral peaks for adularia and sanidine are distinct enough that these minerals can be identified by major peak positions, particularly the distinctive adularia peak present at ~140 cm^{-1}. Overall, this study confirms and demonstrates that adularia and sanidine are structurally and chemically different as well as their potential utility in geothermal fields.

Chapter 2

Early silicic volcanism and rifting in the central Taupo Volcanic Zone, New Zealand from U-Pb dating of subsurface pyroclastic deposits

Alan Eastwood[a]*, Darren Gravley[a], Colin J. N. Wilson[b], Isabelle Chambefort[c], Christopher Oze[a], Jim Cole[a], Trevor Ireland[d]

[a]Department of Geological Sciences, University of Canterbury, Private Bag 4800, Christchurch 8140, New Zealand

[b]School of Geography, Environment and Earth Sciences, Victoria University of Wellington, PO Box 600, Wellington 6140, New Zealand

[c]GNS Science, Wairakei Research Centre, Taupo 3384, New Zealand

[d]Research School of Earth Sciences, Australian National University, Canberra, ACT 0200, Australia

*Email: alan.eastwood@pg.canterbury.ac.nz

Contributions:

Alan Eastwood conducted the literature review, undertook the petrographic analysis of the rock core and cuttings, separated the zircons, assisted with taking SIMS measurements, interpreted the SIMS results and wrote the manuscript. Dr. Gravley helped conceive the study and reviewed the manuscript. Prof. Wilson undertook the SIMS measurements and data analysis, and provided comments on the manuscript. Dr. Chambefort provided assistance with sample selection and collection, and provided comments on the manuscript. Dr. Oze and Prof. Cole helped conceive the study and reviewed the manuscript. Prof. Ireland assisted with the SIMS measurements.

2.1 Abstract

The central Taupo Volcanic Zone (TVZ) is one of the most active and well-studied volcanic regions on Earth. However, understanding its early history has been elusive due to burial of the oldest deposits. As such, the drilled geothermal systems are of major importance to evaluate the early volcano-tectonic evolution of the TVZ. Here, secondary ion mass spectrometry (SIMS) techniques are used to obtain U-Pb crystallisation ages for zircons from the pyroclastic deposits of the Tahorakuri Formation at Ngatamariki and Rotokawa geothermal fields. The age distributions are used to estimate eruption ages, with the oldest two ages placed at 1.89 ± 0.02 Ma and 1.88 ± 0.03 Ma; 200-300 ka older than the oldest exposed silicic deposits from the TVZ. Samples dated at 0.92 ± 0.06 Ma and 0.87 ± 0.03 Ma correlate with the Akatarewa ignimbrite which has previously been dated at nearby geothermal fields. The youngest units were dated at 0.81 ± 0.03 Ma and 0.70 ± 0.04 Ma, and were followed by a long period with no large-scale explosive volcanism until the Whakamaru-group ignimbrites at ~350 ka. Combined with stratigraphic observations, these results indicate that silicic volcanism within TVZ potentially started earlier than previously thought, and may have been tectonically and volcanically active by ~1.9 Ma. The Rotokawa Andesite must have been erupted prior to ~1.9 Ma; demonstrating that early andesitic volcanism was not restricted to the western margin of the TVZ. Rifting within TVZ must also have begun prior to ~1.9 Ma, as shown by significant subsidence and basin development that occurred prior to the emplacement of the oldest silicic deposits. At Ngatamariki subsidence appears to have been reasonably constant at 1-2 mm/yr for the last 1.88 Ma. However, following the initial phase of rifting at Rotokawa, the rift axis appears to have shifted westwards, closer to the modern day rift axis, with subsidence rates of ≤0.2 mm/yr until ~350 ka when rapid subsidence resumed. Overall, silicic volcanism and rifting are closely linked processes in the TVZ, and the data presented here suggests that both have been occurring in the central TVZ for most of the last ~2 million years. This suggests that the Coromandel Volcanic Zone (CVZ) may have extended beneath the current TVZ as far south as Rotokawa, and early andesitic volcanism and rifting may have been related to activity in the more northerly trending CVZ arc system. This in turn suggests that a combination of slab rollback and rotation of the NE part of the North Island may have resulted in the CVZ-TVZ hinge migrating south-eastwards with time, and at ~1.9 Ma was near the current location of Ngatamariki.

2.2 Introduction

Understanding the subsurface stratigraphy and geological structure within a geothermal field is important from both a scientific and industry perspective. Successful management of high-temperature geothermal systems for electricity production requires detailed knowledge of the geothermal reservoir, which is largely controlled by the constituent rocks and geological structures. The rock core and cuttings samples recovered from drilling during geothermal exploration and development are, therefore, of significant value as they provide evidence as to the nature of the subsurface stratigraphy that is often not available outside of geothermal fields. A good example of this comes from the Ngatamariki and Rotokawa geothermal fields in Taupo Volcanic Zone (TVZ), New Zealand, where new U-Pb dates from subsurface pyroclastic deposits have provided some exciting new information on the early history of TVZ.

A major problem in geothermal fields is that high-temperature fluids circulating within the geothermal systems can alter distinctive chemical, mineralogical, and textural characteristics, making correlation of units between different fields, and even different wells, extremely difficult. Most of the pre-Whakamaru sequence in many TVZ geothermal fields is, therefore, simply called 'Tahorakuri Formation' (e.g. *Rae et al.,* 2007; *Bignall,* 2009; *Rosenberg et al.,* 2009; *Bignall et al.,* 2010; *Boseley et al.,* 2010; *Chambefort et al.,* in prep). Within TVZ, early correlations of units were based on mineralogy and petrographic characteristics (e.g. *Grindley,* 1970; *Grindley et al.,* 1994). *Bignall et al.* (1996) also correlated units based on chemical compositions of elements considered to be immobile, in addition to mineralogical and petrographic characteristics. However, there is uncertainty as to the accuracy of this approach in strongly altered rocks typical of those at depth within geothermal fields, and U-Pb zircon dating shows that in some cases existing correlations are inaccurate (*Wilson et al.,* 2010). Unlike minerals used in K-Ar or Ar-Ar age dating, which are commonly altered under hydrothermal conditions, zircons are more resistant to hydrothermal alteration and have successfully been used to date rocks within geothermal fields in the TVZ and elsewhere (*Dalrymple et al.,* 1999; *Schmitt et al.,* 2003; *Wilson et al.,* 2008, 2010; *Milicich et al.,* 2013).

In this paper we report U-Pb age data for selected intervals within the Tahorakuri Formation from the Ngatamariki and Rotokawa geothermal fields (Figure 2.1). This is compared with data from possible correlative units in other geothermal fields, as well as

samples from formations exposed at the surface. Despite extensive alteration of the primary mineral assemblage, the zircons appear unaffected by hydrothermal activity. We show how age data, in addition to petrographic observations, is an important tool in constraining the stratigraphy within geothermal fields, where alteration has a homogenising effect on different lithologies. This data also provides valuable insight into volcanic activity and rifting during the early stages in the history of the TVZ.

2.3 Geological setting

The TVZ (Figure 2.1) is a rifted arc resulting from the oblique subduction of the Pacific Plate beneath the North Island of New Zealand. The eastern part of the North Island is rotating clockwise as a series of discrete tectonic blocks (*Wallace et al.,* 2004), resulting in rifting within the TVZ such that extension generally increases from south to north (*Darby et al.,* 2000; *Villamor and Berryman,* 2001; *Villamor and Berryman,* 2006; *Lamarche et al.,* 2006; *Begg and Mouslopoulou,* 2010). At the surface, this extension is expressed as a NE-SW trending system of normal faults commonly referred to as the Taupo Fault Belt (*Grindley,* 1960) or Taupo Rift (*Acocella et al.,* 2003; *Villamor and Berryman,* 2006). This is partitioned into a series of variably oriented and offset rift segments separated by accommodation zones (*Rowland and Sibson,* 2001).

When rifting in the TVZ began is uncertain. Some authors (e.g. *Stern,* 1987; *Stern and Davey,* 1987; *Stratford and Stern,* 2006) refer to the Central Volcanic Region (CVR); a wedge-shaped area of low density, low velocity volcanic rocks that consists of both the TVZ and the southern section of the Coromandel Volcanic Zone (CVZ). Extension in the CVR may have begun as early as 4-5 Ma, and some consider the TVZ to represent merely the young (~2 Ma) activity within this region (e.g., *Stern,* 1987; *Stern and Davey,* 1987). *Wilson et al.* (1995a) suggest that NE-SW oriented rifting in the TVZ has been confined to the last ~0.9 Ma.

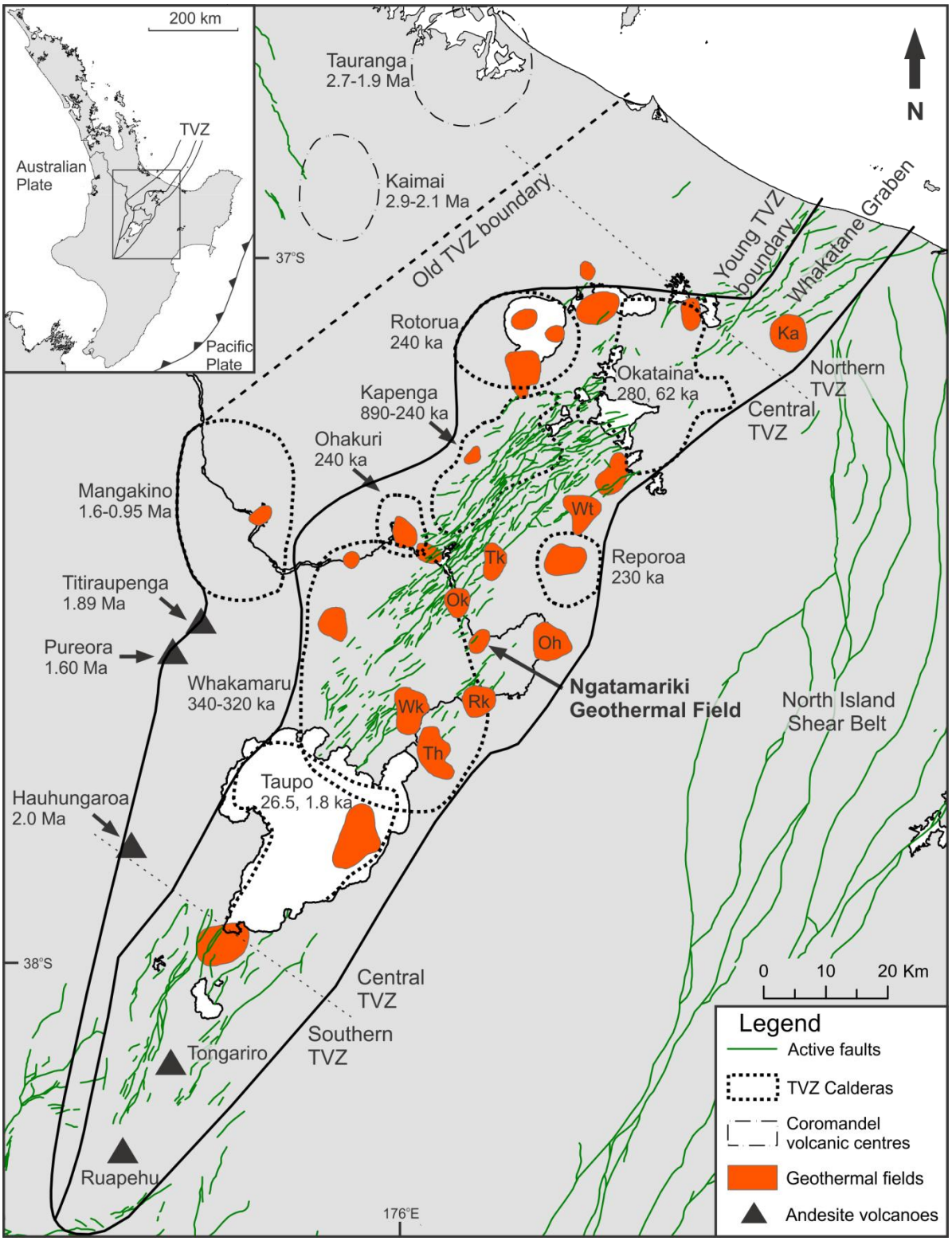

Figure 2.1: Map of the Taupo Volcanic Zone (TVZ). Old (1.6 Ma to 340 ka) and young (340 ka to present) TVZ boundaries are shown along with boundaries for the andesite dominated northern and southern sections and the rhyolite dominated central section (from *Wilson et al.*, 2009). Known calderas (from *Wilson et al., 2009*) and the youngest Coromandel volcanic centres are shown with their ages (from *Briggs et al.*, 2005). Geothermal fields are from *Bibby et al.* (1995), with fields mentioned in this paper marked as: Th – Tauhara; Wk – Wairakei; Rk – Rotokawa; Oh – Ohaaki-Broadlands; Ok – Orakei Korako; Tk – Te Kopia; Wt – Waiotapu; Ka – Kawerau. Ages for andesite cones are from *Graham et al.* (1995) and *Leonard et al.* (2010). Active faults are also shown (from *Leonard et al.*, 2010; *Lee et al.*, 2011; *Townsend et al.*, 2008).

Rifting is an important process in creating depositional basins within the TVZ. For example, the Whakatane Graben is a purely tectonic feature in the northern TVZ and offshore, with rapid subsidence within the graben as a result of extension. Estimates of subsidence rates vary, but maximum rates reported or inferred are in the order of 2-4 mm/yr (*Nairn and Beanland,* 1989; *Wright,* 1990; *Lamarche et al.,* 2006; *Begg and Mouslopoulou,* 2010). Based on the depths to stratigraphic formations within the Kawerau Geothermal Field, *Milicich et al.* (2013) suggest these modern subsidence rates may only be representative of the last ~50 ka, with long-term rates of <1 mm/yr. Variations in subsidence rates with time have also been observed at other geothermal fields (*Wilson et al.,* 2010), suggesting the location of the rift axis may have varied with time. Geophysical studies suggest that the upper ~3 km of the crust in the TVZ is composed of low density volcanic and volcaniclastic deposits (*Rogan,* 1982; *Bibby et al.,* 1995; *Ogawa et al.,* 1999; *Sherburn et al.,* 2003; *Harrison and White,* 2004, 2006; *Stratford and Stern,* 2004, 2006), confirmed by recent drilling within geothermal fields. Rifting is an important process in creating room for the deposition of these volcaniclastic deposits, and establishing subsidence rates can give clues as to the longevity of rifting.

Basins within the TVZ may be formed by rifting, but also by processes such as caldera collapse, which can account for hundreds to over a thousand metres of instantaneous displacement, such as at Mangakino Caldera (e.g., *Wilson et al.,* 2008) and Whakamaru Caldera (*Leonard,* 2003). Three of the youngest calderas in the TVZ contain caldera lakes (*Cole and Spinks,* 2009), indicating the importance of caldera collapse in creating depositional environments. Rifting and caldera formation are commonly inter-related. For example, during the paired Mamaku-Ohakuri eruptions at ~240 ka, syneruptive volcano-tectonic displacement along NNE-SSW trending faults between the 2 calderas may have accounted for >400 m of subsidence (*Gravley et al.,* 2007). Post-eruptive faulting within years to decades following these eruptions may have resulted in a further ~300 m of subsidence. There is commonly a relationship between caldera volcanism and rifting (e.g., *Gravley et al.,* 2007; *Cole and Spinks,* 2009), and *Cole* (1990) suggests that many calderas are related to transtension, where there is also a strike-slip component in addition to extension.

Volcanic activity in the TVZ followed a long period of volcanism in the NNW oriented CVZ, which began at ~18 Ma (*Adams et al.,* 1994). Andesitic arc volcanism dominated until ~9 Ma, with silicic volcanism occurring as early as 12 Ma (*Carter et al.,* 2003, 2004). From ~9 Ma, rhyolitic and basaltic volcanism dominated, and this change in

erupted composition was accompanied by an eastward shift in activity (*Adams et al.*, 1994). Deposits from the CVZ become progressively younger to the south; with the last activity attributed to the CVZ between 2.9 and 1.9 Ma at the Tauranga and Kaimai volcanic centres (*Briggs et al.*, 2005). Activity then transitioned to the TVZ, with andesitic volcanic activity in the TVZ considered to have begun at ~2 Ma, and silicic volcanism from ~1.6 Ma (*Wilson et al.*, 1995a). The oldest andesitic cones are located along the western margin of the TVZ, with Hauhungaroa, Titiraupenga and Pureora (Figure 2.1) dated at ~2.0 Ma, 1.89 Ma and 1.60 Ma, respectively (*Wilson et al.*, 1995a; *Graham et al.*, 1995; *Leonard et al.*, 2010). The earliest silicic activity originated from Mangakino Caldera in what *Wilson et al.*, (1995a) term the 'old TVZ', with the first known activity from within the area encompassed by the 'young TVZ', or the currently active TVZ, at 0.89 Ma (*Houghton et al.*, 1995). The particularly voluminous Whakamaru-group ignimbrites erupted at ~347 ka (*Leonard et al.*, 2010) mark the boundary between the 'old TVZ' and the 'young TVZ' (*Wilson et al.*, 1995a). Together with other 'young TVZ' products, this obscures the older deposits throughout much of the central North Island. Surface exposures of pre-Whakamaru volcanic deposits are mainly located to the west of the currently active TVZ (*Leonard et al.*, 2010).

Distinct segmentation of the TVZ is present with andesitic volcanism dominating in the northern and southern sections, and voluminous rhyolitic volcanism in the central section associated with eight partially delineated calderas (*Wilson et al.*, 2009*; Cole and Spinks,* 2009). The central TVZ has been the most frequently active and productive silicic volcanic system on Earth in the last 340 ka (*Houghton et al.*, 1995; *Wilson et al.*, 1995a), although most of the heat (~75%) is transferred to the surface through convective geothermal systems, which accounts for 4200 ± 500 MW of heat flux (*Bibby et al.*, 1995; *Hochstein*, 1995). There are 23 active high-temperature geothermal systems in the TVZ, most of which are located to the east of the Taupo Rift (*Bibby et al.*, 1995).

Ngatamariki Geothermal Field (Figure 2.2) is located ~17 km NE of Taupo. It lies just outside the eastern margin of the Whakamaru Caldera as proposed by *Wilson et al.* (1986), with the inferred boundary marked by Whakapapataringa dome. Orakei Korako and Rotokawa geothermal fields are located nearby to the north and south, but a hydrological connection between the fields is not apparent (*Bignall*, 2009; *O'Brien,* 2010). Four exploration wells were drilled in the mid-1980's with a further seven wells drilled since 2008 as the field has been further explored and developed. There is a shallow low resistivity

anomaly associated with hydrothermal alteration to the south of the Waikato River and the hydrothermal system extends further to the south at depth (*Urzua*, 2008). The NE-SW trending faults mapped at the surface reflect the regional structure of the TVZ. The Aratiatia Fault passes just to the south of NM6, with Rotokawa located a further ~3 km to the south.

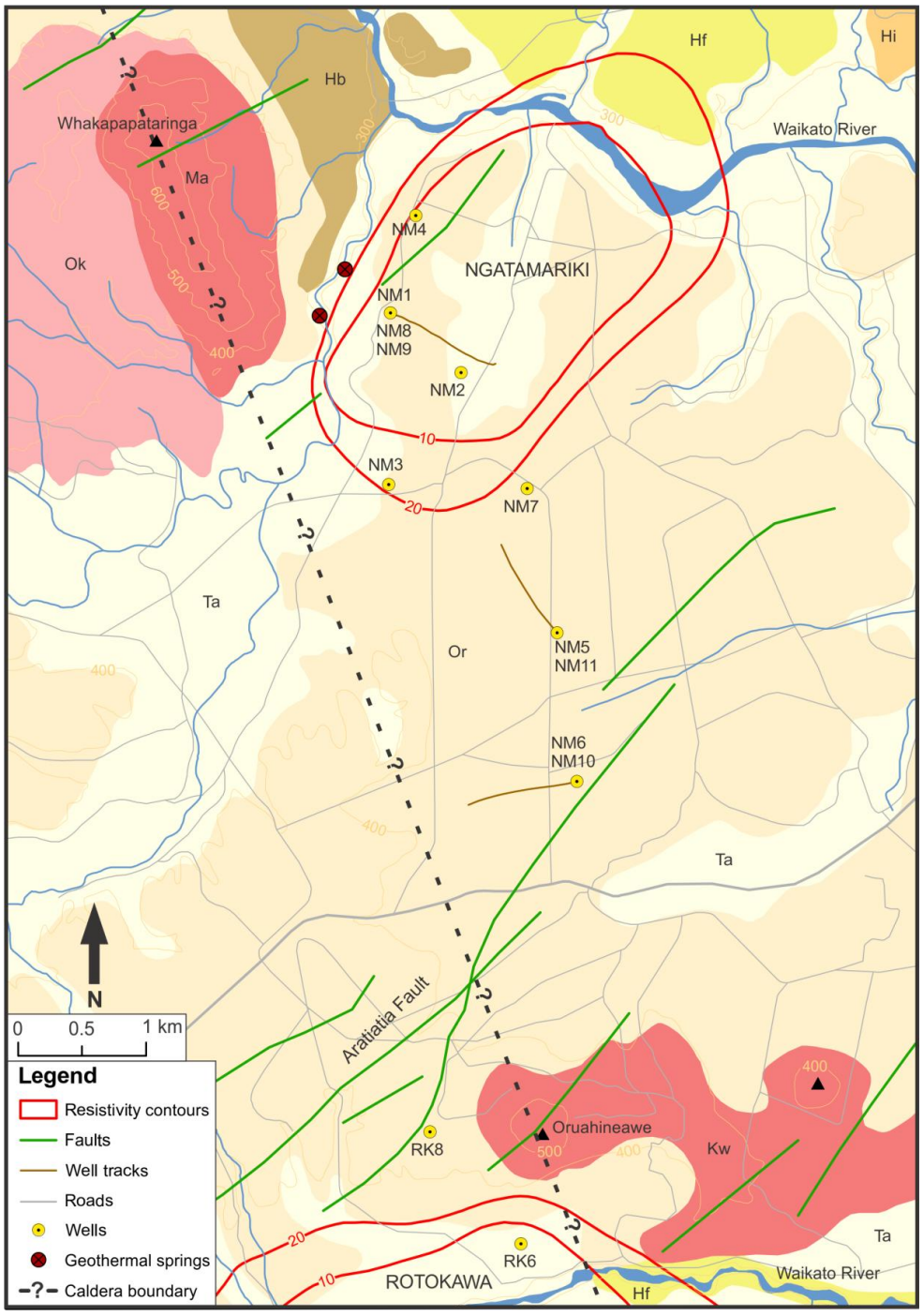

Figure 2.2: Map of Ngatamariki and the northern part of Rotokawa. Resistivity contours indicate the resistivity anomaly at ~500 m depth (from *Stagpoole et al.*, 1985). Geological formations and active faults are from *Leonard et al.* (2010). Units are: Ta – Taupo pumice; Or – Oruanui Formation; Hb – hydrothermal explosion breccias; Hi – Hinuera Formation; Hf – lake sediments, Huka Falls Formation and similar (Tauranga Group); Ok – Orakonui Formation; Kw – Kaimanawa rhyolite dome; Ma – Maroa Group rhyolite. The Whakamaru Caldera boundary it that proposed by *Wilson et al.* (1986).

2.4 Subsurface stratigraphy

The focus of this paper is on the pre-Whakamaru deposits, in particular the pyroclastic deposits of the Tahorakuri Formation, although younger deposits are briefly discussed. Surficial deposits at Ngatamariki are described by *Lloyd* (1972), and consist largely of Taupo Pumice Alluvium from the ~233 AD Taupo eruption (*Lowe et al.*, 2008) and soft pumice breccias and ignimbrites of the Oruanui and Orakonui formations. In the immediate vicinity there are also the Whakapapataringa and Oruahineawe rhyolite domes, bedded rhyolitic sands and gravels of the Hinuera Formation, and an andesite dike. Lacustrine sediments to the north of Ngatamariki were mapped as the Huka Falls Formation by *Lloyd* (1972), but were classified as the Tauranga Group by *Leonard et al.* (2010). In addition, *Leonard et al.* (2010) also mapped hydrothermal explosion breccias to the NE of Whakapapataringa.

The regional subsurface stratigraphy is summarised in Table 2.1 and shown in Figures 2.3 and 2.4. At Ngatamariki it is described by *Chambefort et al*. (in prep) and various reports including *Wood* (1985a, 1985b, 1986a, 1986b), *Ramirez and Rae* (2009); *Rae et al.* (2009a, 2009b); *Bignall* (2009), *Chambefort and Bignall* (2011); and *Lewis et al.* (2012a, 2012b, 2012c, 2013). Major post-Whakamaru units include the Huka Falls Formation, crystal-poor rhyolite, and pyroclastics and tuffaceous sediments of the Waiora Formation. The correlative of the Whakamaru-group ignimbrites, termed the Wairakei ignimbrite in the geothermal wells of the central TVZ (*Chambefort et al.*, in prep), ranges in thickness from ~100-500 m.

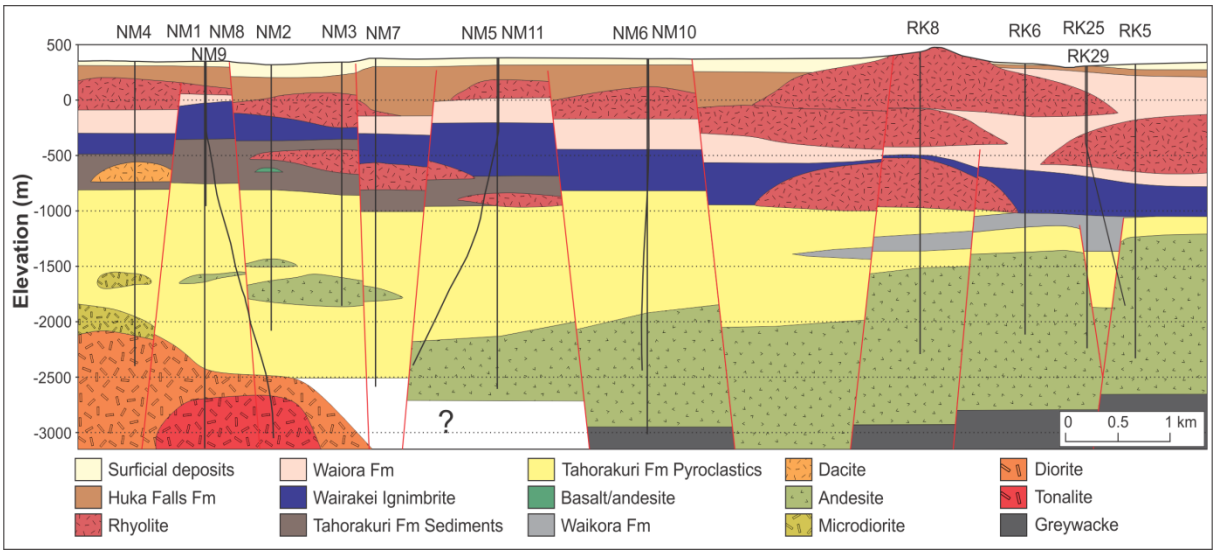

Figure 2.3: Simplified cross section showing the subsurface stratigraphy at Ngatamariki and Rotokawa. The stratigraphy from Ngatamariki is simplified from *Chambefort et al*. (in prep) and has been extended to the south following descriptions from *Nairn* (1984, 1985, and 1986), *Rae* (2007), and *Powell et al.* (2011). Reports courtesy of Mighty River Power Ltd.

Table 2.1: Summary of the main stratigraphic units at Ngatamariki and Rotokawa.

Formation	Thickness (m)	Lithology
Surficial deposits	50-115	Unconsolidated sands, gravels and pyroclastics (includes Taupo Pumice, Orakonui and Oruanui Formations)
Huka Falls Formation	15-285	Siltstone, sandstone, and minor gravel of fluvial or lacustrine origin
Parariki Breccia	20-220	Quartz-feldspar-rich tuffaceous breccia with a silty-clay matrix
Waiora Formation	0-550	Vitric and crystal pyroclastics, tuffaceous sandstone and siltstone
Rhyolite lava	110-660	Rhyolite lava and breccia, sometimes with flow-banding, spherulitic, or perlitic textures (pl, qz ± pyx ± amp)
Wairakei Ignimbrite	100-325	Crystal-rich, ignimbrite with variable welding and common large embayed quartz (qz, pl, pyx ± amp ± bt)
Rhyolite lava	0-285	Quartz-rich rhyolite, sometimes flow-banded (qz, pl ± pyx ± amp)
Waikora Formation	0-250	Rounded to sub-rounded greywacke and argillite gravels.
Tahorakuri Formation sedimentary succession	0-700	Interbedded sediments and pyroclastics dominated by brown-black siltstones and sandstones, sometimes laminated
Tahorakuri Formation pyroclastic succession	>200-1735	Pyroclastic deposits including welded and non-welded ignimbrites and breccias with variable crystal contents
Andesite lava/breccias	0-2190	Andesite lava, sometimes brecciated (pl, pyx, ± amp)
Microdiorite	0-250	Intensely altered volcanic rock with rare relict granophyric or myrmekitic textures (qz, pl, ksp ± pyx ± amp)
Diorite	0->300	Medium-grained, quartz-bearing diorite (pl, qz, amp, pyx)
Tonalite	0->450	Medium-grained, quartz-phyric tonalite (qz, pl, amp)
Greywacke basement		Grey, massive, meta-sandstone with no obvious bedding

Abbreviations used are: pl = plagioclase; qz = quartz; ksp = K-feldspar; pyx = pyroxene; amp = amphibole; bt = biotite. From *Wood* (1985a, 1985b, 1986a, 1986b); *Rae* (2007); *Ramirez and Rae* (2009); *Rae et al.* (2009a, 2009b); *Chambefort and Bignall* (2011); *Lewis et al.* (2012a, 2012b, 2012c, 2013).

The pre-Whakamaru deposits within the geothermal fields of the central TVZ have been termed the Reporoa Group (*Gravley et al.*, 2006). This consists of: 1) the Tahorakuri Formation, including un-correlated volcanic, volcaniclastic, and sedimentary deposits; 2) the Waikora Formation, consisting of greywacke-rich conglomerate; and 3) named ignimbrites and lava flows at individual geothermal fields (Figure 2.4). At Ngatamariki, the Tahorakuri Formation can be divided into a sedimentary succession and a pyroclastic succession (*Chambefort and Bignall*, 2011; *Chambefort et al.*, in prep). The sedimentary succession is dominated by fine-grained sediments described as black mudstones and fine sandstones with minor interbedded pyroclastic deposits, suggestive of a lacustrine environment (*Wood*, 1985a, 1985b, 1986a, 1986b). They are absent in the southern-most wells, suggesting a lake was located in the northern part of the field prior to the Whakamaru-group eruptions. The presence of these sediments led to the suggestion that this may have been a caldera lake, with the thick pyroclastic sequence below being intracaldera fill (*Powell et al.*, 2011). Within the sedimentary succession are small bodies of rhyolite, dacite and basalt lava and breccia.

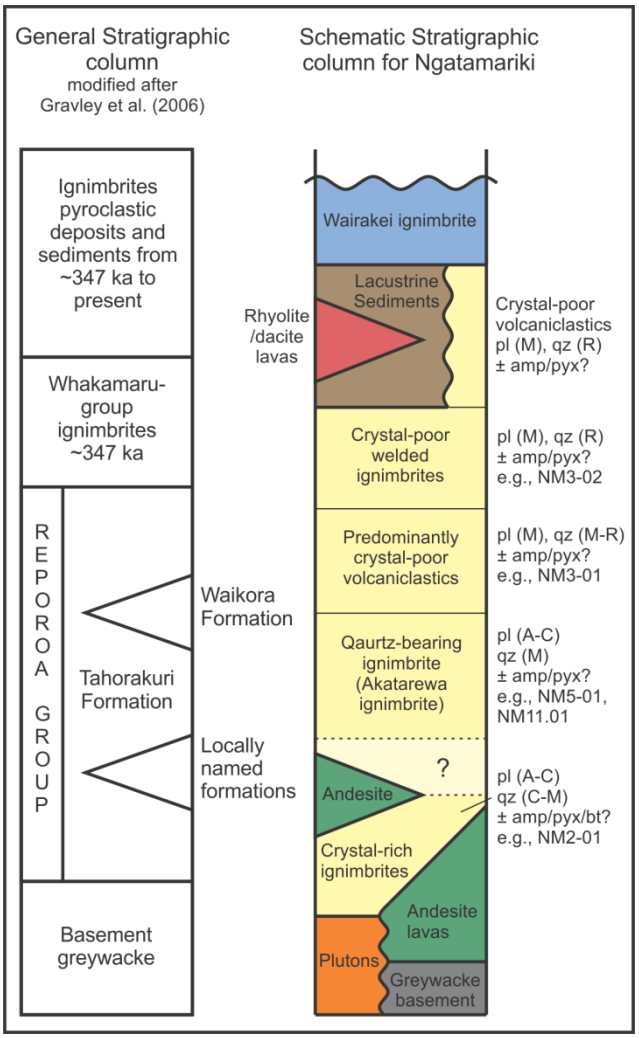

Figure 2.4: The stratigraphic column on the left shows the general subsurface stratigraphy encountered in the geothermal fields of the central TVZ, modified from *Gravley et al.* (2006) with dates from *Leonard et al.* (2010). The schematic stratigraphic column illustrates the different lithologies, and their typical mineralogy, encountered within the Tahorakuri Formation at Ngatamariki as identified in this study. Primary lithologies are after *Chambefort et al.* (in prep). Abbreviations used are: pl = plagioclase; qz = quartz; pyx = pyroxene; amp = amphibole; bt = biotite; A = abundant (>20 %); C = common (10-20 %); M = minor (1-10 %); R = rare (<1 %).

The Tahorakuri Formation pyroclastic succession consists of different lithologies described mainly as ignimbrites, tuffs and breccias (*Wood,* 1985a, 1985b, 1986a, 1986b; *Ramirez and Rae,* 2009; *Rae et al.,* 2009a, 2009b; *Boseley et al.,* 2010; *Chambefort and Bignall,* 2011; and *Lewis et al.,* 2012a, 2012b, 2012c, 2013). However, strong to intense alteration throughout much of the formation, as well as the often fine-grained nature of the drill cuttings complicates any detailed correlations. Hand-sample and thin section descriptions of cores and cuttings from the Tahorakuri Formation are given in Appendix 1, along with a summary of the cuttings from NM5 and NM6 in Appendix 2. This is also summarised in Figure 2.4. The upper part of the formation is dominated by intensely altered, crystal-poor

pyroclastic deposits with minor plagioclase pseudomorphs, very rare quartz, and completely altered ferromagnesian minerals. Welded textures are sometimes preserved, and suggest one or more welded ignimbrites are present towards the top of this succession. Perhaps the best indication of change within the formation is the abundance and size of quartz phenocrysts, which are largely unaffected by hydrothermal alteration. In the lower part of the formation quartz is common and phenocrysts are larger, while the upper part of the succession is notable for the rarity of quartz phenocrysts. This can be seen in cores from NM3 at 1743-1745 mRF (metres below the drilling rig floor), NM5 at 1775-1778 mRF, and possibly NM11 at 2083.0-2089.9 mRF, which are all quartz-bearing ignimbrites (refer to Figures 2.2 and 2.3 for well locations). It can also be recognised in the cuttings from NM5 (~1700-1825 mRF) and NM6 (~1775-1890 mRF) from the size and abundance of the quartz crystals (Appendix 2). Based on geochemical similarities, *Bignall et al.* (1996) suggested core from 1743-1745 mRF in NM3 is the Akatarewa ignimbrite, a quartz-bearing ignimbrite encountered in nearby geothermal fields, and U-Pb dated at 0.95 ± 0.05 Ma at Orakei Korako and Te Kopia (*Wilson et al.,* 2010).

The deepest deposits also differ between the northern and southern parts of the field. A thick sequence of andesite lava is present in the southern wells, and likely represents the northern margin of the andesite found at Rotokawa (*Anderson,* 2011). This deep andesite is not related to the shallower andesite/andesite breccia found in the wells to the north (*Browne et al.,* 1992; refer to wells NM2, NM3 and NM7 in Figure 2.3). The shallower andesite in NM3 has previously been placed at >1.28 Ma by *Arehart et al.* (2002) based on Ar-Ar ages of sericite relating to hydrothermal alteration. Diorite and tonalite bodies, the only intrusives yet encountered in the TVZ, have been encountered at depth in the northern wells (*Browne et al.,* 1992; *Arehart et al.,* 2002; *Chambefort et al.,* in prep). The greywacke basement has also been encountered at depth in NM6 (*Rae et al.,* 2009a).

The shallow stratigraphy encountered at Rotokawa is similar to Ngatamariki, but differs notably at depth. Here, the majority of the pre-Whakamaru sequence consists of the Rotokawa Andesite (*Rae,* 2007). This rests on the greywacke basement, and likely formed a large andesitic cone volcano, with the northern margins reaching as far as the southern Ngatamariki wells (*Anderson,* 2011). Overlying this, but only present in some wells, is a thin (20-250 m) pyroclastic sequence of the Tahorakuri Formation (*Rae,* 2007). Also present in

some wells is a thin (10-250 m) sequence of greywacke-rich gravels known as the Waikora Formation.

2.5 Samples

Six core samples from the Tahorakuri Formation were chosen for this study, five from Ngatamariki and one from Rotokawa. All of the samples are significantly affected by hydrothermal alteration, with little of the primary mineralogy or textures remaining intact. Plagioclase is partially to completely altered, primarily to albite, adularia, clay and calcite. Ferromagnesian minerals are completely altered in all samples, but are sometimes able to be identified by shape. Quartz is the only major primary mineral phase preserved, and its abundance and size is useful for helping distinguish between different units. Samples are summarised in Table 2.2 and discussed below.

Table 2.2: Summary of samples chosen for zircon dating in this study.

Sample	Depth (mRF)	Depth (mRL)	Mineralogy	Description
NM2-01	2254.7 to 2255.2	–1926 to –1926.5	pl (A), qz (C), amp (R), bt (R), ± pyx?	Crystal-rich (40-45%) ignimbrite with large (up to 3 mm), often embayed quartz and vague welding textures
NM11-01	2083.0 to 2089.9	–1610 to –1616	pl (A), qz (M), ± amp/pyx?	Pumice-, crystal- and lithic-rich ignimbrite, with aligned, flattened pumice, and minor quartz fragments
NM5-01	1775 to 1778	–1384 to –1387	pl (C), qz (M), amp ± pyx (M)	Welded ignimbrite with large (>1 mm), rounded, often embayed quartz, pumice fiamme, and minor lithics
NM3-01	1495.7 to 1497.7	–1145.7 to – 1147.7	pl (M), qz (M), ± amp/pyx?	Crystal-poor volcaniclastic unit with mostly fine (<1 mm), quartz fragments, minor lithics, and altered pumice
NM3-02	1246 to 1248	–896 to –898	pl (M), qz (R) ± amp/pyx?	Crystal-poor welded ignimbrite with common elongate pumice fiamme, minor lithics, and rare, mostly fine quartz
RK6-01	1612 to 1614	–1275.4 to –1277.4	pl (A), pyx ± amp (R)	Welded ignimbrite with small, wispy pumice fiamme, minor lithics, and moderate crystal content lacking quartz

Depths of the samples are given in metres below the drilling rig floor (mRF) and relative to sea level (mRL). Mineralogy refers to estimates of the primary mineral phases, which in many cases are completely altered and identified based on shape. Abbreviations used are: pl = plagioclase; qz = quartz; pyx = pyroxene; amp = amphibole; bt = biotite; A = abundant (>20 %); C = common (10-20 %); M = minor (1-10 %); R = rare (<1 %).

The deepest unit, NM2-01, is a crystal-rich ignimbrite. Primary textures are poorly preserved, although relict welding textures are rarely visible. The mineralogy is distinct from all other units observed at Ngatamariki due to the abundance of large, often embayed quartz phenocrysts and relict biotite. It is the only sample dated in this study from below the andesite and andesite breccia encountered in NM2, NM3, and NM7. Two cores of the shallower quartz-bearing ignimbrite were sampled (Figure 2.4), although there are minor differences

between them. Both samples are relatively crystal- and quartz-rich compared to the majority of the overlying Tahorakuri Formation, and are dominated by plagioclase with minor quartz. NM11-01 is moderately welded, with common flattened pumice and lithics. Quartz is mostly relatively fine (<0.5 cm), and possible rare ferromagnesian minerals are completely altered. NM5-01 appears more strongly welded, but again contains common flattened pumice and lithics. Quartz phenocrysts are larger (often >1 mm) and often embayed. Ferromagnesian minerals are completely altered, but based on shape, amphibole appears to dominate.

Sample NM3-01 is intensely altered and no primary textures were observed, making identification difficult. It has a moderate crystal content consisting of quartz and altered crystal pseudomorphs (most likely plagioclase), with minor lithics and pumice in a fine groundmass. Quartz is generally fine, and appears to consist primarily of broken crystal fragments. NM3-02 is a welded ignimbrite, with common pumice fiamme. The mineralogy is characteristic of much of the shallow Tahorakuri Formation pyroclastic succession, with a crystal-poor nature and very rare, mostly small (<0.3 mm) quartz phenocrysts. Although completely altered, primarily to clay, the majority of the crystal pseudomorphs were probably plagioclase. RK6-01 is also a welded ignimbrite with small, highly attenuated fiamme, indicating intense welding. The mineralogy is notable for the apparent lack of quartz, being dominated by plagioclase pseudomorphs, with rare, completely altered ferromagnesian minerals. It is relatively crystal-rich compared to the shallow Tahorakuri Formation pyroclastic succession at Ngatamariki, although the scarcity of quartz is more typical.

2.6 Methods

2.6.1 Sample preparation

Samples were roughly crushed and then ground in a ringmill, before being sieved to yield a <250 µm size fraction. When possible, obvious lithic clasts were removed during the crushing process in order to minimise inheritance. Heavy minerals were concentrated by density separation using lithium polytungstate and methylene iodide. Concentrates were rinsed in nitric acid to remove pyrite, and then magnetic minerals were removed by passing the samples through a Frantz magnetic separator. Zircons were hand-picked from the remaining concentrate material, mounted in epoxy resin, and polished to expose the cores of

the grains. Mounts were imaged by cathodoluminescence (CL) on a JEOL 6610 Scanning Electron Microprobe using a Robinson Detector.

2.6.2 Analytical techniques for ion probe

Age determinations on zircons were made by Secondary Ion Mass Spectrometry (SIMS) techniques using the Sensitive High-Resolution Ion Microprobe - Reverse Geometry (SHRIMP-RG) in the Research School of Earth Sciences, Australian National University (ANU). Techniques used were similar to those described in *Milicich et al.* (2013), as modified from *Dalrymple et al.* (1999). In order to minimise contamination by common Pb, the mounts were rinsed in detergent, petroleum spirits and HCl prior to gold coating for both CL imaging and ion probe analysis. The primary beam was rastered for 180 s on a 35 × 45 µm area prior to data acquisition in order to remove the gold coating and any possible surface contamination. Ions were sputtered from the zircons with a 3-4 nA primary O_2^- beam focussed to a ~25 × 35 µm spot. The mass spectrometer was cycled through peaks corresponding to $^{90}Zr_2{}^{16}O$, ^{204}Pb, background, ^{206}Pb, ^{207}Pb, ^{208}Pb, ^{238}U, $^{232}Th^{16}O$ and $^{238}U^{16}O$, with a total analysis time of ~900 s. Extended count times were used for ^{206}Pb (30 s) and ^{207}Pb (20 s), and six scans were run through the mass sequence. The concentration standard used was SL13 (238 ppm U) and the age standard was R33 (420 Ma ID-TIMS age from: http://earth.boisestate.edu/isotope/analytical-capabilities/id-tims-u-pb). Data reduction was carried out using SQUID 2 (Version 1.51, *Ludwig,* 2009).

The zircon/melt partition coefficient is higher for U than for Th, therefore, an initial deficit of ^{230}Th occurs in zircon during crystallisation. This creates a temporal gap in the $^{230}Th/^{234}U$ secular equilibrium of the ^{238}U decay chain and an underestimation of the zircon crystallisation age. Using the measured Th and U concentrations (relative to concentration standard SL13), and a whole rock Th/U value of 4.4, a correction factor was applied using $f = (Th/U_{zir}) / (Th/U_{magma})$ (*Schärer,* 1984). The age corrections resulting from initial Th-U disequilibrium ranged from 55 ka to 103 ka.

The young age of the zircons make the results particularly susceptible to contamination by common Pb. The presence of common Pb was monitored by using ^{204}Pb, and applying a correction using the measured $^{207}Pb/^{206}Pb$ values for the sample and a common Pb isotopic composition of $^{207}Pb/^{206}Pb = 0.836$ from the average crustal values of *Stacey and*

Kramers (1975). Samples vary in the proportion of ^{206}Pb attributable to common Pb, with the younger units in general having higher percentages. In the younger units these values were often >20%, and cut-offs of common Pb of >30% to >50% were used to exclude analyses with sometimes plausible, but imprecise ages from consideration. The older samples generally had lower proportions of common Pb, and a cut-off of >10% or >20% was used (Table 2.3). High proportions of ^{206}Pb attributable to common Pb are unlikely to be the result of hydrothermal alteration, as the crystals do not display breakdown or replacement textures seen in altered grains elsewhere (for discussion see *Milicich et al.,* 2013).

2.7 Results and discussion

2.7.1 Sample ages and possible correlative ignimbrites

Full data sets are shown in Appendix 4, with histograms and probability density function (pdf) curves, created using Isoplot (*Ludwig,* 2011), for each sample shown in Figures 2.5-2.9. A summary of the age data is also shown in Table 2.3. Individual zircon ages determined for a single crystal are interpreted to represent a crystallisation age, not necessarily an eruption age. The peaks in the crystallisation age distribution (pdf peaks) for all zircons in a given sample may predate the eruption ages by tens to hundreds of thousands of years. Data presented in *Simon et al.* (2008) suggest an average difference between peak crystallisation age and eruption age of 70 ka for explosive eruptions and 92 ka for extrusive eruptions, while *Wilson et al.* (2008) suggest a figure of roughly 100 ka based on explosive eruptions in the TVZ. The youngest zircons, therefore, provide a closer approximation for the eruption age. Here, eruption ages are estimated from the weighted mean ages of only the youngest (typically ~10) viable ages. This method was used successfully at Kawerau Geothermal Field where ^{40}Ar/^{39}Ar dates were also available for comparison (*Milicich et al.,* 2013). Results are presented below in order of decreasing age, firstly from Ngatamariki followed by the Rotokawa sample.

Table 2.3: Summary of the age data for samples from the Tahorakuri Formation.

Sample	Number of analyses		Comm. Pb cut-off (%)	Youngest age determinations				Number of spots
	Total	Viable		Age (Ma)	2 s.d.	MWSD	Prob.	
NM2-01	33	30	20	1.88	0.03	1.16	0.30	16
NM5-01	31	30	40	0.92	0.06	0.66	0.68	7
NM11-01	41	21	30	0.87	0.03	0.97	0.46	10
NM3-01	37	36	30	0.80	0.03	0.51	0.68	4
NM3-02	20	19	50	0.70	0.04	1.04	0.41	12
RK6-01	33	27	10	1.89	0.02	0.82	0.63	13

2.7.1.1 NM2-01 (2254.7-2255.2 mRF)

A total of 33 grains were analysed from this sample, 3 of which have >20 % of ^{206}Pb attributable to common Pb and were excluded from the data set. The age distribution is bimodal, with a pdf peak at 1.93 Ma (Figure 2.5). The weighted mean of the 16 viable ages in the younger mode is 1.88 ± 0.03 Ma, which is considered to be the best estimate for the eruption age of this unit. This is significantly older than any published dates for silicic rocks originating from the TVZ. Although it is similar in age to the core sample from nearby NM8A dated at 1.85 ± 0.06 Ma (*Chambefort et al.*, in prep), petrographic characteristics suggest they may be separate units, with distinctive large quartz phenocrysts and relict biotite in NM2-01. The lateral extent of this unit is unknown as it has not been recognised in other wells, while the vertical extent is also unknown due to complete loss of cuttings during drilling. However, pyroclastic deposits do extend ~550 m deeper in NM8A (*Lewis et al.*, 2012a).

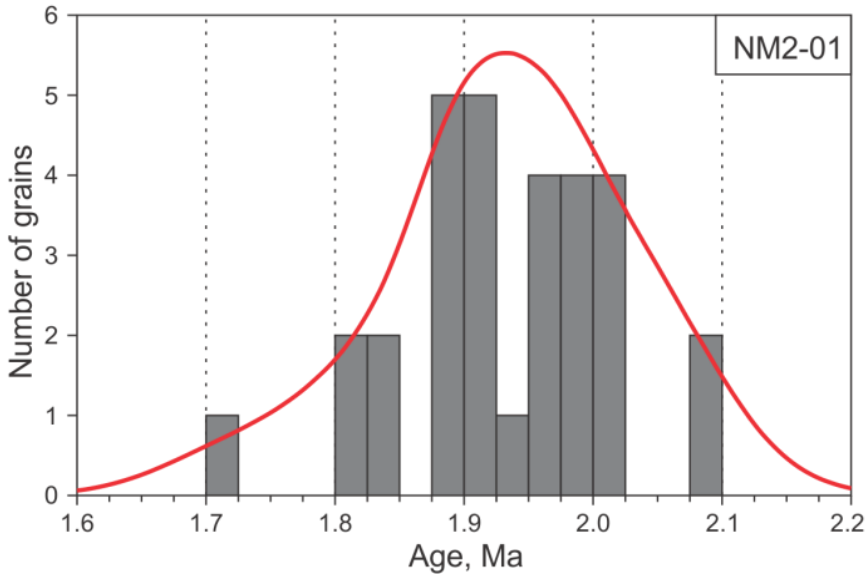

Figure 2.5: Histogram and probability density curve (created using Isoplot: *Ludwig*, 2011) for zircons from sample NM2-01.

2.7.1.2 NM5-01 (1775-1778 mRF)

This sample produced 30 viable analyses containing <40 % of ^{206}Pb attributable to common Pb. It shows a weakly bimodal age distribution, with a pdf peak at ~1.07 Ma (Figure 2.6). The weighted mean for the 7 grains in the younger mode is 0.92 ± 0.06, which is considered to be the best estimate for the eruption age of this deposit. Comparisons were made with other ignimbrites from the TVZ for which U-Pb zircon data is available (Table 2.4), but correlation based solely on this age data is difficult as there are a number of ignimbrites of similar age. The Kidnappers ignimbrite has a pdf peak at around 1.11 Ma, but lacks the younger mode observed in the NM5-01 age distribution (*Wilson et al.,* 2008). The Akatarewa ignimbrite, which is only encountered in geothermal wells, has younger pdf peaks at 1.02 and 1.00 Ma at Orakei Korako and Te Kopia respectively (*Wilson et al.,* 2010). However, both data sets show a weakly bimodal distribution (Figure 2.6), and the estimated eruption age of 0.95 ± 0.05 Ma is similar to the eruption age estimated here.

Further, the ignimbrites of a similar age that are exposed at the surface can be eliminated as likely correlatives due to petrographic characteristics, while some, such as the Marshall and Tikorangi ignimbrites, also appear to have limited distributions (*Wilson,* 1986; *Hildyard et al.,* 2000). The 0.95 Ma Marshall ignimbrites (*Houghton et al.,* 1995) are crystal-poor with only trace amounts of quartz and no amphibole, and are only exposed in the Mangakino area (*Martin,* 1961; *Wilson,* 1986). The 0.89 Ma Tikorangi ignimbrite (*Houghton et al.,* 1995) meanwhile is quartz-free, and is restricted to limited exposures in the Matahana Basin to the NW of the Kapenga Caldera (*Hildyard et al.,* 2000). The 1.00 Ma Rocky Hill ignimbrite (*Houghton et al.,* 1995) is notable for the unusual abundance of amphibole and the presence of biotite (*Martin,* 1961; *Blank,* 1965; *Schipper,* 2004), while the 1.01 Ma Kidnappers ignimbrite (*Wilson et al.,* 2009) is crystal-poor, and contains biotite with only trace amounts of quartz (*Schipper,* 2004). The mineralogy and appearance of NM5-01 is most similar to the Akatarewa ignimbrite. This is described as a welded ignimbrite with a crystal content of 20-25% consisting of plagioclase, quartz, and completely altered ferromagnesian minerals, most likely amphibole based on shape (*Grindley,* 1965b; *Bignall et al.,* 1996). Due to the similarity of the mineralogy and the zircon age distribution, NM5-01 is most likely the Akatarewa ignimbrite.

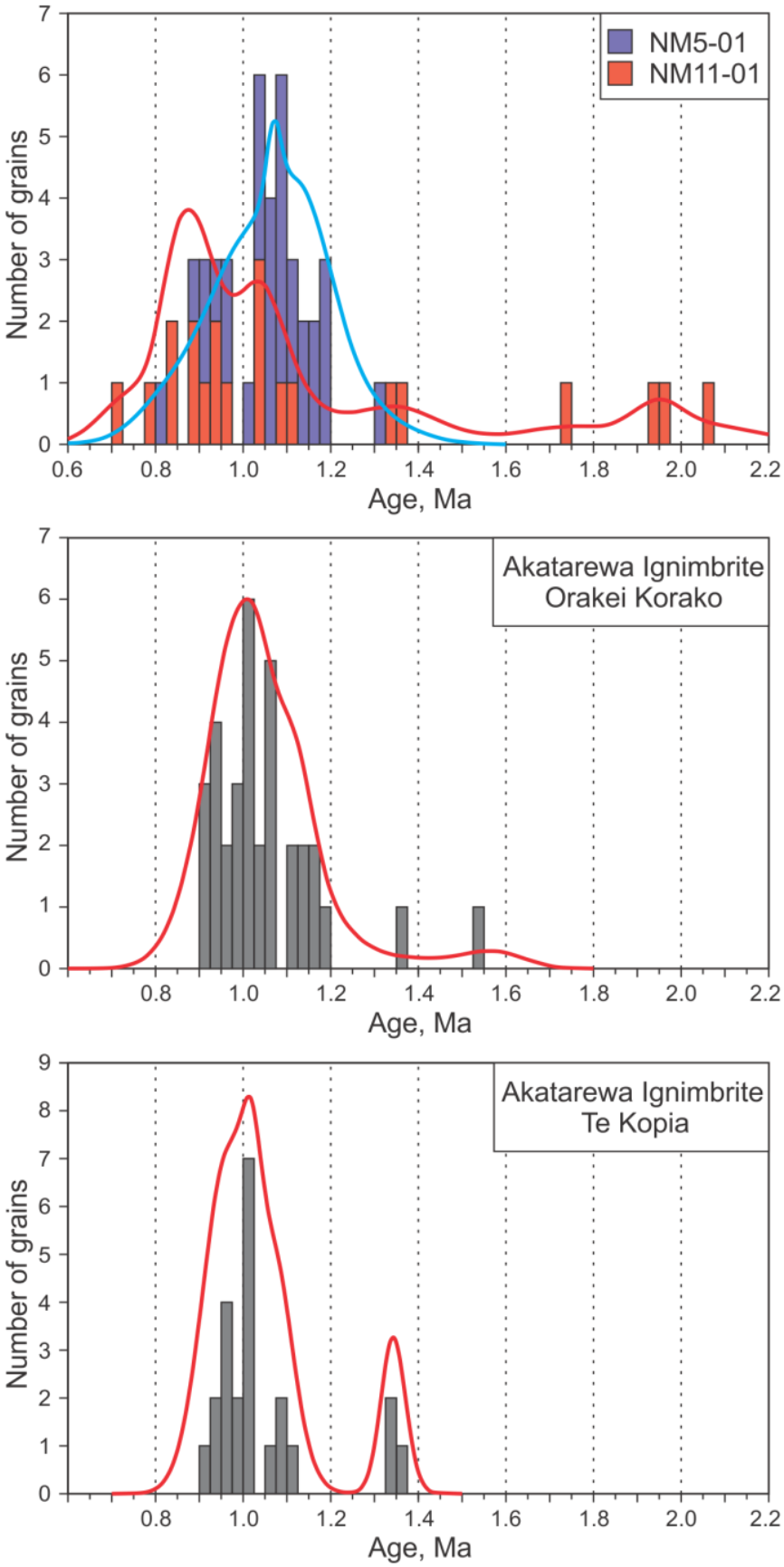

Figure 2.6: Histogram and probability density curve (created using Isoplot: *Ludwig*, 2011) for zircons from samples NM5-01 and NM11-01, as well as the Akatarewa ignimbrite from Orakei Korako and Te Kopia (from *Wilson et al.*, 2010). All samples show a weakly bimodal age distribution.

Table 2.4: Summary of sample ages and possible correlative ignimbrites.

Sample	Age (Ma)	Possible correlatives			
		Name	Age (Ma)	Comments	Refs
NM2-01	1.88 ± 0.03	No known correlatives			
NM5-01	0.92 ± 0.06	Akatarewa ignimbrite	0.95 ± 0.05	Similar appearance and zircon age spectra	1, 2, 3
		Kidnappers ignimbrite	1.01 ± 0.01	Older eruption age, differing mineralogy	4, 5
		Rocky Hill ignimbrite	1.00 ± 0.05	Older eruption age, differing mineralogy	5, 6
		Marshall ignimbrites	0.95 ± 0.03	Differing mineralogy, limited distribution	6, 7, 8
		Tikorangi ignimbrite	0.89 ± 0.04	Differing mineralogy, limited distribution	6, 9
NM11-01	0.87 ± 0.03	As for NM5-01			
NM3-01	0.81 ± 0.03	Waiotapu ignimbrite	0.71 ± 0.06	Older eruption age, differing mineralogy	6, 10
		Rahopaka ignimbrite	0.77 ± 0.03	Differing mineralogy, limited distribution	6, 11
NM3-02	0.70 ± 0.04	Waiotapu ignimbrite	0.71 ± 0.06	Similar appearance, differing age spectra	1, 6
RK6-01	1.89 ± 0.03	No known correlatives			

References are: 1, *Wilson et al.* (2010); 2, *Grindley* (1965b); 3, *Bignall et al.* (1996); 4, *Wilson et al.* (2009); 5, *Schipper* (2004); 6, *Houghton et al.* (1995); 7, *Martin* (1961); 8, *Wilson* (1986); 9, *Hildyard et al.* (2000); 10, *Ritchie* (1996); 11, *Murphy and Seward* (1981).

2.7.1.3 NM11-01 (2083-2089.9 mRF)

Zircons from this sample generally have low U concentrations, resulting in low count rates, and often have high common Pb values. In order to reduce the uncertainty resulting from this, only grains with >180 ppm U and <30% of ^{206}Pb attributable to common Pb have been considered here. The 21 grains that meet these specifications have a bimodal age distribution, with small peaks resulting from inheritance back to ~2 Ma (Figure 2.6). The average of the 10 grains in the youngest mode is 0.87 ± 0.03 Ma, which is considered to be the best estimate of the eruption age of this deposit.

This age is slightly younger than that of NM5-01, despite this deposit being deeper. However, the ages do overlap within uncertainties, and both have a bimodal age distribution spanning the 1 Ma mark. The simplest interpretation is that both samples are from the same unit, and probably correlate with the Akatarewa ignimbrite. Petrographically they are similar, with common flattened pumice and lithics, although NM11-01 lacks the large embayed quartz phenocrysts observed in NM5-01. This variation can also be observed in the Akatarewa ignimbrite at Orakei Korako, and NM11-01 is considered likely to be part of this unit.

2.7.1.4 *NM3-01 (1495.7-1497.7 mRF)*

Of the 37 grains analysed, one contained >30 % of ^{206}Pb attributable to common Pb and was excluded from the data set. This unit has a very mixed population of zircon ages,

with pdf peaks at ~0.80, 0.99, 1.06 and 1.89 Ma, although the majority of grains contribute to the peaks at around 1 Ma (Figure 2.7). The average of the 4 grains that make up the youngest peak is 0.81 ± 0.03 Ma, which is considered the best estimate for the age of this deposit. The youngest pdf peak is similar in age to that of the Waiotapu ignimbrite, which has a zircon pdf peak at ~0.79 Ma (*Wilson et al.*, 2010). However, the Waiotapu ignimbrite has a homogenous zircon age population (*Wilson et al.*, 2010), while the eruption age of 0.71 ± 0.06 Ma is significantly younger than that estimated here (*Houghton et al.*, 1995). In addition, it is a strongly welded, crystal- and quartz-poor ignimbrite with highly attenuated pumice (*Ritchie*, 1996). In comparison, NM3-01 contains no obvious welding textures and has a moderate crystal content including quartz. The 0.77 ± 0.03 Ma Rahopaka ignimbrite (*Houghton et al.*, 1995) is similar in age, but is described as a hornblende-rich ignimbrite with a restricted distribution close to its proposed Kapenga Caldera source (*Murphy and Seward*, 1981), making a correlation with this doubtful.

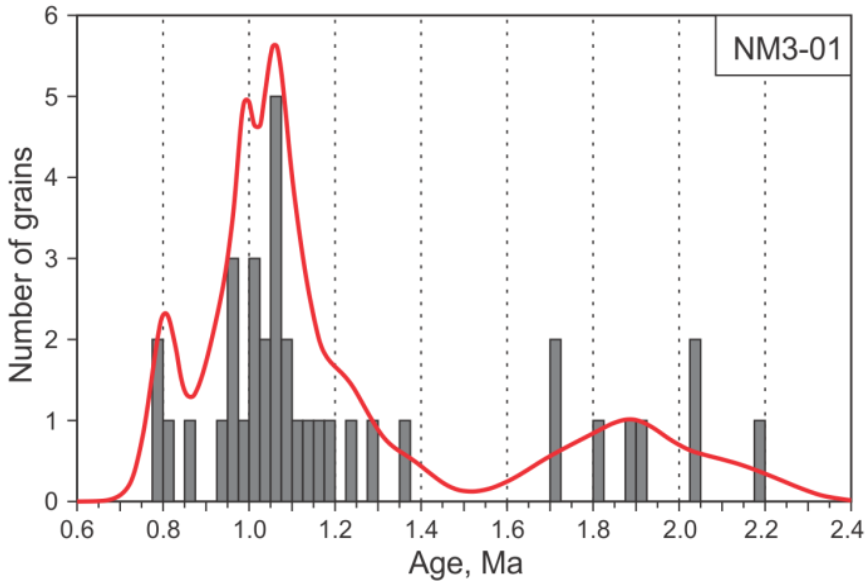

Figure 2.7: Histogram and probability density curve (created using Isoplot: *Ludwig*, 2011) for zircons from sample NM3-01.

The mixed zircon population highlights the possibility that this might not be a primary unit, and instead might be a secondary (re-sedimented) volcaniclastic deposit that has incorporated material from numerous older units. For example, the peaks at around 1 Ma are similar in age to the Akatarewa ignimbrite dated in NM5, while the peak at ~1.9 Ma is similar to the oldest units dated here. Close to 90% of the zircons analysed appear to be related to inheritance from these older deposits, which would likely have been exposed over a wide area

at the time of deposition. The presence of lithics contaminating the sample may also explain the older populations; however, care was taken to remove any obvious lithic fragments prior to crushing for zircon sampling. In addition, this sample was more zircon-rich than other samples analysed here, and it seems unlikely that the relatively small amount of lithics from these older deposits would be able to contribute the amount of zircons observed. Therefore, the fine-grained groundmass likely contains a large population of inherited zircons, such as might be expected in a secondary volcaniclastic deposit. As this sample is intensely altered, primary textures are poorly preserved. *Wood* (1986a) highlighted lenticular patches of altered pumice in suggesting the unit is an ignimbrite. However, the altered pumice observed within the sample dated here were not significantly elongate, and may simply represent the secondary sedimentation of non-spherical pumice clasts.

2.7.1.5 *NM3-02 (1246-1248 mRF)*

This sample is particularly zircon-poor compared to the other samples presented here, and as a result only a relatively small number of suitable grains were available for analysis. Only 19 viable ages with <50% of ^{206}Pb attributable to common Pb were obtained. There is a dominant pdf peak at 0.7 Ma, with an older peak at ~1.2 Ma attributed to inheritance (Figure 2.8). A single anomalously young grain at 0.4 Ma may be the result of contamination from sample preparation. The 12 grains in the dominant peak have a weighted mean age of 0.70 ± 0.04 Ma, which is considered the best estimate for the age of this unit.

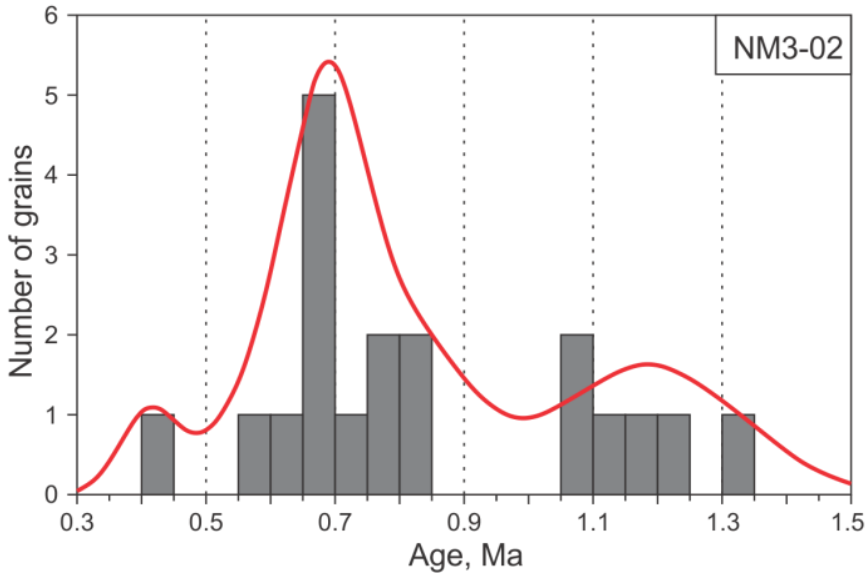

Figure 2.8: Histogram and probability density curve (created using Isoplot: *Ludwig*, 2011) for zircons from sample NM3-02.

The Waiotapu ignimbrite is the only ignimbrite of similar age that outcrops in the TVZ. Both are strongly welded ignimbrites with low crystal contents, and it is possible NM3-02 correlates to the Waiotapu ignimbrite. However, the zircon age data presented by *Wilson et al.* (2010) for the Waiotapu ignimbrite at Waiotapu Geothermal Field is somewhat older, with a pdf peak at 0.79 Ma, almost 100 ka older than the pdf peak for NM3-02. The Waiotapu ignimbrite also has a narrow spectrum of dates, whereas NM3-02 has significant inheritance of zircons from ~1.0-1.3 Ma. On this basis a correlation to the Waiotapu ignimbrite is uncertain, and this may be a unit not exposed at the surface.

2.7.1.6 *RK6-01 (1612-1614 mRF)*

This sample provided 27 viable analyses with <10 % of ^{206}Pb attributable to common Pb. It has a weakly bimodal age distribution, with peaks shortly after 1.9 Ma and shortly before 2.0 Ma (Figure 2.9). The weighted mean age for the 13 grains that form the younger mode is 1.89 ± 0.03 Ma, and this is considered the best estimate for the eruption age of this deposit. This sample is similar in age to both NM2-01 and a sample from NM8A presented by *Chambefort et al.* (in prep). However, petrographically the samples are very different, and it is considered unlikely that they represent the same unit. Quartz is common in the oldest units at Ngatamariki, but appears absent entirely in this unit, indicating multiple ignimbrites of a similar age may be present at Ngatamariki and Rotokawa.

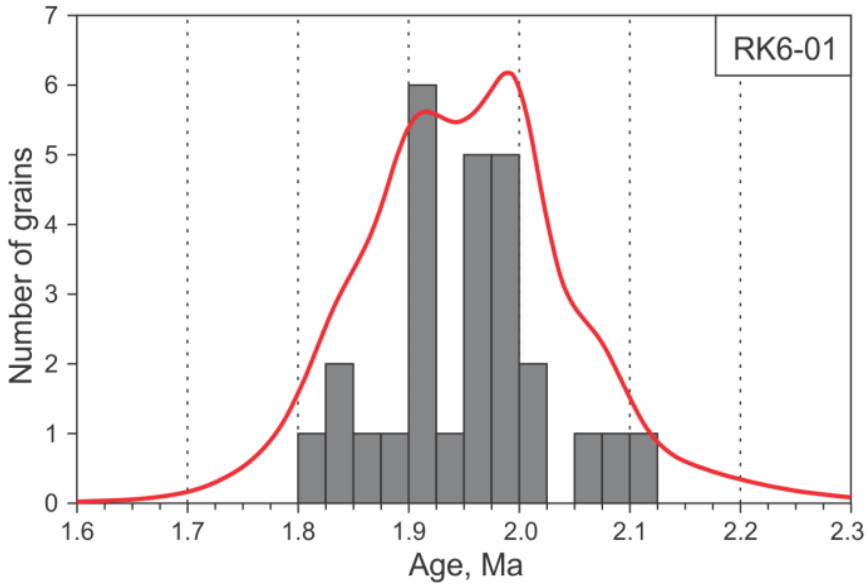

Figure 2.9: Histogram and probability density curve (created using Isoplot: *Ludwig*, 2011) for zircons from sample RK6-01.

2.7.2 Early (Pre-Whakamaru) central TVZ volcanism

The age data presented here for units within the Tahorakuri Formation include the oldest published dates for silicic rocks from within the central TVZ. Samples from Ngatamariki and Rotokawa have ages of 1.88 ± 0.03 and 1.89 ± 0.03 Ma respectively. This is significantly older than the 1.60 ± 0.09 Ma age reported by *Soengkono et al.* (1992), the oldest date published for an exposed silicic unit originating from the TVZ (excluding the age of 1.68 Ma for Ignimbrite C by *Houghton et al.* (1995) as this is thought to be younger based on stratigraphic constraints). Another age determination of 1.85 ± 0.06 Ma presented by *Chambefort et al.* (in prep) indicates vigorous silicic volcanism during this period. All 3 of these ignimbrites appear to be different based on petrographic observations; however, it is important to note that multiple magma types may be erupted during a single event. For example, within the Whakamaru-group, 5 distinct magma types have been recognised, including 3 related rhyolitic magmas and a completely unrelated rhyolitic magma (*Brown et al.,* 1998). This can result in varying mineralogy within a single deposit. On the other hand, it has been widely noted that within the TVZ there is often a clustering of closely spaced eruptions followed by periods with little activity (*Houghton et al.,* 1995; *Gravley et al.,* 2007; *Wilson et al.,* 2009).

The source of these ignimbrites is uncertain, primarily because of the problems with quantifying their thicknesses, as discussed earlier in this paper. However, the samples presented here suggest a central TVZ source, possibly close to Ngatamariki and Rotokawa. The oldest ages obtained here are similar in age to the youngest CVZ deposits. The Upper Papamoa ignimbrite has previously been dated at 1.90 ± 0.10 Ma (*Briggs et al.,* 2005); but this has restricted distribution close to its inferred source, the Tauranga Volcanic Centre (Figure 2.1). This suggests a correlation with ignimbrites at Ngatamariki and Rotokawa (>80 km away) is unlikely. The Waiteariki ignimbrite from the Kaimai Volcanic Centre is more widespread, but is also somewhat older at 2.09 ± 0.03 Ma (*Briggs et al.,* 2005). It is therefore considered unlikely that the ignimbrites at Ngatamariki and Rotokawa originated from either of these volcanic centres in the southern CVZ.

It is also possible that they originated to the west of the currently active TVZ in the ‘old TVZ’ (*Wilson et al.,* 1995a). Indeed, ignimbrites originating from Mangakino are preserved at depth within some geothermal fields of the TVZ (*Wilson et al.,* 2010). However, these have particularly widespread distributions and are exposed widely today (i.e.,

Kidnappers and Ongatiti ignimbrites; *Wilson,* 1986; *Wilson et al.,* 1995b). The oldest exposed ignimbrites surrounding Mangakino are somewhat limited in their distribution, and overlie the basement and Cenozoic sedimentary rocks (*Leonard et al.,* 2010). No ~1.9 Ma ignimbrites from Mangakino have been recognised, and the presence of the younger ignimbrites overlying old sediments suggests it is unlikely there were any ignimbrites of this age originating from Mangakino.

There is no inheritance of zircons at ~1.6 Ma in any of the younger samples presented here (Figures 2.6-2.8), indicating that the earliest phase of activity from Mangakino was not important in the volcanic sedimentation at Ngatamariki. In contrast, there is a small but significant amount of inheritance at ~1.9 Ma (Figures 2.6 and 2.7). No zircons of this age were analysed in the whole rock samples of four Mangakino ignimbrites dated by *McCormack et al.* (2009). There is also no zircon inheritance of this age in subsurface deposits originating from Mangakino that were dated at Waiotapu and Mangakino geothermal fields, although a fresh pumice clast from the Ongatiti ignimbrite yielded one zircon age at ~1.9 Ma (*Wilson et al.,* 2008; *Wilson et al.,* 2010). The almost complete lack of inheritance of old zircons in the Mangakino eruptives suggest it is unlikely that Mangakino was active at ~1.9 Ma, and a source further east in the TVZ (i.e., the 'young TVZ') is considered most likely for these deposits.

These ages also provide age constraints on the Rotokawa Andesite. Based on geochemical characteristics, it is likely the andesite encountered in the southern Ngatamariki wells is the northern continuation of the Rotokawa Andesite (*Anderson,* 2011). The andesite directly overlies the greywacke basement, and must have formed a sizeable composite cone volcano, with a known thickness of up to 2100 m (*Rae,* 2007). *Anderson* (2011) considered the volcano to be centred along the western margin of Rotokawa Geothermal Field based on known thicknesses. If this is the case, the minimum estimate of the radius of the volcano is ~7 km based on the distance to the furthest known occurrences at Ngatamariki. In comparison, the largest cone volcano in the TVZ, Ruapehu, rises ~1700 m above the surrounding ring plain and has a radius of ~7-10 km. Although the size of the Rotokawa Andesite is not well constrained, it is clearly a large structure. It must have formed prior to 1.89 Ma, making it one of the oldest known andesite cones in the TVZ. Tongariro and Ruapehu have been active for at least the last 275 ka and 205 ka respectively, indicating the longevity of these large andesitic volcanoes (*Hobden et al.,* 1996; *Gamble et al.,* 2003). A period of rifting and

subsidence must also have preceded the silicic eruptions (see section 2.7.5), suggesting the Rotokawa volcano likely started forming prior to 2 Ma.

The only unit encountered at Ngatamariki that can be positively correlated with a previously known central TVZ ignimbrite is the Akatarewa ignimbrite. It is present across Ngatamariki, with the zircon age spectra of NM5-01 similar to those from Orakei Korako and Te Kopia. Although the NM11-01 data is not as clear, the stratigraphic position, mineralogy and age data suggest this is the Akatarewa ignimbrite. *Grindley* (1970) suggested the Akatarewa ignimbrite is also present at Ohaaki-Broadlands geothermal field, and it has been identified at Wairakei based on geochemical similarities (*Bignall et al.,* 1996). Despite the uncertainty of the correlations further afield, it is clearly a regionally widespread unit, with a maximum thickness of >400 m at Orakei Korako (*Bignall,* 1991). As the Akatarewa ignimbrite has not been identified to the north at Waiotapu, it seems likely it originated from a volcanic centre in the southern part of the central TVZ that was active in the period shortly after 1 Ma.

The relatively crystal-rich, quartz-bearing, Akatarewa ignimbrite contrasts with the overlying deposits that are generally crystal-poor with very rare or absent quartz. Sample NM3-01, dated at 0.81 ± 0.03 Ma, was previously described as a primary volcanic ignimbrite (*Wood,* 1986a), but the zircon age distribution suggests it may be a re-sedimented deposit. If so, much of the upper Tahorakuri Formation pyroclastic succession must be of uncertain origin as alteration has generally destroyed the primary textures. However, near the top of the pyroclastic succession, welded ignimbrites can be recognised in many of the wells. They are crystal-poor, with very rare or no quartz, but any correlations are uncertain. Dated at 0.70 ± 0.04 Ma in NM3, this seems to represent the last major phase of volcanic activity at Ngatamariki prior to the Whakamaru eruptions at ~350 ka (*Leonard et al.,* 2010).

The lacustrine sediments of the Tahorakuri Formation sedimentary succession lead to the suggestion that they formed in a Tahorakuri caldera lake (*Powell et al.,* 2011). However, age data presented here shows the Tahorakuri Formation formed over a long period of time (>1 Ma), and there is little evidence for thick intracaldera fill such as that found within the Mangakino Caldera (*Wilson et al.,* 2008). While most lakes in the TVZ today are associated with calderas, the sediments at Ngatamariki were deposited during a prolonged period with little volcanic activity in the TVZ (*Houghton et al.,* 1995; *Carter et al.,* 2003, 2004; *Allan et*

al., 2008). If rifting, and therefore subsidence, continued throughout this period, topographic lows where lakes can form would be the logical result.

2.7.3 Transition from andesitic to rhyolitic volcanism

Previously the oldest dated andesitic volcanism attributed to the TVZ was found along the western margin at ~2 Ma (*Wilson et al.*, 1995a; Figure 2.1). The offshore continuation of the TVZ, the Kermadec Arc, was probably also active by ~2 Ma (*Ballance et al.*, 1999). Here we provide age constraints on the Rotokawa Andesite that suggests andesitic volcanism was also occurring within TVZ prior to 1.9 Ma. This contradicts the proposal that andesitic arc volcanism has migrated progressively eastwards across the CVR over the last ~4 Ma (e.g., *Stern*, 1987), as andesite in the central and eastern TVZ should be considerably younger.

Early activity in the central TVZ was dominantly andesitic in composition, but has become dominantly rhyolitic with time. This transition from andesitic volcanism to more silicic volcanism as the system matures is recognised in many arc systems in New Zealand and worldwide (*Adams et al.*, 1994; *Grunder et al.*, 2006; *Lipman et al.*, 2007). *Deering et al.* (2011) highlight an acceleration of rifting at ~0.9 Ma (see also *Wilson et al.*, 1995a) as the cause of this transition in the central TVZ, with a progressive transition in composition until ~0.7 Ma when rhyolite became dominant. However, the results presented here suggest rhyolite may have become the dominant composition earlier than proposed by Deering et al. (2011). Significant silicic volcanism occurred following the initial andesitic volcanism, and has dominated the depositional record at Ngatamariki since ~1.9 Ma.

2.7.4 Clustering of eruptions

Two of the largest eruptions in the history of the TVZ, the Kidnappers and Rocky Hill ignimbrites, occurred in quick succession from Mangakino at around 1 Ma (*Wilson et al.*, 2009). This was followed by the Akatarewa ignimbrite and the Marshall ignimbrites over the next ~50-100 ka. This was closely followed by more activity at 0.89 Ma, most likely from a completely different source at Kapenga (*Houghton et al.*, 1995). It was, therefore, a very active period in the history of the TVZ, with activity from multiple sources both within and outside the currently active TVZ.

Clustering of ignimbrite-forming eruptions in the TVZ has previously been recognised by a number of authors (e.g. *Houghton et al.*, 1995; *Gravley et al.*, 2007; *Wilson et al.*, 2009). The most notable 'flare-up' was at 340-240 ka, where 7 caldera forming eruptions evacuated >3,000 km^3 of silicic magma (*Wilson et al.*, 2009; *Gravley et al.*, in prep). In some cases ignimbrite-forming eruptions from different caldera sources occurred no more than weeks to months apart (*Nairn and Kohn*, 1973; *Gravley et al.*, 2007), and *Gravley et al.* (2007) highlight enhanced rifting as the likely cause. The relationship between regional tectonics and volcanism has been well documented, both within TVZ and internationally (*Gravley et al.*, 2007 and references therein; *Wilson et al.*, 2009). Stress changes associated with enhanced rifting are likely to control volcanic eruptions, and the clustering of events from multiple sources at ~1 Ma may indicate a period of enhanced rifting within the TVZ at this time. The period from 1.89 to 1.85 Ma also appears to be a period of increased silicic volcanism (3 ages presented here and by *Chambefort et al.*, in prep) that may include multiple units. This possible clustering of events seems to mark the initial phase of silicic deposition at Ngatamariki and Rotokawa, and may be related to the onset of rifting within the TVZ.

2.7.5 Subsidence rates and rifting in the TVZ

The link between rifting and volcanism can be further explored by looking at long-term subsidence rates. First-order estimates of subsidence rates can be made by comparing the depths of dated units (e.g., *Wilson et al.*, 2010). If the current ground surface is taken as a datum, subsidence rates are given by the thickness of the material separating 2 units divided by the time between them. At Ngatamariki, this is complicated by the fact that thicknesses of the dated units below the Whakamaru-group ignimbrites are often uncertain due to a combination of poor cuttings recovery, the similarity of the deposits and the extremely fine-grained nature of cuttings at depth. This creates added uncertainty in the subsidence rates over the short term, but over a longer-term the subsidence rates are more accurate.

All wells where dating has been conducted at Ngatamariki show subsidence rates of 1-2 mm/yr (Figure 2.10). These rates do not appear to have changed significantly over time, although there is a slight increase in the subsidence rate in all wells following the Whakamaru-group ignimbrites. However, it is different in RK6 at Rotokawa, where there is a large increase in the subsidence rate from 0.2 mm/yr to 2.8 mm/yr following the eruption of the Whakamaru-group ignimbrites. One possibility is that the current correlation of the

Wairakei ignimbrite to the Whakamaru-group ignimbrites at Rotokawa is incorrect. Wairakei ignimbrite has never been dated here, but the similar distinctive mineralogy and features of the deposit to the Whakamaru-group ignimbrites (*Chambefort et al.*, in prep) support this correlation. If so, the change represents a much higher rate of subsidence at Rotokawa.

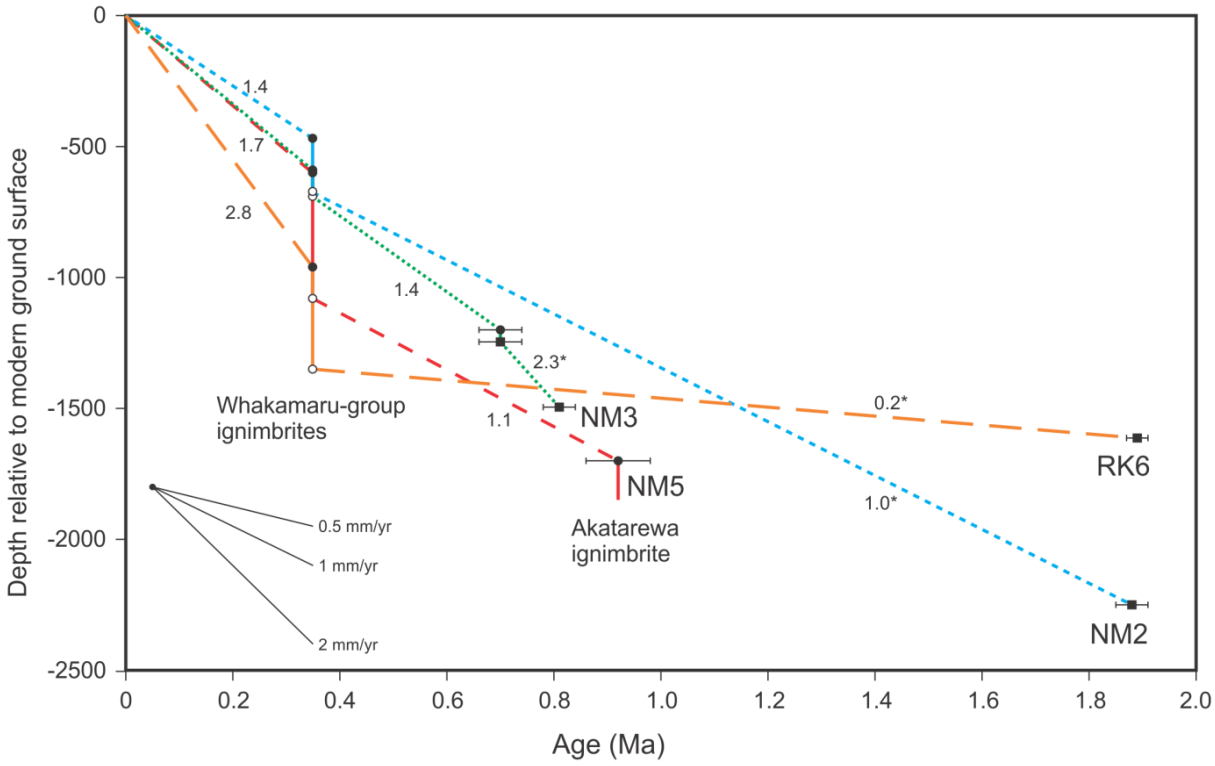

Figure 2.10: Plot showing the depth of stratigraphic units relative to their age for wells at Ngatamariki and Rotokawa. The age for the Whakamaru-group ignimbrites is from *Leonard et al.* (2010); all other ages are reported in this paper and are shown with their 2 s.d. uncertainties. Open circles represent the bottom of a deposit, closed circles represent the top of a deposit, and squares represent cores dated where the extent of the deposits are unknown. Lines connecting the deposits represent estimated subsidence rates, which are shown in mm/yr. Those marked with a * are the maximum possible rate due to the unknown extent of the deposits. Over the long term these rates are considered close approximations (e.g., NM2 and RK6), but over the short term the rate is less accurate (e.g., NM3).

As subsidence is indicative of rifting, this data provides insight into rifting in the TVZ. *Wilson et al.* (1995a) suggest that rifting of the TVZ may be restricted to the last ~0.9 Ma, or if it was rifting prior to this, that the rate has increased with time. This is based partly on the observations that deformation associated with rifting has been confined to the currently active TVZ over the last 0.9 Ma and evidence for major tectonic activity over large parts of the North Island between ~1 Ma and 0.34 Ma. Geodetically determined extension rates were also believed to have been capable of producing the thinned crust of the TVZ over that time period. By restoring the thinned crust of the TVZ to the same thickness as that proposed for

the crust NW of the TVZ, *Wilson et al*. (1995a) calculated that the TVZ has widened by 11-14 km as a result of rifting. Assuming this has been confined to the last 0.9 Ma, average extension rates would be 12-16 mm/yr. The geodetically determined extension rate highlighted by *Wilson et al.* (1995a) of 18 mm/yr (*Darby and Williams,* 1991) would suggest that this is a likely scenario; however, this rate has subsequently been re-examined, resulting in a rate now determined to be only 8 mm/yr (*Darby et al.,* 2000). *Villamor and Berryman* (2001) also determined an extension rate of 6.4 mm/yr at seismogenic depths based on fault slip rates. Assuming these rates represent a long-term average of the extension rates in the TVZ, a longer period of rifting would clearly be necessary to account for these slower rates in the method used by *Wilson et al.* (1995a).

If we assume that rifting has accompanied volcanism throughout the ~2 Ma history of activity in the TVZ, as it is important to establish the silicic magmatic system prior to the ~1.9 Ma ignimbrite eruptions (*Price et al.,* 2005), average subsidence rates would be ~1.5 mm/yr based on an average volcaniclastic thickness of 3 km. Although crude in approach, this gives a rate similar to those observed at Ngatamariki. While maximum observed subsidence rates of 3-4 mm/yr (*Villamor and Berryman,* 2001; *Lamarche et al.,* 2006; *Begg and Mouslopoulou,* 2010) could account for this subsidence over a shorter period of time, long-term rates observed here and within other geothermal fields suggest it is unlikely maximum rates would continue long-term in any given area (e.g., *Wilson et al.,* 2010; *Milicich et al.,* 2013).

In Ngatamariki well NM2, it is not certain how thick the pyroclastic deposits are below the 1.88 Ma dated sample, but similar pyroclastic deposits extend down another ~550 m in nearby NM8A (*Lewis et al.,* 2012a). No fault that may have down-dropped the deposits in NM8A has been identified, so a significant amount of material ~1.88 Ma or older must be present. Therefore, it does not simply represent a veneer resting on a topographically high area, but must have been deposited in topographical lows. As discussed earlier in this paper, basins in the TVZ may be the result of volcanic processes (i.e., caldera collapse), tectonic processes, or a combination of these, but all are ultimately linked to rifting. If the early basin development at Ngatamariki is simply the result of tectonic extension, to generate 550 m of subsidence, even at maximum observed rates of ~3.5 mm/yr, would require a period of >150 ka.

In Rotokawa well RK6, ~250 m of the Tahorakuri Formation overlies the Rotokawa Andesite, with ~100 m between the andesite and the core dated at 1.89 Ma. Such significant thicknesses of silicic deposits overlying what was a large volcano again illustrates that subsidence must pre-date 1.9 Ma. Interbedded within the Tahorakuri Formation, as well as overlying it, are the greywacke gravels of the Waikora Formation (*Nairn*, 1985; *Rae*, 2007). These formations do not extend right across Rotokawa, and appear to be infilling a graben or 'rift' structure (*Rae*, 2007; *Powell et al.*, 2011). This was described by *Rae* (2007) as a normal block fault-controlled graben structure that has displaced the andesite and the greywacke basement. Both the Tahorakuri and Waikora formations are thicker within this structure, suggesting it is not simply younger faulting. Although no samples of the Tahorakuri Formation were dated from directly within this structure, the age of 1.89 Ma from nearby RK6 suggests this is a very old feature. An alternative explanation is that this was a canyon (*T Powell*, personal communication, 2013); however, the offset of the andesite on either side of the structure (*Rae*, 2007; *Powell et al.*, 2011) suggests fault displacement, while the NE-SW trend is similar to the overall trend of the TVZ. In order to deposit greywacke within a canyon on an andesite volcano it would require significant subsidence in the first place, and if this were the case, it might be expected to be dominantly filled with andesitic debris instead of greywacke. It is, therefore, most likely an old tectonic structure, and provides further evidence of early rifting.

A model of the proposed variations in subsidence at Ngatamariki and Rotokawa is shown in Figure 2.11. Initial subsidence related to rifting pre-dates 1.9 Ma, creating depositional basins which are filled by pyroclastic deposits, partially burying the Rotokawa Andesite. The rift axis then appears to shift away from Rotokawa, as indicated by the slow subsidence rate between 1.89 Ma and 0.35 Ma in RK6 (Figure 2.10). Subsidence continued at Ngatamariki, with relatively uniform rates until the present day, suggesting the rift axis may have shifted further west towards the modern day rift axis of the TVZ. Minor andesitic volcanism and extensive siliciclastic deposition continued until ~0.7 Ma. Subsidence continued after 0.7 Ma, but rarity of explosive volcanism until ~0.35 Ma (*Houghton et al.* 1995; *Leonard et al.*, 2010), and the resulting paucity of new volcaniclastic input, resulted in the developing basin being filled with lacustrine sediments.

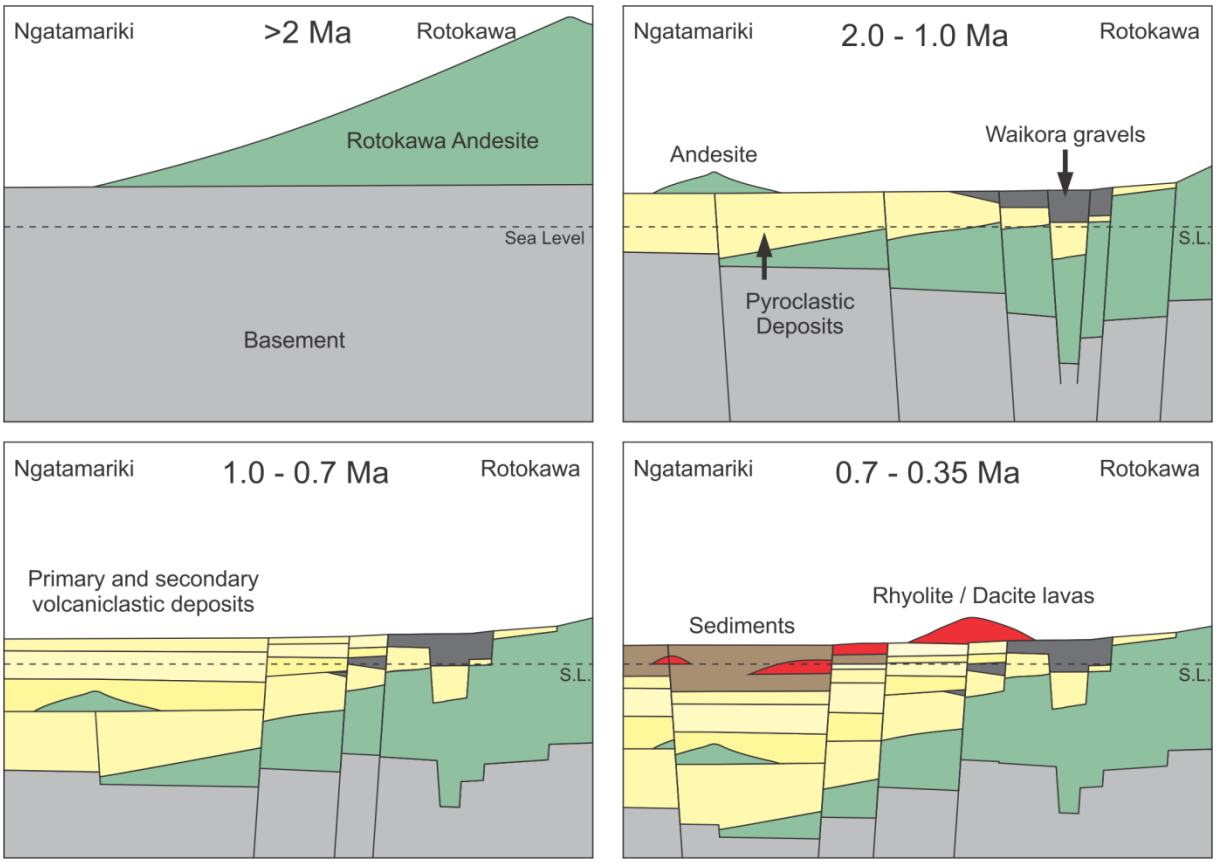

Figure 2.11: Block models illustrating early volcanism and rifting at Ngatamariki and Rotokawa until emplacement of the Whakamaru-group ignimbrites. >2 Ma: the Rotokawa Andesite is erupted. 2.0-1.0 Ma: rifting results in subsidence of the Rotokawa Andesite and graben development followed by deposition of silicic pyroclastic deposits and the Waikora Formation gravels. Minor andesitic volcanism continues at Ngatamariki. 1.0-0.7 Ma: the rifting axis has shifted away from Rotokawa, and subsidence is greatest at Ngatamariki, where primary and secondary volcaniclastic deposits, including the Akatarewa Ignimbrite, are deposited. 0.7-0.35 Ma: no major explosive volcanism occurs during this time, but subsidence continues at Ngatamariki, with the resulting basin filled with lacustrine sediments. Extrusive volcanism, predominantly rhyolitic in composition, continues during this period.

2.7.6 The CVZ – TVZ transition

The transition to the TVZ has generally been considered to be marked by the gap in silicic volcanism between the last activity in CVZ at 1.9 Ma and the earliest phase of activity from Mangakino Caldera starting at ~1.6 Ma (*Houghton et al.*, 1995; *Carter et al.*, 2003, 2004; *Briggs et al.*, 2005; *Allan et al.*, 2008). *Cole and Spinks* (2009) even suggest that activity during this phase may itself be transitional as Mangakino lies outside the current structural boundaries of TVZ. This perceived break in silicic volcanism that marks the transition is in the order of ~300 ka, which is similar in magnitude to some of the gaps within the record for the rocks exposed within TVZ (*Wilson et al.*, 2009), and certainly shorter than

gaps in the CVZ record (*Adams et al.,* 1994; *Carter et al.,* 2003, 2004). This indicates the relative continuity of volcanism through the transition.

The data presented here is important when considering this transition. It suggests that significant silicic volcanism was occurring in central TVZ at ~1.9 Ma, with multiple deposits of similar age. Offshore tephra records may indicate little large-scale activity for a time from ~2 Ma, although activity appears to have resumed as early as ~1.8 Ma in the record from one offshore site (*Carter et al.,* 2004). Tephra layers in the Wanganui Basin also indicate volcanic activity was occurring between 1.7-1.8 Ma (*Shane et al.,* 1996; *Pillans et al.,* 2005). Breaks between volcanic episodes over this period are, therefore, less than 100 ka, further highlighting the relative continuity of volcanism.

The nature and exact timing of the CVZ to TVZ transition is still unclear (see Figure 2.12). Extension in the CVR may have started as early as 4-5 Ma (*Stern,* 1987; *Stern and Davey,* 1987), while offshore the Havre Trough is also thought to have been extending over this time (*Wright,* 1993). In this view, the transition from the more northerly trending CVZ to the NE-SW trending TVZ can be thought of as a long lived process (>2 Ma) of rotation involving extension within the CVR and the opening of the Havre Trough (Figure 2.12A). However, *Wilson et al.*, (1995a) suggest a more rapid transition, with TVZ structural features superimposed over earlier CVZ structures, rather than continuous rotation.

While the data presented here indicates that rifting, and probably also silicic volcanism, was occurring in the central TVZ by ~1.9 Ma, extension was not necessarily in a NW-SE direction. Possible NE-SW trending structures at Rotokawa (e.g., *Rae,* 2007) may indicate the TVZ was tectonically active at that time, while the offshore continuation of the TVZ, the Kermadec Arc, was probably active by ~2 Ma (*Ballance et al.*, 1999). However, *Cole* (1990) has suggested that southward rift extension from CVZ could extend beneath the central TVZ (Figure 2.12B), and this may have been important in generating the early rifting and volcanism observed at Ngatamariki and Rotokawa. The Rotokawa Andesite most likely started forming prior to 2 Ma, as shown by the size of the volcanic structure and the amount of subsidence that preceded the silicic eruptives. Therefore, it seems likely that the southern extent of the CVZ extended to Rotokawa, resulting in early rifting and volcanism within what is now the TVZ (Figure 2.12D).

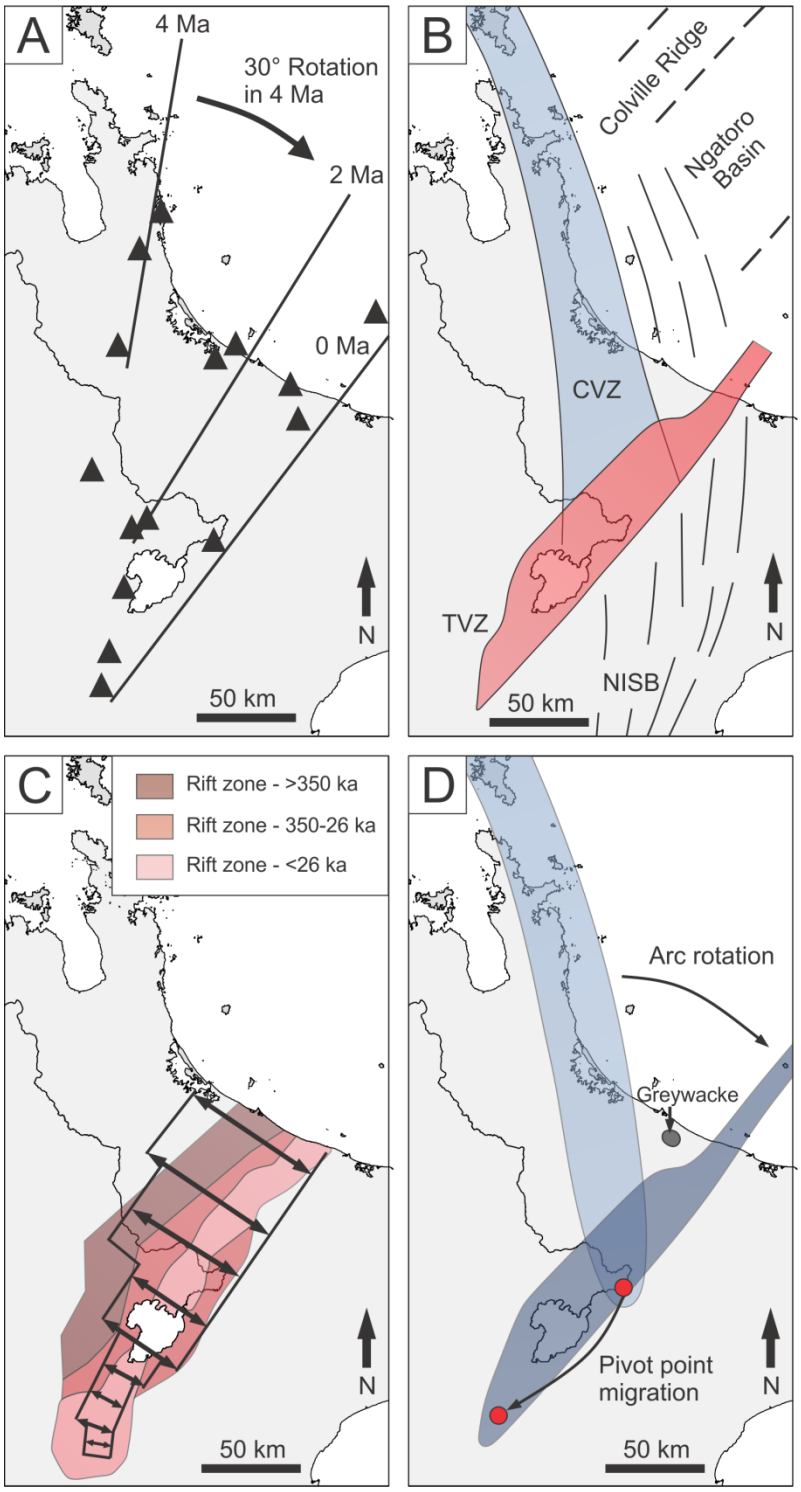

Figure 2.12: Models illustrating the opening of the CVR. (A) The rotating arc model, where the volcanic front has rotated clockwise 30° over the last 4 Ma to the present position near the eastern margin of the TVZ (from *Stratford and Stern*, 2006). (B) The transtension model of *Cole* (1990), in which the rotation of the east coast is the result of dextral shear on the North Island Shear Belt (NISB), with the CVZ extending beneath the TVZ resulting in both NW and NNE fault trends. (C) The step-wise southward propagating rift of *Villamor and Berryman* (2006), where rifting in the TVZ is propagating south in a step-wise fashion, with parallel-sided rift sectors that are extending at different rates. (D) The CVZ pivots around a point as a result of slab-rollback along the obliquely convergent subduction zone. The pivot point also migrates south as a result of the oblique convergence. In this way, the CVZ rapidly re-aligns as the NW-SE trending TVZ, with little rifting in the wedge between the arcs as evidenced by the outcropping of greywacke. See text for discussion.

The evidence presented here for the earliest TVZ volcanism occurring near its eastern boundary, has potential implications for large-scale tectonic reconstruction and invoking of ideas postulated by *Cole* (1990). Collision of the Hikurangi Plateau with the subduction zone to the east of the North Island has resulted in clockwise rotation of the fore-arc region and extension within the arc/back-arc region (*Wallace et al.,* 2004). Rapid slab rollback can significantly enhance this process (*Wallace et al.,* 2009), and this may have been important in the transition from the CVZ to the TVZ. A combination of rollback and rotation would effectively result in the TVZ arc pivoting about a point. At the same time, this pivot point would migrate to the south (Figure 2.12D). This rapid rotation of the volcanic arc as a result of slab rollback can explain early rifting and volcanism at Ngatamariki and Rotokawa. An added consideration is the presence of greywacke outcropping at the surface in the northern CVR (Figure 2.12D), between CVZ and TVZ (*Cole,* 1990), indicating that little rifting took place in this zone, but strongly supporting rifting in central TVZ to the south.

2.8 Conclusions

U-Pb dating of zircons from hydrothermally altered volcanic rocks located within geothermal fields offers insight into the history of volcanism and rifting in the TVZ that is not available from rocks exposed at the surface. It also allows confident correlations between similar units where alteration has destroyed other primary minerals and textures.

1) Samples of the Tahorakuri Formation from Ngatamariki and Rotokawa were dated between 1.89 and 0.70 Ma, highlighting the long time period represented by this formation. There is no evidence of thick intracaldera fill at Ngatamariki, and following ~0.7 Ma, there was a long period with little volcanic activity until the Whakamaru eruptions in which dominantly fine-grained sediments were deposited at Ngatamariki.
2) The Akatarewa ignimbrite is also present at Ngatamariki, with 2 samples similar to the Akatarewa ignimbrite dated at Orakei Korako and Te Kopia. It probably originated from somewhere in the southern part of the central TVZ, and was part of a period of heightened activity in the TVZ at ~1 Ma and shortly after. No deposits that are exposed at the surface were definitively identified at Ngatamariki or Rotokawa.
3) Early volcanic activity within the central TVZ was andesitic, but was not restricted to the western margin, with a large >1.89 Ma andesitic volcano centred at Rotokawa. Significant

silicic volcanism, likely originating from within the currently active TVZ, was underway by 1.89 Ma, and may have rapidly become the dominant composition erupted. Silicic volcanism prior to ~1 Ma was not restricted to the Mangakino Caldera.

4) Rifting of the TVZ also began prior to ~1.89 Ma, as shown by thick accumulations of pyroclastic deposits in a subsiding basin at Ngatamariki and Rotokawa. A structure interpreted to be a block faulted graben is apparent at Rotokawa, and has a similar trend to the TVZ. Significant displacement of the Rotokawa Andesite must predate deposition of the Tahorakuri Formation, which infills the graben along with Waikora Formation gravels.
5) The CVZ might have extended at least as far south into the current TVZ as Rotokawa, which may account for the earliest andesitic volcanism and rifting observed and created conditions favourable for widespread silicic activity by ~1.9 Ma. The transition to the TVZ may have been a product of rapid rotation as a result of slab rollback.

Conclusions

Petrographic examination of the Tahorakuri Formation at Ngatamariki and Rotokawa geothermal fields showed that there are significant variations in the types of lithology present. It is dominated by fine-grained volcaniclastic deposits, and a combination of hydrothermal alteration destroying primary textures and minerals, the generally fine-grained nature of the drill cuttings, the similarity of the deposits, and cuttings losses during drilling make detailed correlations difficult. Therefore, a combination of analytical techniques was used in order to further investigate this formation.

Potassium feldspars in the fine-grained drill cuttings from NM5 were definitively identified as adularia using Raman spectroscopy and electron microprobe analysis. Both methods conclusively showed that no sanidine is present in the cuttings, despite many of the feldspars appearing optically similar to sanidine, a diagnostic mineral in the TVZ. Raman spectroscopy was found to be ideal for analysing a large number of grains quickly. The small spectral peak in adularia at ~140 cm^{-1} was the main peak used for identification purposes as it is absent in sanidine. Where this could not be distinguished, the peak at 162-177 cm^{-1} was used, with a peak of ~176 cm^{-1} being indicative of adularia, and a peak of ~172 or less being indicative of sanidine. Major element data indicates that it is unlikely sanidine ever existed in these deposits, with the potassium-rich compositions of Or^{94-99} being typical of adularia. As unaltered plagioclase is present in the samples, some unaltered sanidine might also be expected if it was originally present, resulting in a greater spread of compositions.

U-Pb dating of zircons shows that the Tahorakuri Formation was emplaced over a long period of more than 1.5 Ma. Primary silicic units range in age from 1.89 ± 0.02 Ma to 0.70 ± 0.04 Ma, with sediments then dominating until ~0.35 Ma. On the basis of the observed stratigraphy and the age data, there is no evidence to suggest that any of the Tahorakuri Formation represents intracaldera fill. Rather, it represents multiple deposits that were likely deposited in a subsiding basin.

It is sometimes uncertain whether core samples represent primary volcanic deposits or secondary deposits that have been re-sedimented due to the destruction of primary textures. The overwhelming abundance of inherited zircons in one unit from NM3 suggests that it may be a re-sedimented deposit, and this may also be the case for some of the similar deposits in the upper part of the formation. However, the majority of the formation appears to be primary

volcanic deposits, and a number of welded ignimbrites can be recognised. Perhaps the most notable of these is the quartz-bearing ignimbrite dated at ~0.9 Ma and correlated with the Akatarewa ignimbrite, as the relatively quartz-rich nature differs from the overlying deposits. It is also the only unit recognised that can be confidently correlated with a known ignimbrite.

The source of the silicic deposits remains uncertain. It seems likely that the Akatarewa ignimbrite originated in the southern part of the central TVZ considering its distribution. Likewise, the welded ignimbrite dated at 0.7 Ma appears to be of limited extent as it has not been identified further afield, although a correlation with the Waiotapu ignimbrite cannot definitively be ruled out. This would also suggest a source in the southern part of the central TVZ is likely. However, it is the source of the oldest deposits that is of most interest, as the oldest deposits known to have originated from the TVZ were erupted 200-300 ka earlier at ~1.6 Ma. Based on the limited distribution of ignimbrites dated at ~1.9 in the southern CVZ, it seems most likely that they originated from somewhere in the TVZ, and possibly within the currently active TVZ. Rifting and silicic volcanism are closely linked processes in the TVZ, and the observations made here that rifting began prior to 1.9 Ma suggest the earliest phase silicic volcanism at Ngatamariki and Rotokawa may also have originated in the currently active TVZ.

Early rifting is shown by the significant thickness of volcaniclastic deposits below the unit dated in NM2, and the presence of thick silicic deposits dated at 1.89 Ma overlying the Rotokawa Andesite. The Rotokawa Andesite must have formed a large composite cone volcano that began forming prior to ~2 Ma, and significant subsidence must have occurred prior to emplacement of the silicic deposits in order to create a low-lying depositional environment. This indicates that rifting within the TVZ was occurring prior to 1.9 Ma. It also shows that early andesitic volcanism was not restricted to the western margin of the TVZ. These observations are consistent with the suggestion that the CVZ extended beneath what is now the TVZ, and the early activity recorded at Ngatamariki and Rotokawa may be related to activity in the older CVZ. Subsidence rates at Ngatamariki appear to be relatively constant at 1-2 mm/yr over the last 1.88 Ma. However, at Rotokawa the variation in subsidence indicates the axis of rifting shifted away from Rotokawa following the early silicic deposits, with rapid subsidence resuming only in the last ~350 ka.

References

Acocella, V., K. Spinks, J. Cole, and A. Nicol (2003), Oblique back arc rifting of Taupo Volcanic zone, New Zealand, *Tectonics*, *22*(4), 1045, doi:10.1029/2002TC001447.

Adams, C. J., I. J. Graham, D. Seward, and D. N. B. Skinner (1994), Geochronological and geochemical evolution of late Cenozoic volcanism in the Coromandel Peninsula, New Zealand, *New Zealand Journal of Geology and Geophysics*, *37*, 359–379, doi:10.1080/00288306.1994.9514626.

Allan, A. S. R., J. A. Baker, L. Carter, and R. J. Wysoczanksi (2008), Reconstructing the Quaternary evolution of the world's most active silicic volcanic system: insights from an ~1.65Ma deep ocean tephra record sourced from Taupo Volcanic Zone, New Zealand, *Quaternary Science Reviews*, *27*(25-26), 2341–2360, doi:10.1016/j.quascirev.2008.09.003.

Anderson, L. C. A. (2011), A comparison of buried andesites at Ngatamariki and Rotokawa geothermal fields, Taupo, M.Sc. thesis, University of Waikato, Hamilton, New Zealand.

Arehart, G. B., B. W. Christenson, C. P. Wood, K. A. Foland, and P. R. L. Browne (2002), Timing of volcanic, plutonic and geothermal activity at Ngatamariki, New Zealand, *Journal of Volcanology and Geothermal Research*, *116*(3-4), 201–214, doi:10.1016/S0377-0273(01)00315-8.

Ballance, P. F., A. G. Ablaev, I. K. Pushchin, S. P. Pletnev, M. G. Birylina, T. Itaya, H. A. Follas, and G. W. Gibson (1999), Morphology and history of the Kermadec trench–arc–backarc basin–remnant arc system at 30 to 32°S : geophysical profile, microfossil and K–Ar data, *Marine Geology*, *159*, 35–62.

Begg, J. G., and V. Mouslopoulou (2010), Analysis of late Holocene faulting within an active rift using lidar, Taupo Rift, New Zealand, *Journal of Volcanology and Geothermal Research*, *190*(1-2), 152–167, doi:10.1016/j.jvolgeores.2009.06.001.

Bibby, H. M., T. G. Caldwell, F. J. Davey, and T. H. Webb (1995), Geophysical evidence on the structure of the Taupo Volcanic Zone and its hydrothermal circulation, *Journal of Volcanology and Geothermal Research*, *68*(1-3), 29–58.

Bignall, G. (1991), Subsurface stratigraphy and structure of the Orakeikorako and Te Kopia geothermal systems, New Zealand, *Proceedings of the 13th New Zealand Geothermal Workshop, University of Auckland*, 199–205.

Bignall, G. (2009), Ngatamariki Geothermal Field geoscience overview, *GNS Science consultancy report 2009/94*, 41p.

Bignall, G., P. R. L. Browne, and P. R. Kyle (1996), Geochemical characterisation of hydrothermally altered ignimbrites in active geothermal fields from the central Taupo Volcanic Zone, New Zealand, *Journal of Volcanology and Geothermal Research*, *73*(1-2), 79–97, doi:10.1016/0377-0273(96)00015-7.

Bignall, G., S. Milicich, L. Ramirez, M. Rosenberg, G. Kilgour, and A. Rae (2010), Geology of the Wairakei-Tauhara Geothermal System, New Zealand, *Proceedings of the World Geothermal Congress, Bali, Indonesia*, (25-29 April 2010).

Blank, H. R. (1965), Ash-flow deposits of the central King Country, New Zealand, *New Zealand Journal of Geology and Geophysics*, *8*, 588–610, doi:10.1080/00288306.1965.10423193.

Boseley, C., W. Cumming, L. Urzúa-Monsalve, T. Powell, and M. Grant (2010), A Resource Conceptual Model for the Ngatamariki Geothermal Field Based on Recent Exploration Well Drilling and 3D MT Resistivity Imaging, in *Proceedings of the World Geothermal Congress, Bali, Indonesia*, (25-29 April 2010).

Briggs, R. M., B. F. Houghton, M. McWilliams, and C. J. N. Wilson (2005), $^{40}Ar/^{39}Ar$ ages of silicic volcanic rocks in the Tauranga-Kaimai area, New Zealand: Dating the transition between volcanism in the Coromandel Arc and the Taupo Volcanic Zone, *New Zealand Journal of Geology and Geophysics*, *48*, 459–469, doi:10.1080/00288306.2005.

Brown, S. J. A. (1994), Geology and geochemistry of the Whakamaru Group ignimbrites, and associated rhyolite domes, Taupo Volcanic Zone, New Zealand, Ph.D. thesis, University of Canterbury, Christchurch, New Zealand.

Brown, S. J. A, C. J. N. Wilson, J. W. Cole, and J. Wooden (1998), The Whakamaru group ignimbrites, Taupo Volcanic Zone, New Zealand: evidence for reverse tapping of a zoned silicic magmatic system, *Journal of volcanology and geothermal research*, *84*, 1–37.

Browne, P. R. L. (1970), Hydrothermal alteration as an aid in investigating geothermal fields, *Geothermics, Special Issue 2,* 564-570.

Browne, P. R. L., and A. J. Ellis (1970), The Ohaki-Broadlands hydrothermal area, New Zealand; mineralogy and related geochemistry, *American Journal of Science*, *269*, 97-131.

Browne, P. R. L., I. J. Graham, R. J. Parker, and C. P. Wood (1992), Subsurface andesite lavas and plutonic rocks in the Rotokawa and Ngatamariki geothermal systems, Taupo Volcanic Zone, New Zealand, *Journal of Volcanology and Geothermal Research*, *51*, 199–215.

Carter, L., P. Shane, B. Alloway, I. R. Hall, S. E. Harris, and J. A. Westgate (2003), Demise of one volcanic zone and birth of another–A 12 my marine record of major rhyolitic eruptions from New Zealand, *Geology*, *31*, 493–496.

Carter, L., B. Alloway, P. Shane, and J. Westgate (2004), Deep-ocean record of major late Cenozoic rhyolitic eruptions from New Zealand, *New Zealand Journal of Geology and Geophysics, 47*, 481–500, doi:10.1080/00288306.2004.9515071.

Chambefort, I., and G. Bignall (2011), Petrographic Review of Stratigraphic Units of the Ngatamariki Geothermal Field, *GNS Science consultancy report 2011/298*, 102p.

Chambefort, I., B. Lewis, G. Bignall, C. J. N. Wilson, A. J. Rae, C. Boseley, and T. R. Ireland (in preparation), Stratigraphy and structure of the Ngatamariki geothermal system: New U-Pb geochrononlogy and its implications for the Taupo Volcanic Zone evolution.

Cole, J. W. (1990), Structural control and origin of volcanism in the Taupo volcanic zone, New Zealand, *Bulletin of volcanology*, *52*, 445–459.

Cole, J. W., and K. D. Spinks (2009), Caldera volcanism and rift structure in the Taupo Volcanic Zone, New Zealand, *Geological Society, London, Special Publications*, *327*, 9–29, doi:10.1144/SP327.2.

Craw, D., P. Upton, and D. J. Mackenzie (2009), Hydrothermal alteration styles in ancient and modern orogenic gold deposits, New Zealand, *New Zealand Journal of Geology and Geophysics*, *52*, 11-26, doi:10.1080/00288300909509874.

Dalrymple, G. B., M. Grove, O. M. Lovera, T. M. Harrison, J. B. Hulen, and M. A. Lanphere (1999), Age and thermal history of the Geysers plutonic complex (felsite unit), Geysers geothermal field, California: a $^{40}Ar/^{39}Ar$ and U–Pb study, *Earth and Planetary Science Letters*, *173*, 285–298.

Darby, D. J., and R. O. Williams (1991), A new geodetic estimate of deformation in the Central Volcanic Region of the North Island, New Zealand, *New Zealand Journal of Geology and Geophysics*, *34*, 127–136, doi:10.1080/00288306.1991.9514450.

Darby, D. J., K. M. Hodgkinson, and G. H. Blick (2000), Geodetic measurement of deformation in the Taupo Volcanic Zone, New Zealand: The north Taupo network revisited, *New Zealand Journal of Geology and Geophysics*, *43*, 157–170, doi:10.1080/00288306.2000.9514878.

Deer, W. A., R. A. Howie, and J. Zussman (1992), An introduction to the rock-forming minerals, second ed. Longman, Harlow.

Deering, C. D., O. Bachmann, J. Dufek, and D. M. Gravley (2011), Rift-Related Transition from Andesite to Rhyolite Volcanism in the Taupo Volcanic Zone (New Zealand) Controlled by Crystal-melt Dynamics in Mush Zones with Variable Mineral Assemblages, *Journal of Petrology*, *52*(11), 2243–2263, doi:10.1093/petrology/egr046.

Dugdale, A. L., C. J. L. Wilson, and R. J. Squire (2006), Hydrothermal alteration at the Magdala gold deposit, Stawell, western Victoria, *Australian Journal of Earth Sciences*, *53*(5), 733–757, doi:10.1080/08120090600827421.

Freeman, J. J., A. Wang, K. E. Kuebler, B. L. Jolliff, and L. A. Haskin (2008), Characterization of Natural Feldspars By Raman Spectroscopy for Future Planetary Exploration, *The Canadian Mineralogist*, *46*(6), 1477–1500, doi:10.3749/canmin.46.6.1477.

Gamble, J. A., R. C. Price, I. E. M. Smith, W. C. McIntosh, and N. W. Dunbar (2003), $^{40}Ar/^{39}Ar$ geochronology of magmatic activity, magma flux and hazards at Ruapehu volcano, Taupo Volcanic Zone, New Zealand, *Journal of Volcanology and Geothermal Research*, *120*, 271–287.

Graham, I. J., J. W. Cole, R. M. Briggs, J. A. Gamble, and I. E. M. Smith (1995), Petrology and petrogenesis of volcanic rocks from the Taupo Volcanic Zone: a review, *Journal of Volcanology and Geothermal Research, 68*, 59–87.

Gravley, D. M., C. J. N. Wilson, M. D. Rosenberg, and G. S. Leonard (2006), The nature and age of Ohakuri Formation and Ohakuri Group rocks in surface exposures and geothermal drillhole sequences in the central Taupo Volcanic Zone, New Zealand, *New Zealand Journal of Geology and Geophysics, 49*, 305–308, doi:10.1080/00288306.2006.9515169.

Gravley, D. M., C. J. N. Wilson, G. S. Leonard, and J. W. Cole (2007), Double trouble: Paired ignimbrite eruptions and collateral subsidence in the Taupo Volcanic Zone, New Zealand, *Geological Society of America Bulletin*, *119*(1-2), 18–30, doi:10.1130/B25924.1.

Gravley, D. M., et al., (in preparation).

Grindley, G. W. (1960), Sheet 8 – Taupo, Geological map of New Zealand 1:250:000, Department of Scientific and Industrial Research, Wellington.

Grindley, G. W. (1965a), The geology, structure, and exploitation of the Wairakei geothermal field, Taupo, New Zealand, *New Zealand Geological Survey Bulletin, 75*, 1-131.

Grindley, G. W. (1965b), Subsurface Geology of the Orakei Korako and Te Kopia Geothermal Fields, *New Zealand Geological Survey, Geological Geothermal Report No. 3*.

Grindley, G. W. (1970), Subsurface structures and relation to steam production in the Broadlands geothermal field, New Zealand, *Geothermics, Special Issue 2*, 248–261.

Grindley, G. W. (1982), The deeper structure of the Wairakei geothermal field, *Proceedings of the Pacific Geothermal Conference*, 69-74.

Grindley, G. W., T. C. Mumme, and B. P. Kohn (1994), Stratigraphy, paleomagnetism, geochronology and structure of silicic volcanic rocks, Waiotapu/Paeroa Range area, New Zealand, *Geothermics*, *23*(5), 473–499.

Grunder, A. L., E. W. Klemetti, T. C. Feeley, and C. M. McKee (2008), Eleven million years of arc volcanism at the Aucanquilcha Volcanic Cluster, northern Chilean Andes: implications for the life span and emplacement of plutons. *Earth and Environmental Science Transactions of the Royal Society of Edinburgh, 97,* 415–436.

Harrison, A. J., and R. S. White (2004), Crustal structure of the Taupo Volcanic Zone, New Zealand: Stretching and igneous intrusion, *Geophysical Research Letters, 31*, L13615, doi:10.1029/2004GL019885.

Harrison, A. J., and R. S. White (2006), Lithospheric structure of an active backarc basin: the Taupo Volcanic Zone, New Zealand, *Geophysical Journal International*, *167*(2), 968–990, doi:10.1111/j.1365-246X.2006.03166.x.

Hedenquist, J. W., and P. R. L. Browne (1989), The evolution of the Waiotapu geothermal system, New Zealand, based on the chemical and isotopic composition of its fluids, minerals and rocks, *Geochimica et Cosmochimica Acta*, *53*(9), 2235–2257, doi:10.1016/0016-7037(89)90347-5.

Hildyard, S. C., J. W. Cole, and S. D. Weaver (2000), Tikorangi Ignimbrite: A 0.89 Ma mixed andesite-rhyolite ignimbrite, Matahana Basin, Taupo Volcanic Zone, New Zealand, *New Zealand Journal of Geology and Geophysics*, *43*(1), 95–107. doi:10.1080/00288306.2000.9514872.

Hobden, B. J., B. F. Houghton, M. A. Lanphere, and I. A. Nairn (1996), Growth of the Tongariro volcanic complex: New evidence from K-Ar age determinations, *New Zealand Journal of Geology and Geophysics*, *39*(1), 151–154. doi:10.1080/00288306.1996.9514701.

Hochstein, M. P. (1995), Crustal heat transfer in the Taupo Volcanic Zone (New Zealand): comparison with other volcanic arcs and explanatory heat source models, *Journal of Volcanology and Geothermal Research*, *68*(1-3), 117–151, doi:10.1016/0377-0273(95)00010-R.

Houghton, B. F., C. J. N. Wilson, M. O. McWilliams, M. A. Lanphere, S. D. Weaver, R. M. Briggs, and M. S. Pringle (1995), Chronology and dynamics of a large silicic magmatic system: Central Taupo Volcanic Zone, New Zealand, *Geology*, *23*(1), 13–16.

ID-TIMS U-Pb geochronology, Retrieved from http://earth.boisestate.edu/isotope/analytical-capabilities/id-tims-u-pb/

Lamarche, G., P. M. Barnes, and J. M. Bull (2006), Faulting and extension rate over the last 20,000 years in the offshore Whakatane Graben, New Zealand continental shelf, *Tectonics*, *25*, 1–24, doi:10.1029/2005TC001886.

Lee, J. M., D. Townsend, K. Bland, and P. J. J. Kamp (compilers) (2011) Geology of the Hawke's Bay area, Institute of Geological & Nuclear Sciences 1:250,000 geological map 8, GNS Science, Lower Hutt, New Zealand.

Leitch, C. H. B., C. I. Godwin, T. H. Brown, and B. E. Taylor (1991), Geochemistry of mineralizing fluids in the Bralorne-Pioneer Mesothermal gold vein deposit, British Columbia, Canada, *Economic Geology*, *86*, 318–353.

Leonard, G. S. (2003), The evolution of Maroa Volcanic Centre, Taupo Volcanic Zone, New Zealand, Ph.D. thesis, University of Canterbury, Christchurch, New Zealand.

Leonard, G. S., J. G. Begg, and C. J. N. Wilson (compilers) (2010), Geology of the Rotorua area, Institute of Geological & Nuclear Sciences 1:250,000 geological map 5, GNS Science. Lower Hutt, New Zealand.

Lewis, B., I. Chambefort, and A. J. Rae (2012a), Geology of Injection Well NM8-NM8A, Ngatamariki Geothermal Field, *GNS Science consultancy report 2012/188*.

Lewis, B., I. Chambefort, A. J. Rae, and F. Sanders (2012b), Geology of Well NM9, Ngatamariki Geothermal Field, *GNS Science consultancy report 2012/330*.

Lewis, B., I. Chambefort, A. J. Rae, and F. Sanders (2012c), Geology of Injection Well NM10, Ngatamariki Geothermal Field, *GNS Science consultancy report 2012/231*.

Lewis, B., I. Chambefort, A. J. Rae, F. Sanders, and C. Massiot (2013), Geology of Well NM11, Ngatamariki Geothermal Field, *GNS Science consultancy report 2013/33*.

Lipman, P. W. (2007), Incremental assembly and prolonged consolidation of Cordilleran magma chambers: Evidence from the Southern Rocky Mountain volcanic field, *Geosphere*, *3*(1), 42–70, doi:10.1130/GES00061.1.

Lloyd, E. F. (1972), Geology and hot springs of Orakeikorako, *New Zealand Geological Survey Bulletin*, *85*, 164p.

Lowe, D. J., P. A. R. Shane, B. V. Alloway, and R. M. Newnham (2008), Fingerprints and age models for widespread New Zealand tephra marker beds erupted since 30,000 years ago: a framework for NZ-INTIMATE, *Quaternary Science Reviews*, *27*, 95–126, doi:10.1016/j.quascirev.2007.01.013.

Ludwig, K. (2009), SQUID 2: A User's Manual, revision of 12 April, 2009, Berkeley Geochronology Center Special Publication 5.

Ludwig, K. (2011), Isoplot/Ex version 4.13, a geochronological toolkit for Microsoft Excel, Berkeley Geochronology Centre, Berkeley, California (revision of January 02, 2011).

Martin, R. C. (1961), Stratigraphy and structural outline of the Taupo Volcanic Zone, *New Zealand Journal of Geology and Geophysics*, *4*, 449–478, doi:10.1080/00288306.1961.10420134.

Mauk, J. L., C. M. Hall, J. T. Chesley, and F. Barra (2011), Punctuated evolution of a large epithermal province: The Hauraki goldfield, New Zealand, *Economic Geology*, *106*, 921–943.

McCormack, K. D., M. A. M. Gee, N. J. McNaughton, R. Smith, and I. R. Fletcher (2009), U–Pb dating of magmatic and xenocryst zircons from Mangakino ignimbrites and their correlation with detrital zircons from the Torlesse metasediments, Taupo Volcanic Zone, New Zealand, *Journal of Volcanology and Geothermal Research*, *183*(1-2), 97–111, doi:10.1016/j.jvolgeores.2009.03.005.

Milicich, S. D., C. J. N. Wilson, G. Bignall, B. Pezaro, B. L. A. Charlier, J. L. Wooden, and T. R. Ireland (2013), U–Pb dating of zircon in hydrothermally altered rocks of the Kawerau Geothermal Field, Taupo Volcanic Zone, New Zealand, *Journal of Volcanology and Geothermal Research*, *253*, 97–113, doi:10.1016/j.jvolgeores.2012.12.016.

Mernagh, T. P. (1991), Use of the laser Raman microprobe for discrimination amongst feldspar minerals, *Journal of Raman Spectroscopy, 22*, 453-457.

Mueller, A. G., and D. I. Groves (1991), The classification of Western Australian greenstone-hosted gold deposits according to wallrock-alteration mineral assemblages, *Ore Geology Reviews*, *6*(4), 291–331, doi:10.1016/0169-1368(91)90008-U.

Murphy, R. P., and D. Seward (1981), Stratigraphy, lithology, paleomagnetism, and fission track ages of some ignimbrite formations in the Matahana Basin, New Zealand, *New Zealand Journal of Geology and Geophysics*, *24*(3), 325-331.

Nairn, I. A. (1984), Stratigraphy of RK5 to 2654 m, Department of Scientific and Industrial Research, Wellington.

Nairn, I. A. (1985), Stratigraphy of RK6: Preliminary report, Department of Scientific and Industrial Research, Wellington.

Nairn, I. A. (1986), Rotokawa RK8 stratigraphy, Department of Scientific and Industrial Research, Wellington.

Nairn, I. A., and B. P. Kohn (1973), Relation of the Earthquake Flat Breccia to the Rotoiti Breccia, central North Island, New Zealand, *New Zealand Journal of Geology and Geophysics*, *16*, 269–279, doi:10.1080/00288306.1973.10431457.

Nairn, I. A., and S. Beanland (1989), Geological setting of the 1987 Edgecumbe earthquake, New Zealand, *New Zealand Journal of Geology and Geophysics*, *32*(1), 1–13, doi:10.1080/00288306.1989.10421383.

O'Brien, J. M. (2010), Hydrogeochemical characteristics of the Ngatamariki Geothermal Field and a comparison with the Orakei Korako thermal area, Taupo Volcanic Zone, New Zealand, M.Sc. thesis, University of Canterbury, Christchurch, New Zealand.

Ogawa, Y., H. M. Bibby, T. G. Caldwell, S. Takakura, T. Uchida, N. Matsushima, S. L. Bennie, T. Tosha, and Y. Nishi (1999), Wide-band Magnetotelluric Measurements across the Taupo Volcanic Zone, New Zealand – Preliminary Results, *Geophysical Research Letters*, *26*(24), 3673–3676, doi:10.1029/1999GL010914.

Pillans, B., B. Alloway, T. Naish, J. Westgate, S. Abbott, and A. Palmer (2005), Silicic tephras in Pleistocene shallow-marine sediments of Wanganui Basin, New Zealand, *Journal of the Royal Society of New Zealand*, *35*, 43–90, doi:10.1080/03014223.2005.9517777.

Powell, T., J. O'Brien, and C. Boseley, (2011) A Tahorakuri Formation caldera boundary at Ngatamariki, Presented at: Geosciences Society of New Zealand Meeting, 1 December 2011, Nelson, New Zealand.

Price, R. C., J. A. Gamble, I. E. M. Smith, R. B. Stewart, S. Eggins, and I. C. Wright (2005), An integrated model for the temporal evolution of andesites and rhyolites and crustal development in New Zealand's North Island, *Journal of Volcanology and Geothermal Research*, *140*(1-3), 1–24, doi:10.1016/j.jvolgeores.2004.07.013.

Rae, A. J. (2007), Rotokawa geology and geophysics, *GNS Science consultancy report 2007/83*, 11p.

Rae, A. J., M. D. Rosenberg, G. Bignall, G. N. Kilgour, and S. D. Milicich (2007), Geological Results of Production Well Drilling in the Western steamfield, Ohaaki Geothermal system: 2005–2007, *Proceedings of the 29th New Zealand Geothermal Workshop, University of Auckland*, 6p.

Rae, A. J., L. E. Ramirez, and C. Bardsley (2009a), Geology of Exploration Well NM6, Ngatamariki Geothermal Field, *GNS Science consultancy report 2009/130*, 68p.

Rae, A. J., L. E. Ramirez, and C. Boseley (2009b), Geology of Geothermal Well NM7, Ngatamariki Geothermal Field, *GNS Science consultancy report 2009/289*, 57p.

Ramirez, L. E., and A. J. Rae (2009), Geology of Injection Well NM5, NM5A, Ngatamariki Geothermal Field, *GNS Science consultancy report 2009/41*, 29p.

Ritchie, A. B. H. (1996), Volcanic geology and geochemistry of Waiotapu Ignimbrite, Taupo Volcanic Zone, New Zealand, M.Sc. thesis, University of Canterbury, Christchurch, New Zealand.

Rogan, M. (1982), A geophysical study of the Taupo Volcanic Zone New Zealand, *Journal of Geophysical Research, 87*, 4073–4088.

Rosenberg, M. D., G. Bignall, and A. J. Rae (2009), The geological framework of the Wairakei–Tauhara Geothermal System, New Zealand, *Geothermics*, *38*(1), 72–84, doi:10.1016/j.geothermics.2009.01.001.

Rowland, J. V., and R. H. Sibson (2001), Extensional fault kinematics within the Taupo Volcanic Zone, New Zealand: Soft-linked segmentation of a continental rift system, *New Zealand Journal of Geology and Geophysics*, *44*, 271–283, doi:10.1080/00288306.2001.9514938.

Schärer, U. (1984), The effect of initial ^{230}Th disequilibrium on young U-Pb ages: the Makalu case, Himalaya, *Earth and Planetary Science Letters, 67*, 191–204.

Schipper, C. I. (2004), Chemical and mineralogical characterization of pyroclastic deposits from the ca. 1 Ma Kidnappers and Rocky Hill eruptions, Taupo Volcanic Zone, New Zealand, M.Sc. thesis, University of Otago, Dunedin, New Zealand.

Schmitt, A. K., M. Grove, T. M. Harrison, O. Lovera, J. Hulen, and M. Walters (2003), The Geysers - Cobb Mountain Magma System, California (Part 1): U-Pb zircon ages of volcanic rocks, conditions of zircon crystallization and magma residence times, *Geochimica et Cosmochimica Acta*, *67*(18), 3423–3442, doi:10.1016/S0016-7037(03)00140-6.

Shane, P. A. R., T. M. Black, B. V. Alloway, and J. A. Westgate (1996), Early to middle Pleistocene tephrochronology of North Island, New Zealand: Implications for volcanism, tectonism, and paleoenvironments, *Geological Society of America Bulletin*, *108*(8), 915–925.

Sherburn, S., S. Bannister, and H. Bibby (2003), Seismic velocity structure of the central Taupo Volcanic Zone, New Zealand, from local earthquake tomography, *Journal of*

Volcanology and Geothermal Research, *122*(1-2), 69–88, doi:10.1016/S0377-0273(02)00470-5.

Simmons, S. F., and B. W. Christenson (1994), Origins of calcite in a boiling geothermal system, *American Journal of Science*, *294*, 361-400.

Simon, J. I., P. R. Renne, and R. Mundil (2008), Implications of pre-eruptive magmatic histories of zircons for U–Pb geochronology of silicic extrusions, *Earth and Planetary Science Letters*, *266*(1-2), 182–194, doi:10.1016/j.epsl.2007.11.014.

Soengkono, S., M. P. Hochstein, I. E. M. Smith, and T. Itaya (1992), Geophysical evidence for widespread reversely magnetised pyroclastics in the western Taupo Volcanic Zone (New Zealand), *New Zealand Journal of Geology and Geophysics*, *35*, 47–55, doi:10.1080/00288306.1992.9514499.

Stacey, J. S., and J. D. Kramers (1975), Approximation of terrestrial lead isotope evolution by a two-stage model, *Earth and Planetary Science Letters*, *26*, 207–221.

Stagpoole, V. M., S. L. Bennie, H. M. Bibby, D. J. Graham, and P. H. Newport (1985), Electrical resistivity map of New Zealand, Sheet U17, Wairakei [cartographic material]: Nominal Schlumberger array spacing 500 m. Department of Scientific and Industrial Research, Wellington.

Steiner, A. (1970), Genesis of hydrothermal K-feldspar (adularia) in an active geothermal environment at Wairakei, New Zealand, *Mineralogical Magazine*, *37*(292), 916-922.

Stern, T. A. (1987), Asymmetric back-arc spreading, heat flux and structure associated with the Central Volcanic Region of New Zealand, *Earth and Planetary Science Letters*, *85*, 265–276.

Stern, T. A., and F. J. Davey (1987), A seismic investigation of the crustal and upper mantle structure within the Central Volcanic Region of New Zealand, *New Zealand Journal of Geology and Geophysics*, *30*, 217–231, doi:10.1080/00288306.1987.10552618.

Stratford, W. R., and T. A. Stern (2004), Strong seismic reflections and melts in the mantle of a continental back-arc basin, *Geophysical Research Letters*, *31*, L06622, doi:10.1029/2003GL019232.

Stratford, W. R., and T. A. Stern (2006), Crust and upper mantle structure of a continental backarc: central North Island, New Zealand, *Geophysical Journal International*, *166*(1), 469–484, doi:10.1111/j.1365-246X.2006.02967.x.

Townsend, D., A. Vonk, and P. J. J. Kamp (compilers) (2008), Geology of the Taranaki area, Institute of Geological & Nuclear Sciences 1:250,000 geological map 7. GNS Science. Lower Hutt, New Zealand.

Urzua, L.A. (2008), MT analysis with geology and geochemistry in a conceptual model of the Ngatamariki Geothermal Field, M.Sc. thesis, University of Auckland, Auckland, New Zealand.

Villamor, P., and K. Berryman (2001), A late Quaternary extension rate in the Taupo Volcanic Zone, New Zealand, derived from fault slip data, *New Zealand Journal of Geology and Geophysics*, *44*, 243–269, doi:10.1080/00288306.2001.9514937.

Villamor, P., and K. R. Berryman (2006), Evolution of the southern termination of the Taupo Rift, New Zealand, *New Zealand Journal of Geology and Geophysics*, *49*, 23–37, doi:10.1080/00288306.2006.9515145.

Wallace, L. M. (2004), Subduction zone coupling and tectonic block rotations in the North Island, New Zealand, *Journal of Geophysical Research*, *109*, 1–21, doi:10.1029/2004JB003241.

Wallace, L. M., S. Ellis, and P. Mann (2009), Collisional model for rapid fore-arc block rotations, arc curvature, and episodic back-arc rifting in subduction settings, *Geochemistry, Geophysics, Geosystems*, *10*(5), doi:10.1029/2008GC002220.

White, N. C., and J. W. Hedenquist (1990), Epithermal environments and styles of mineralization: Variations and their causes, and guidelines for exploration, *Journal of Geochemical Exploration*, *36*(1-3), 445–474, doi:10.1016/0375-6742(90)90063-G.

Wilson, C. J. N. (1986). Reconnaissance stratigraphy and volcanology of ignimbrites from Mangakino volcano, in: Smith, I. E. M., (Ed.), Late Cenozoic Volcanism in New Zealand, *Royal Society of New Zealand Bulletin 23*, 179-193.

Wilson, C. J. N., B. F. Houghton, and E. F. Lloyd (1986). Volcanic history and evolution of the Maroa-Taupo area, central North Island, in: Smith I. E. M., (Ed.), Late Cenozoic Volcanism in New Zealand, *Royal Society of New Zealand Bulletin 23*, 194-223.

Wilson, C. J. N., B. F. Houghton, M. O. McWilliams, M. A. Lanphere, S. D. Weaver, and R. M. Briggs (1995a), Volcanic and structural evolution of Taupo Volcanic Zone, New Zealand: a review, *Journal of Volcanology and Geothermal Research*, *68*(1-3), 1–28.

Wilson, C. J. N., B. F. Houghton, P. J. J. Kamp, and M. O. McWilliams (1995b), An exceptionally widespread ignimbrite with implications for pyroclastic flow emplacement, *Nature*, *378*(6557), 605–607.

Wilson, C. J. N., B. L. A. Charlier, C. J. Fagan, K. D. Spinks, D. M. Gravley, S. F. Simmons, and P. R. L. Browne (2008), U–Pb dating of zircon in hydrothermally altered rocks as a correlation tool: Application to the Mangakino geothermal field, New Zealand, *Journal of Volcanology and Geothermal Research*, *176*(2), 191–198, doi:10.1016/j.jvolgeores.2008.04.010.

Wilson, C. J. N., D. M. Gravley, G. S. Leonard, and J. V. Rowland (2009), Volcanism in the central Taupo Volcanic Zone, New Zealand: tempo, styles and controls, *Studies in Volcanology: The Legacy of George Walker, Special Publications of IAVCEI, 2*, 225–247.

Wilson, C. J. N., B. L. A. Charlier, J. V. Rowland, and P. R. L. Browne (2010), U–Pb dating of zircon in subsurface, hydrothermally altered pyroclastic deposits and implications for subsidence in a magmatically active rift: Taupo Volcanic Zone, New Zealand, *Journal*

of Volcanology and Geothermal Research, *191*(1-2), 69–78, doi:10.1016/j.jvolgeores.2010.01.001.

Wood, C. P. (1985a), Stratigraphy and petrology of NM1 Ngatamariki Geothermal Field, Unpublished report of the New Zealand Geological Survey, Department of Scientific and Industrial Research, Lower Hutt.

Wood, C. P. (1985b), Stratigraphy and petrology of NM2 Ngatamariki Geothermal Field, Unpublished report of the New Zealand Geological Survey, Department of Scientific and Industrial Research, Lower Hutt.

Wood, C. P. (1986a), Stratigraphy and petrology of NM3 Ngatamariki Geothermal Field, Unpublished report of the New Zealand Geological Survey, Department of Scientific and Industrial Research, Lower Hutt.

Wood, C. P. (1986b), Stratigraphy and petrology of NM 4 Ngatamariki Geothermal Field, Unpublished report of the New Zealand Geological Survey, Department of Scientific and Industrial Research, Lower Hutt.

Wright, I. C. (1990), Late Quaternary faulting of the offshore Whakatane Graben, Taupo Volcanic Zone, New Zealand, *New Zealand Journal of Geology and Geophysics*, *33*(2), 245–256, doi:10.1080/00288306.1990.10425682.

Wright, I. C. (1993), Pre-spread rifting and heterogeneous volcanism in the southern Havre Trough back-arc basin, *Marine Geology*, *113*(3-4), 179–200, doi:10.1016/0025-3227(93)90017-P.

Appendix 1: Thin section and cuttings descriptions

Note: descriptions are primarily focussed on the original nature of the rock, although descriptions of the hydrothermal alteration are also given. Mineral percentages are estimates. Primary mineral estimates include both unaltered crystals and altered crystal pseudomorphs interpreted to be that primary mineral. Volcaniclastic is used to describe all clastic deposits of volcanic origin. Ignimbrite is used to describe primary deposits inferred to have been emplaced by pyroclastic density currents. Tuff is used to describe deposits inferred to be primary volcanic deposits, where the mode of emplacement is unknown.

Sample: NM1, 1305.5-1307.7 mRF

Rock type: Welded ignimbrite

Hand Sample Description:
Hard grey ignimbrite with a eutaxitic texture. Fiamme are common and highly attenuated. They are variously altered to a white, light grey or medium grey-greenish colour. Some have visible phenocrysts. Lithics are also present, with fragments up to ~2 cm, and are mostly light grey with small white phenocrysts. Phenocrysts are also common within the ignimbrite, and are set in a light to medium grey groundmass. Pyrite-rich veins and voids are also present.

Thin Section Description:
Welding can be seen in the banded nature of the section, with reasonably common pumice fiamme. It is sometimes difficult to distinguish between lithics and pumice due to intense alteration. Crystals are mostly plagioclase, with euhedral crystals up to ~1.5 mm and common smaller fragments. Ferromagnesian minerals are completely altered. Quartz is very rare.

Hydrothermal alteration:
Alteration is intense. The groundmass is altered to fine quartz and clay with common pyrite and Fe-Ti oxides (mostly leucoxene?) disseminated throughout the rock, but particularly common in some lithic and pumice clasts. Plagioclase is altered to clay, calcite, and albite. Ferromagnesian minerals are altered to chlorite, quartz, pyrite, clinozoisite, and calcite.

Mineralogy:
Groundmass ~50-60%
Crystals ~20-30%
Lithics ~5-15%
Pumice ~5-15%

Primary minerals	Abundance	Secondary minerals	Abundance
Plagioclase	20-25%	Quartz	>20%
Quartz	Trace	Clay	>20%
Ferromagnesian minerals?	1-5%?	Calcite	5-10%
Zircon	Trace	Albite	1-5%
		Chlorite	1-5%
		Clinozoisite	1-5%
		Pyrite	5-10%
		Fe-Ti oxides	5-10%

Sample: NM2, 1155.5-1157.5 mRF

Rock type: Welded ignimbrite

Hand Sample Description:
Light grey welded ignimbrite with common white pumice and lithic fragments, rare dark lithic fragments, and common crystal fragments in a fine, light grey groundmass. Some white clasts of flattened pumice are present, while others are angular and appear un-flattened. These are possibly lithics rather than pumice. Also contains dark grey andesite and greywacke lithics. Pale grey lithics are difficult to distinguish from the ignimbrite itself.

Thin Section Description:
Crystal-rich ignimbrite with common pumice fiamme and a variety of lithic fragments in a fine groundmass. The groundmass is still quite glassy in places, but is devitrified in places, giving a weak banded appearance. Pumice fiamme often contain plagioclase phenocrysts and spherulites. Some lithics contain lithic clasts within them

(possibly ignimbrite). Plagioclase phenocrysts are common in the lithics, while at least one contains rare quartz. Andesite lithics are rare. Crystals are dominantly plagioclase in various stages of alteration, with some fresh enough for composition of andesine (An≥42%) to be estimated using the Michel Levy method. Euhedral, often elongate crystals up to ~3 mm in length are present, but most are smaller crystal fragments. Quartz is extremely rare. Ferromagnesian minerals are completely altered but amphibole can be identified by relict cleavage planes, with some crystals up to ~0.9 mm in size. Pseudomorph shapes resembling pyroxene are also present, but most are difficult to identify.

Hydrothermal alteration:
Alteration is moderate. The groundmass remains partly glassy, but in places is altered to fine quartz, clay, Fe-Ti oxides, and disseminated pyrite. The groundmass in most lithics is altered to clay and/or quartz, while pumice is altered mostly to clay with minor Fe-Ti oxides and pyrite. Plagioclase remains fresh in places, but is otherwise altered to albite, calcite, and clay. Ferromagnesian minerals are altered to clay, Fe-Ti oxides, pyrite, and quartz.

Mineralogy:
Groundmass ~50-55%
Crystals ~20-25%
Lithics ~10-15%
Pumice ~10-15%

Primary minerals	Abundance	Secondary minerals	Abundance
Plagioclase	~20%	Clay	>20%
Quartz	<1%	Quartz	>10%
Amphibole	1-3%	Albite	5-10%
Pyroxene?	1-3%	Calcite	1-5%
Zircon	Trace	Fe-Ti oxides	1-5%
		Pyrite	1-5%

Sample: NM2, 1354.2 – 1356.2 mRF

Rock type: Welded ignimbrite

Hand Sample Description:
Pale grey-white ignimbrite with common lithic and pumice clasts. Pumice is often flattened, defining a weakly eutaxitic texture. Lithics are common, some >2 cm in size, with multiple lithologies including; a light grey rock with white phenocrysts (andesite?), and fine-grained dark grey, green, and brownish rocks.

Thin Section Description:
Lithic-rich ignimbrite with crystal fragments and flattened pumice in a fine groundmass. A weak eutaxitic texture is defined by pumice fiamme. Lithics are intensely altered and fine-grained making identification difficult, but probably consist of a range of volcanic and sedimentary rocks. Crystals are mostly plagioclase, with euhedral-subhedral crystals up to ~2 mm long, although most are finer crystal fragments. Michel Levy method gives a plagioclase composition of An≥30. Quartz is rare, with both angular and rounded crystals up to ~0.7 mm. Ferromagnesian minerals cannot be confidently identified.

Hydrothermal alteration:
Alteration is strong. The groundmass is altered to fine quartz and clay, with Fe-Ti oxides and pyrite. Plagioclase is altered to adularia, albite, wairakite, and clinozoisite, but remains fresh in places. Aggregates of clinozoisite, sometimes associated with wairakite and calcite, are possibly altered ferromagnesian minerals, but in places appear to be altered from plagioclase so it is uncertain if ferromagnesian minerals were present.

Mineralogy:
Groundmass ~55%
Crystals ~15%
Lithics ~15-20%
Pumice ~10-15%

Primary minerals	Abundance	Secondary minerals	Abundance
Plagioclase	10-15%	Quartz	>20%
Quartz	<1%	Clay	>20%
Ferromagnesian minerals?	0-3%?	Albite	5-10%
		Adularia	1-5%
		Calcite	1-5%
		Clinozoisite	1-5%
		Wairakite	1-5%
		Fe-Ti oxides	1-5%
		Pyrite	<1%

Sample: NM2, 1415-1417 mRF

Rock type: Volcaniclastic?

Hand Sample Description:
Intensely altered volcaniclastic rock with rare crystals and lithics in a fine groundmass. The groundmass is mostly white with green patches, and no visible textures. Some lithics and possible pumice clasts are also altered to fine-grained green patches. Grey lithics with white crystals and rare light grey-pink lithics are also visible.

Thin Section Description:
The rock is intensely altered making identification difficult. Altered patches consisting primarily of secondary quartz, minor chlorite, clinozoisite, and rare apatite were possibly pumice or lithic clasts, but there is no strong alignment or flattening observed indicating the rock was not welded. Plagioclase is the dominant crystal, with euhedral-subhedral crystals and crystal fragments. Quartz is rare but rounded crystals up to ~1 mm are present.

Hydrothermal alteration:
Alteration is intense. The groundmass is altered to fine quartz, Fe-Ti oxides and pyrite. Possible pumice clasts are altered to coarser quartz, chlorite, and clinozoisite. Rare wairakite veins are also associated with this mineralogy. Plagioclase is altered to adularia, albite, and possibly epidote/clinozoisite.

Mineralogy:
Groundmass ~60-70%
Crystals ~10-15%
Lithics/Pumice ~20-25%

Primary minerals	Abundance	Secondary minerals	Abundance
Plagioclase	10-15%	Quartz	>50%
Quartz	~1%	Chlorite	5-10%
		Albite	1-5%
		Adularia	1-5%
		Clinozoisite	1-5%
		Wairakite	~1%
		Fe-Ti oxides	1-5%
		Pyrite	<1%

Sample: NM2, 1582-1586 mRF

Rock type: Ignimbrite?

Hand Sample Description:
This core is of a strongly altered white rock containing altered lithic (and possibly pumice) clasts and crystals in a fine, white groundmass. Lithics are generally also white and appear similar to the rock as a whole, although fine-grained light grey lithics are also present.

Thin Section Description:
This is probably a partially welded ignimbrite. Wispy fiamme shapes are common and generally lie in a preferred orientation, indicating partial welding. Glass shard shapes can also be seen. Some lithics are difficult to distinguish from the groundmass while others are darker, although it is difficult to identify rock type due to alteration. Some have visible phenocrysts. Crystals are predominantly altered plagioclase, although very rare quartz crystals up to ~0.5 mm are present. Possible completely altered ferromagnesian minerals.

Hydrothermal alteration:
Alteration is intense. The groundmass is altered to fine quartz, clay, Fe-Ti oxides and pyrite. Pumice fiamme are altered to clay. Plagioclase is altered to albite, adularia and possibly clay. Crystal shapes altered to quartz, wairakite, clinozoisite, and rare acicular apatite could have originally been plagioclase, but some may also have been ferromagnesian minerals. Wairakite veins are reasonably common.

Mineralogy:
Groundmass ~50-70%
Crystals ~5-15%
Lithics ~10-20%
Pumice ~15-25%

Primary minerals	Abundance	Secondary minerals	Abundance
Plagioclase	5-15%	Quartz	>20%
Quartz	<1%	Clay	>20%
Ferromagnesian minerals?		Albite	1-5%
		Adularia	1-5%
		Wairakite	1-5%
		Clinozoisite	1-5%
		Apatite	<1%
		Fe-Ti oxides	1-5%
		Pyrite	1-5%

Sample: NM2, 2254.7-2255.2 mRF

Rock type: Crystal-rich ignimbrite

Hand Sample Description:
This is a dense, light to medium grey rock with common felsic crystals, white lithic grains, and possibly pumice clasts in a fine groundmass. Some lithics contain visible phenocrysts. No textures are observed.

Thin Section Description:
Very crystal-rich ignimbrite, with abundant plagioclase crystals and crystal fragments up to ~2 mm in size, and common large embayed quartz phenocrysts up to ~3 mm in size. While many quartz phenocrysts are rounded and embayed, angular fragments of quartz and feldspar are common. Possible ferromagnesian minerals are completely altered, but biotite and amphibole are identified based on shape. No shapes resembling pyroxene are observed. Lithics are rare and hard to differentiate from the groundmass. Possible rare pumice fiamme.

Hydrothermal alteration:
Alteration is strong. The groundmass is altered to quartz and clay, with minor Fe-Ti oxides and pyrite throughout the rock. Plagioclase is altered to albite, rare calcite, and clay. Ferromagnesian minerals are altered to clinozoisite/epidote, chlorite, calcite, and Fe-Ti oxides.

Mineralogy:
Crystals ~40-45%

Primary minerals	Abundance	Secondary minerals	Abundance
Plagioclase	~25%	Quartz	>10%
Quartz	15-20%	Clay	>20%
Amphibole (± pyroxene?)	<1%	Albite	10-20%
Biotite?	<1%	Clinozoisite/Epidote	1-5%
Zircon	Trace	Chlorite	1-5%
		Calcite	<1%
		Fe-Ti oxides	1-5%
		Pyrite	1-5%

Sample: NM2, 2409.7-2410.5 mRF?

Rock type: Welded ignimbrite

Hand Sample Description:
A single cobble was recovered and it is doubtful it actually came from this depth. It is a white coloured ignimbrite with crystals, angular lithics, and flattened pumice fiamme in a fine, white groundmass. Lithics are

also often white, some with phenocrysts, although some grey lithics are also present. The largest observed is ~1 cm in size, but most are much smaller. Pumice fiamme are altered to clay.

Thin Section Description:
This core is similar in appearance to the core at 1582-1586 mRF. Wispy pumice fiamme are common, indicating a degree of welding, and glass shard shapes are also observed. Lithic clasts are of fine grained, altered rocks, making identification difficult; however, some are clearly darker than others indication there is more than one rock type. Crystals are predominantly altered plagioclase, although rare quartz crystals up to ~0.5 mm are present, and one large (~1.5 mm) embayed quartz crystal is also present. Possible completely altered ferromagnesian minerals.

Hydrothermal alteration:
Alteration is intense. The groundmass is altered to fine quartz, clay, Fe-Ti oxides (mainly leucoxene), and pyrite. Pumice fiamme are altered to clay. Plagioclase is altered to adularia, albite, calcite, and possibly clay. Crystal shapes altered to quartz, wairakite, clinozoisite, and rare apatite could have originally been plagioclase, but some may have also been ferromagnesian minerals.

Mineralogy:
Groundmass ~60-80%
Crystals ~5-10%
Lithics ~5-15%
Pumice ~10-20%

Primary minerals	Abundance	Secondary minerals	Abundance
Plagioclase	5-10%	Quartz	>20%
Quartz	<1%	Clay	>20%
		Albite	1-5%
		Adularia	1-5%
		Wairakite	1-5%
		Clinozoisite/Epidote	1-5%
		Apatite	<1%
		Fe-Ti oxides	1-5%
		Pyrite	1-5%

Sample: NM3, 1246-1248 m

Rock type: Welded ignimbrite

Hand Sample Description:
Hard, welded ignimbrite with a eutaxitic texture defined by common elongate pumice fiamme. The pumice and altered crystals appear to be altered to clay. They are set in a light grey groundmass. Some lithic clasts are visible, with altered phenocrysts in a fine grey groundmass (andesite?). Dark, pyrite-rich veins are common.

Thin Section Description:
Welded ignimbrite with a well developed eutaxitic texture. Fiamme are common and most are highly attenuated indicating strong welding. Lithics are minor in comparison to pumice and crystals, with multiple lithologies including andesite. Quartz crystals are very rare, and range in size from mostly small fragments <0.3 mm to extremely rare rounded grains up to ~1 mm. Plagioclase is completely altered, but crystal pseudomorphs are visible, indicating a moderate crystal content. Some shapes resemble pyroxene.

Hydrothermal alteration:
Alteration is intense. The groundmass is altered to fine quartz and clay, with minor Fe-Ti oxides and pyrite. Pyrite and quartz veins are visible, and secondary quartz often surrounds lithics. Pumice is mostly altered to clay. Plagioclase and possible ferromagnesian minerals are altered mainly to clay, but also quartz and Fe-Ti oxides.

Mineralogy:
Groundmass ~60%
Crystals ~10%
Lithics ~1-2%
Pumice ~25-30%

Primary minerals	Abundance	Secondary minerals	Abundance
Plagioclase	~10%	Quartz	>30%
Quartz	<1%	Clay	>20%
Ferromagnesian minerals?	<1%	Fe-Ti oxides	1-5%
Zircon	Trace	Pyrite	1-5%

Sample: NM3, 1495.7-1497.7 mRF

Rock type: Volcaniclastic

Hand Sample Description:
Pale grey rock with a moderate crystal and lithic content and minor pumice clasts. Pumice is not significantly elongate to suggest welding, and are altered to a green colour. Lithics are common and mostly white with visible phenocrysts. Light grey-greenish lithic clasts are also present, while dark grey greywacke lithics are rare.

Thin Section Description:
Dominated by intensely altered groundmass, with common extensively altered lithics including sandstone, mudstone, and possible rhyolite (with common embayed quartz phenocrysts). Quartz is minor, rarely reaching sizes of >1 mm, and commonly 0.5-1 mm. It is only rarely embayed compared to the rhyolite lithics. Feldspar is completely altered, but appears to have been common in the original rock. Cavities are common, and many appear to be due to dissolution of crystals; probably mainly feldspar, but possibly also ferromagnesian minerals. Many have later been partly or wholly in-filled. Some altered pumice clasts are observed. Rare zircons.

Hydrothermal alteration:
Alteration is intense. The groundmass is altered to a clay-quartz-chlorite-rich assemblage, with minor leucoxene. Pumice clasts are altered to chlorite and clay. Quartz phenocrysts in lithics sometimes have secondary quartz overgrowths. Plagioclase is altered to clay, wairakite, clinozoisite, epidote, chlorite, quartz, or adularia. Much of this appears to infill cavities caused by dissolution of crystals, commonly growing in from the cavity walls. Some chlorite may be altered ferromagnesians. Quartz and wairakite veins are present, with rare apatite in some.

Mineralogy:
Groundmass ~75-85%
Crystals ~5-15%
Lithics ~5-10%
Pumice ~4-5%

Primary minerals	Abundance	Secondary minerals	Abundance
Plagioclase	5-10%	Clay	>20%
Quartz	1-2%	Quartz	10-20%
Ferromagnesian minerals?	1-2%	Chlorite	5-10%
Zircon	Trace	Wairakite	1-5%
		Adularia	1-5%
		Clinozoisite/Epidote	1-5%
		Apatite	<1%
		Fe-Ti oxides	1-5%
		Pyrite	1-5%

Sample: NM3, 1743-1745 mRF

Rock type: Welded ignimbrite

Hand Sample Description:
Grey-greenish ignimbrite with common crystals, and minor pumice and lithics. Lithics are generally small (<5 mm) and rounded, consisting of dark sandstone/mudstone as well as light grey and green grains. Pumice is generally small and flattened, giving the rock a eutaxitic texture, indicating welding. Common felsic crystals.

Thin Section Description:
Dominated by altered groundmass, but crystals are common. Relict pumice fiamme are common giving the rock a eutaxitic texture. Andesite lithics are also present, with rare recrystallised, fine-grained sedimentary rock. Quartz is minor and reaches ~1 mm in size, although it is generally <0.5 mm. Plagioclase crystals and crystal fragments are common, with twinning preserved in places. Possible rare ferromagnesian minerals. Rare zircon.

Hydrothermal alteration:
Alteration is moderate to strong. The groundmass is mainly altered to quartz and clay, with chlorite commonly replacing pumice and lithic groundmass. In some fiamme secondary quartz forms euhedral crystals surrounded by chlorite, possibly infilling cavities caused by partial dissolution of pumice. Calcite and epidote/clinozoisite also appear to be related to alteration of pumice. Plagioclase is replaced by albite, calcite and clay. Possible ferromagnesian minerals are completely altered to chlorite. Pyrite and leucoxene occur throughout the rock.

Mineralogy:
Groundmass ~55-65%
Crystals ~20-25%
Lithics ~2-3%
Pumice ~10-15%

Primary minerals	Abundance	Secondary minerals	Abundance
Plagioclase	~20%	Quartz	>20%
Quartz	~1%	Clay	>20%
Ferromagnesian minerals?	1-2%	Chlorite	5-10%
Zircon	Trace	Albite	5-10%
		Calcite	5-10%
		Epidote/clinozoisite	<1%
		Fe-Ti oxides	1-5%
		Pyrite	1-5%

Sample: NM4, 1225 – 1226 mRF

Rock type: ?

Thin Section Description:
Intensely altered rock with primary textures virtually obliterated, although in places there is a hint of possible banding. Rare primary quartz fragments are <0.5mm. Relict pseudomorphs indicate plagioclase may have been common in the original rock. Open cavities and veins are common.

Hydrothermal alteration:
Alteration is intense. The groundmass and primary crystals excluding quartz are completely altered to clay or quartz. Pyrite is common, some disseminated in the groundmass, but particularly lining cavities/veins.

Mineralogy:

Primary minerals	Abundance	Secondary minerals	Abundance
Quartz	0-5%	Quartz	>40%
Plagioclase?	?	Clay	>30%
		Pyrite	5-10%

Sample: NM4 1475.2-1477.2 mRF

Rock type: ?

Thin Section Description:
Intensely altered volcaniclastic rock. Rare quartz up to ~0.5 mm are the only primary crystals preserved, but crystal pseudomorphs indicate they were reasonably common in the original rock. Small lithics up to ~4 mm.

Hydrothermal alteration:
Alteration is intense. The groundmass is strongly silicified, with common clay altered patches. Some are clearly crystal pseudomorphs, but some of the larger, more irregular patches may have been pumice or lithics. Pyrite is common throughout, with rare Fe-Ti oxides.

Mineralogy:
Crystals ~10-30%?

Primary minerals	Abundance	Secondary minerals	Abundance
Quartz	<1%	Quartz	>50%
Plagioclase?		Clay	20-50%
		Pyrite	5-10%
		Fe-Ti oxides	1-5%

Sample: NM5, 1775-1778 mRF

Rock type: Welded Ignimbrite

Hand Sample Description:
Light grey to pale green, strongly welded ignimbrite, with a eutaxitic texture defined by common flattened, altered (green) pumice fragments. Minor amount of lithics are mainly andesite or rhyolite, with possible greywacke, and are up to ~1 cm in size. Moderate crystal component set in a highly altered groundmass.

Thin Section Description:
Contains clasts of altered, flattened pumice with quartz and feldspar phenocrysts. Rare andesite and rhyolite (with quartz and feldspar phenocrysts) lithics. The groundmass is strongly altered, but weak flow banding is visible. Quartz crystals are commonly embayed and some are >1 mm in size. Rare skeletal quartz crystals. Plagioclase crystals are large (many >1 mm), and twinning is preserved in places (estimated composition An≥40%). Altered ferromagnesian minerals are mostly amphibole, with possible pyroxene (based on shape).

Hydrothermal alteration:
Alteration is moderate to strong. Pumice and groundmass is commonly altered to quartz and clay. Plagioclase crystals are wholly or partly replaced by albite, calcite, rare adularia, and to a lesser extent clay and Fe-Ti oxides, particularly along cleavage planes. Ferromagnesian minerals are completely altered to chlorite, calcite, and Fe-Ti oxides. Rare pyrite. Rare calcite veins.

Mineralogy:
Groundmass ~50-60%
Crystals ~20%
Lithics ~10%
Pumice ~10-15%

Primary minerals	Abundance	Secondary minerals	Abundance
Plagioclase	~15%	Quartz	20-50%
Quartz	1-2%	Albite	10-20%
Ferromagnesian minerals		Calcite	5-10%
(amphibole ± pyroxene?)	1-2%	Chlorite	1-5%
Zircon	Trace	Clay	5-10%
		Adularia	<1%
		Fe-Ti oxides	<1%
		Pyrite	<1%

Sample: NM8A, 2525.0-2526.8 mRF

Rock type: Volcaniclastic

Hand Sample Description:
Intensely altered volcaniclastic rock with common quartz veins. The rock is very hard, altered to a light grey/greenish colour, and contains dark grey/green patches that are possibly altered crystals, although some may also be altered lithic fragments. Pyrite is sometimes visible in these patches. Rare quartz phenocrysts are visible.

Thin Section Description:
Crystals and possible lithic/pumice fragments are contained in an altered groundmass, with no primary textures observed. Quartz veins are common. Quartz phenocrysts are minor, are sometimes embayed, and sometimes show undulose extinction. Plagioclase is rare in parts, but is more common in some places. It is generally partially altered, although it is sometimes relatively fresh with twinning visible. Altered clay and chlorite patches are possibly altered ferromagnesian minerals, although some of the larger patches may be altered pumice or lithics.

Hydrothermal alteration:
Alteration is strong to intense. The groundmass is intensely altered, mostly to secondary quartz, with common quartz veins. In places it is clay-rich, with minor chlorite, with the more defined clay and chlorite patches resembling altered pumice, lithics and crystals. Plagioclase is partially altered to albite, rare calcite, and quartz.
Mineralogy:
Groundmass >60%
Crystals ~10-25%
Lithics ~0-10%
Pumice ~0-10%

Primary minerals	Abundance	Secondary minerals	Abundance
Plagioclase	10-20%	Quartz	>50%
Quartz	5-10%	Clay	10-20%
Ferromagnesian minerals?	<5%?	Chlorite	0-5%
		Albite	0-5%
		Calcite	<1%
		Epidote	<1%
		Fe-Ti oxides	0-5%
		Pyrite	<1%

Sample: NM11, 2083.0-2089.1 mRF

Rock type: Welded ignimbrite

Hand Sample Description:
Light grey, welded ignimbrite containing common pumice fiamme and lithics. Some fiamme, particularly the smaller ones, are altered to a greenish colour. Large pumice clasts up to 5 cm in length remain vesicular in places, with a brown-orange colour, although parts are sometimes altered to clay and/or chlorite. Lithics are common, and are up to ~2 cm in size. Dark greywacke or andesite lithics are present, while light grey-greenish, and some pinkish lithics, some with visible phenocrysts, indicate a variety of volcanic lithics are also present.

Thin Section Description:
Common crystals, lithics, and pumice in a fine, altered groundmass. Large flattened pumice often have open voids. Alignment of pumice and wispy fiamme shapes indicate welding. Lithics include fine-grained sediments, andesite, and possibly rhyolite. Crystals are mostly plagioclase, with minor quartz and completely altered ferromagnesian minerals.

Hydrothermal alteration:
Alteration is moderate to strong. Pumice is altered to clinozoisite, epidote, chlorite, clay, and quartz. Plagioclase is often partially altered to albite and rarely adularia, but remains fresh in places. Possible ferromagnesian minerals are altered to chlorite and epidote. Lithics are often strongly altered to clinozoisite, quartz, and clay.

Mineralogy:
Groundmass ~40-50%
Crystals ~30%
Lithics ~10-15%
Pumice ~10-15%

Primary minerals	Abundance	Secondary minerals	Abundance
Plagioclase	20-30%	Quartz	>10%
Quartz	1-2%	Albite	10-20%
Ferromagnesian minerals?	1-5%	Clay	5-10%
		Chlorite	5-10%
		Clinozoisite/epidote	5-10%
		Calcite	1-5%
		Adularia	1-5%
		Fe-Ti oxides	1-5%

Sample: RK6, 1612-1614 mRF

Rock type: Welded ignimbrite

Hand Sample Description:
Light grey welded ignimbrite with wispy, highly attenuated fiamme. These are mostly small (~1 cm by <1 mm) and well aligned. Altered lithic clasts up to ~1 cm are also present, many altered to clay, although light grey lithics are also present. Crystals are visible in some lithics as well as in the fine, light grey groundmass.

Thin Section Description:
The alignment of fiamme is clear in sections cut vertically through the core. These are highly elongate and mostly small, although some of the larger fiamme, mostly containing phenocrysts within them, exceed 1 mm in width. Altered, fine-grained lithics with phenocrysts are visible. The crystal content is dominated by altered plagioclase, although rare pyroxene can be identified by shape. Most of the completely altered ferromagnesian minerals cannot be identified.

Hydrothermal alteration:
Alteration is strong. The groundmass is altered primarily to quartz, with minor Fe-Ti oxides. Pumice is primarily altered to clay. Plagioclase is altered to albite, adularia, calcite, epidote and quartz. Ferromagnesian minerals are altered to chlorite, epidote, clinozoisite, and quartz.

Mineralogy:
Groundmass ~50-70%
Crystals ~20-25%
Lithics ~1-10%
Pumice ~10-15%

Primary minerals	Abundance	Secondary minerals	Abundance
Plagioclase	20-25%	Quartz	>20%
Ferromagnesian minerals	<1%	Albite	5-10%
		Clay	10-20%
		Chlorite	<1%
		Clinozoisite/epidote	<1%
		Calcite	1-5%
		Adularia	1-5%
		Fe-Ti oxides	1-5%

Cuttings:

Sample: NM5, 1100 mRF

Rock type: Mixed cuttings

Hand Sample Description:
The cuttings are mixed, with colour ranging from white to black, although they are most commonly white to pale-grey. Size ranges from fine sand to almost 1 cm in size. Darker coloured crystals/lithics are often visible within the light coloured grains, whereas they are not visible in the dark grains which are probably sedimentary.

Optical Microscope Description:
The very dark grey-black grains are fine-grained, without obvious phenocrysts, although some contain small white grains (andesite?). They have some vein material, and some are pyrite-rich. Light grey grains are crystal-rich, with common large quartz phenocrysts, plagioclase, and altered ferromagnesian minerals and/or Fe-Ti oxides. The white grains are most common, and have much fewer crystals than the grey ones, although felsic crystals are a minor component. Glass shard shapes can rarely be seen in the groundmass of these grains.

Thin Section Description:
At least 3 different lithologies are observed in thin section, and can be matched with those described above. The darkest grains appear to be fine-grained sediments, ranging from light brown to very dark brown. Small, angular quartz and feldspar fragments are sometimes present, and weak layering is sometimes visible. The light grey grains appear to be rhyolite, with common quartz and plagioclase phenocrysts, rare ferromagnesians, and a fine groundmass with well developed flow banding. The white grains appear to be an altered crystal-poor tuff, containing large embayed quartz phenocrysts up to ~1.5 mm, completely altered plagioclase, and possible completely altered ferromagnesian minerals. The groundmass is intensely altered, and no textures are preserved.

Hydrothermal alteration:
Alteration varies with rock type, being low in the rhyolite, but much stronger in the sediments and tuff. The groundmass of the tuff is intensely altered to fine-grained quartz, clay, Fe-Ti oxides, and pyrite. Plagioclase is completely altered, mostly to clay, but also to quartz and possibly calcite. Calcite might also represent altered ferromagnesians. Some voids are filled by mosaics of quartz, others have quartz rims and are filled with calcite.

Mineralogy: (of the tuff only)
Crystals ~10-20%

Primary minerals	Abundance	Secondary minerals	Abundance
Quartz	5-10%	Quartz	>50%
Plagioclase	5-10%	Calcite	5-10%
Ferromagnesian minerals?	<1%	Clay	5-10%
		Fe-Ti oxides	1-5%
		Pyrite	1-5%

Sample: NM5, 1125 mRF

Rock type: Vitric tuff

Hand Sample Description:
Cuttings are rusty-brown in colour caused by extensive Fe-staining. Moderately-well sorted, being mostly fine-medium sand size. Most of the larger grains (coarse sand size) are white, but rare black grains are also present.

Optical Microscope Description:
Fe-staining is extensive. Cuttings are a mix of white (tuff?) grains and felsic crystals, with a moderate amount of grey (lithic?) grains. Some light rhyolitic lithics are also present. Minor pyrite.

Thin Section Description:
Dominated by fine, altered tuff fragments. There is a minor component of fine-grained sedimentary grains, and some fine-grained, carbonate-rich grains. Fe-oxides are common. Quartz fragments are common, and reach a maximum size of ~0.7mm. Plagioclase is completely altered.

Hydrothermal alteration:
Alteration is strong. Groundmass of the tuff is altered to quartz and clay, while some of the grains are carbonate-rich. Calcite mostly occurs as either as an infill material or as an alteration product of plagioclase. Rare adularia and possible albite are also alteration products of plagioclase. Pyrite is minor. Quartz mosaics infill voids/veins.

Mineralogy:
Crystals ~10-15%

Primary minerals	Abundance	Secondary minerals	Abundance
Quartz	10-15%	Quartz	20-50%
Plagioclase	~1%	Clay	5-10%
		Calcite	5-10%
		Adularia	<1%
		Albite?	<1%
		Pyrite	1-5%

Sample: NM5, 1175 mRF

Rock type: Vitric tuff?

Hand Sample Description:
Cuttings are a rusty, pale brown colour, with extensive Fe-staining. Moderately-well sorted, ranging from very fine to medium sand size. Many of the larger grains are rusty to white, but minor dark grains are present.

Optical Microscope Description:
Most grains are white (tuff ?) although felsic crystals are also common. High degree of Fe-staining surrounds dark grains, and also coats surrounding grains. Possible rare ferromagnesian minerals. Minor amount of grey grains which could represent lithic fragments. Minor pyrite is often cubic.

Thin Section Description:
Dominated by altered groundmass (tuff?). Some of the darker grains appear to be fine-grained sediments. The tuff appears crystal-poor as most crystals are separate from the groundmass. Rarely quartz crystals reach ~1 mm, but are generally <0.5 mm. Plagioclase is very rare and altered. Extensive Fe-staining.

Hydrothermal alteration:
Alteration is strong. The groundmass is extensively clay and quartz altered. Plagioclase is replaced by calcite, albite, adularia, and possibly clay. Some calcite may also be due to alteration of the groundmass, and some may be due to void/vein infill. Interlocking quartz mosaics are likely infill material. Pyrite is reasonably common.

Mineralogy:
Crystals ~10-15%

Primary minerals	Abundance	Secondary minerals	Abundance
Quartz	10-15%	Quartz	20-50%
Plagioclase	1%	Clay	20-50%
		Calcite	5-10%
		Albite	<1%
		Adularia	<1%
		Fe-Ti oxides	5-10%
		Pyrite	1-5%

Sample: NM5, 1225 mRF

Rock type: Vitric tuff?

Hand Sample Description:
Cuttings are moderately-well sorted, mostly very fine-medium sand size. Pale grey in colour, with Fe-staining.

Optical Microscope Description:
Mostly white grains which are likely altered groundmass material. Minor amount of felsic crystals and rare grey lithic fragments. Possible rare rhyolite lithic fragments. Some rare black grains may be ferromagnesian minerals. Minor pyrite and moderate Fe-staining.

Thin Section Description:
Dominated by fine, altered groundmass material (tuff?). Rare lithics include andesite (common microphenocryst feldspar laths). Rarely quartz crystals exceed 0.5 mm in size, but mostly they are finer than this. Plagioclase is rare, although it may have originally been more abundant as it often appears to be completely altered.

Hydrothermal alteration:
Alteration is strong to intense. Groundmass is altered to quartz (± albite?), with common clay. Plagioclase is replaced by calcite, albite, and adularia in rare cases.

Mineralogy:
Crystals ~10%

Primary minerals	Abundance	Secondary minerals	Abundance
Quartz	5-10%	Quartz	20-50%
Plagioclase	1-5%	Clay	20-50%
		Calcite	5-10%
		Albite	<1%
		Adularia	<1%
		Fe-Ti oxides	1-5%
		Pyrite	<1%

Sample: NM5, 1300 mRF

Rock type: Vitric tuff?

Hand Sample Description:
Cuttings are moderately-well sorted, being mostly fine to very fine sand size, but ranges up to coarse sand size. Pale grey in colour, but with an orange tinge caused by Fe-staining.

Optical Microscope Description:
Grains are mostly white, but many have common small black and/or pyrite inclusions. Moderate amount of felsic crystals. Grey lithic grains are a minor component, and include andesite (feldspar laths), and possibly greywacke. Moderate amount of pyrite, and minor Fe-staining. Rare small black grains.

Thin Section Description:
Grains mostly consist of fine, altered groundmass material (tuff?). Some grains are slightly darker and may be rhyolite/dacite, but most appear to be a crystal-poor tuff. Quartz crystals are up to 1 mm in size, but most are <0.5 mm. Plagioclase is rare or entirely replaced. Andesite lithic fragments can rarely be identified, sometimes within the tuff grains, and have small plagioclase laths. Possible relict biotite and pyroxene.?

Hydrothermal alteration:
Alteration is strong to intense. The groundmass is strongly quartz and clay altered, although parts are carbonate-rich (lithics?). Plagioclase is altered to calcite, albite, adularia, and probably clay. Pyrite and Fe-Ti oxides are minor. Mosaics of quartz are likely infill material.

Mineralogy:

Crystals ~5-10%

Primary minerals	Abundance	Secondary minerals	Abundance
Quartz	~5%	Quartz	20-50%
Plagioclase	1-5%	Clay	10-20%
Pyroxene?	<1%	Calcite	5-10%
Biotite?	Trace	Albite	1-5%
		Adularia	<1%
		Pyrite	1-5%
		Fe-Ti oxides	1-5%

Sample: NM5, 1350 mRF

Rock type: Vitric tuff / rhyolite breccia?

Hand Sample Description:

Cuttings are well sorted, pale grey to white in colour, and mostly fine to very fine sand size. Rare larger grains are a mix of white, dark grey, and Fe-stained grains.

Optical Microscope Description:

Grains are mostly white, with a minor amount of felsic crystals. Grey lithic fragments are rare. Pyrite and Fe-staining are both also quite rare. Small amount of black grains.

Thin Section Description:

Dominated by altered groundmass, although there is some variation in colour. The lightest grains are intensely altered and appear similar to the tuff above. Some grains are darker and less altered. Spherulites and weak banding are sometimes visible in these grains and could indicate rhyolite. Possible rare andesite and argillite lithics. Quartz is rare and up to 0.8 mm, but are generally <0.5 mm. Rare plagioclase. Possible relict biotite?

Hydrothermal alteration:

Alteration is moderate to strong. Banding textures can be seen in some grains, but the groundmass is generally strongly altered to quartz or clays. Plagioclase is altered to calcite or albite, and rarely adularia.

Mineralogy:

Crystals ~5-10%

Primary minerals	Abundance	Secondary minerals	Abundance
Quartz	1-5%	Quartz	20-50%
Plagioclase	1-5%	Clay	10-20%
Biotite?	<1%	Calcite	5-10%
		Albite	<1%
		Adularia	<1%
		Fe-Ti oxides	1-5%
		Pyrite	1-5%

Sample: NM5, 1400 mRF

Rock type: Tuff?

Hand Sample Description:

Cuttings are pale grey to white, moderately-well sorted, and mostly medium to fine sand size. Rare dark grains.

Optical Microscope Description:

Grains are mostly white (altered groundmass?), with a minor amount of felsic crystals. Rare dark grey grains are likely lithics. Rare pyrite, and rare Fe-staining. Rare small black grains.

Thin Section Description:

Dominated by altered groundmass (tuff?), with rare lithics including andesite, and possibly greywacke. Quartz is relatively rare, and reaches ~0.8 mm, although it is generally <0.5 mm. Plagioclase is rare and strongly altered.

Hydrothermal alteration:

Alteration is strong. The groundmass is strongly altered to clay and quartz. Clay minerals often form around the edge of grains consisting of glassy groundmass. Plagioclase crystals are replaced by calcite, albite, and adularia. Mosaics of large quartz crystals are likely vein infill material. Rare pyrite and Fe-oxides.

Mineralogy:
Crystals ~10-15%

Primary minerals	Abundance	Secondary minerals	Abundance
Quartz	1-5%	Clay	20-50%
Plagioclase	~10%	Quartz	20-50%
		Calcite	1-5%
		Albite	~1%
		Adularia	~1%
		Fe-Ti oxides	1-5%
		Pyrite	<1%

Sample: NM5, 1450 mRF

Rock type: Vitric tuff?

Hand Sample Description:
Cuttings are moderately well sorted, pale grey to white in colour, and mostly medium to very fine sand size. White grains are common, but dark grey and rust coloured grains are also present.

Optical Microscope Description:
Grains are mostly white, with a small amount of felsic crystals. Grey lithic grains are a minor component. Pyrite is a minor component, and Fe-staining is minor. Rare small black grains.

Thin Section Description:
Dominated by altered groundmass (tuff?), with rare lithics of andesite. Spherulite-like textures can be seen in places. Slightly darker grains are possibly lithic fragments. Quartz is rare and fine <0.5mm. Plagioclase is rare and strongly altered.

Hydrothermal alteration:
Alteration is strong. Groundmass is altered to quartz and clay. Plagioclase is altered to albite, calcite or adularia.

Mineralogy:
Crystals ~10-20%

Primary minerals	Abundance	Secondary minerals	Abundance
Plagioclase	10-15%	Quartz	20-50%
Quartz	1-5%	Clay	20-30%
Zircon	Trace	Albite	1-5%
		Calcite	1-5%
		Adularia	~1%
		Fe-Ti oxides	1-5%
		Pyrite	<1%

Sample: NM5, 1500mRF

Rock type: Tuff?

Hand Sample Description:
Cuttings are pale grey to white, moderately-well sorted, and very fine sand to medium sand size. Grey grains are rare, as is Fe-staining.

Optical Microscope Description:
Grains are mostly white (altered groundmass?), with a minor amount of felsic crystals. Rare dark grey grains are likely lithics, some of which appears to be andesite, but some is likely greywacke. Rare pyrite, and rare Fe-staining. Rare greenish grains, possibly chlorite. Possible rare ferromagnesian minerals.

Thin Section Description:
Dominated by altered groundmass, probably of crystal-poor tuff? While most quartz crystals are <0.3 mm, they commonly reach sizes of 0.5-0.7 mm. Plagioclase is rare and completely altered. Rare andesite lithics.

Hydrothermal alteration:
Alteration is strong. Groundmass is intensely clay and quartz altered. Plagioclase is replaced by calcite, albite and possibly quartz. Minor pyrite, Fe-Ti oxides, and adularia. Coarse, interlocking quartz mosaics infill voids.

Mineralogy:
Crystals ~10-20%

Primary minerals	Abundance	Secondary minerals	Abundance
Quartz	1-5%	Quartz	20-50%
Plagioclase	10-15%	Clay	20-50%
Zircon	Trace	Calcite	1-5%
		Albite	1-5%
		Adularia	1-2%
		Fe-Ti oxides	1-5%
		Pyrite	<1%

Sample: NM5, 1550 mRF

Rock type: Crystal-vitric tuff?

Hand Sample Description:
Cuttings are moderately well sorted, pale grey-white in colour, and mostly medium to very fine sand size. Some of the larger grains (up to coarse sand size) are dark grey, some are white, and rare Fe-staining is present.

Optical Microscope Description:
Grains are mostly white with a minor amount of felsic crystals. Rare dark grey grains are likely lithics, some of which appear to be andesite. Rare pyrite, and rare Fe-staining. Rare small black grains.

Thin Section Description:
Dominated by altered groundmass. Minor amount of andesite lithics (possible greywacke/argillite?). Quartz crystals reach a size of >1 mm, but are commonly between 0.5-1 mm, and sometimes embayed. They are often set within the altered, fine-grained groundmass. Altered plagioclase is reasonably common. Possible relict biotite.

Hydrothermal alteration:
Alteration is strong. The groundmass is strongly quartz and clay altered. Plagioclase is commonly replaced by calcite, albite, and in some cases adularia. Rare pyrite.

Mineralogy:
Crystals ~15-20%

Primary minerals	Abundance	Secondary minerals	Abundance
Plagioclase	5-10%	Quartz	20-50%
Quartz	5-10%	Clay	10-20%
Biotite?	Trace	Albite	5-10%
		Calcite	1-5%
		Adularia	1-5%
		Fe-Ti oxides	<1%
		Pyrite	<1%

Sample: NM5, 1600 mRF

Rock type: Tuff?

Hand Sample Description:
Cuttings are pale grey/white, moderately sorted, and very fine sand to coarse sand size. Minor dark grey grains.

Optical Microscope Description:
Grains are mostly white (altered groundmass?), with a minor amount of felsic crystals. Minor amount of dark grey grains are likely lithics – they are more common than above. Rare pyrite, and rare Fe-staining. Rare greenish grains are likely chlorite? Possible rare ferromagnesian minerals?

Thin Section Description:
Dominated by altered groundmass, and is crystal-poor. While most quartz crystals are <0.5 mm, they sometimes reach sizes of 1 mm, while one crystal forms a ribbon ~3 mm long. Plagioclase is rare or entirely replaced. Rare lithics; many appearing to be carbonate-rich. Some have small micas and rounded quartz grains.

Hydrothermal alteration:
Alteration is strong. Groundmass is intensely clay and quartz altered (possibly with albite?). Plagioclase is entirely replaced by calcite, albite, and adularia. Minor pyrite and Fe-Ti oxides. Coarse, interlocking quartz mosaics are likely infill material, with rare veins visible.

Mineralogy:
Crystals ~10%

Primary minerals	Abundance	Secondary minerals	Abundance
Quartz	1-5%	Quartz	20-50%
Plagioclase	5-10%	Clay	20-50%
		Adularia	1-5%
		Calcite	1-5%
		Albite	1-5%
		Pyrite	1-5%
		Fe-Ti oxides	>1%

Sample: NM5, 1650 mRF

Rock type: Vitric tuff?

Hand Sample Description:
Cuttings are well sorted, mostly medium to very fine sand size, with a white colour. Rare dark and rusty grains.

Optical Microscope Description:
Mostly white grains with a small component of felsic crystals. Very few grey lithic grains – most dark grains appear crystalline. Rare greenish (chlorite?) grains. Minor amount of pyrite. Rare Fe-staining.

Thin Section Description:
Dominated by fine fragments of altered groundmass. Rarely quartz crystals are between 0.5-1 mm in size, but more commonly they are <0.3 mm. Plagioclase appears to have been fairly common in the original rock.

Hydrothermal alteration:
Alteration is strong to intense. The groundmass is strongly quartz and clay altered. Probable plagioclase is completely altered to calcite, adularia and possibly albite. Rare chlorite is also present. Rare vein quartz.

Mineralogy:
Crystals ~10-15%

Primary minerals	Abundance	Secondary minerals	Abundance
Plagioclase	~10%	Quartz	20-50%
Quartz	1-5%	Clay	20-50%
		Calcite	~5%
		Adularia	1-5%
		Albite	1-5%
		Chlorite	<1%
		Fe-Ti oxides	1-5%
		Pyrite	<1%

Sample: NM5, 1700 mRF

Rock type: Vitric tuff?

Hand Sample Description:
Cuttings are pale grey to white, moderately-well sorted, and mostly very fine sand to medium sand size. Dark grey grains are minor, and Fe-staining is rare.

Optical Microscope Description:
Grains are mostly white (altered groundmass?), with a minor amount of felsic crystals. Rare dark grey grains are likely lithics. Rare pyrite, and rare Fe-staining. Some greenish grains are likely chlorite.

Thin Section Description:
Dominated by altered groundmass – crystal-poor. Quartz crystals reach ~1mm in size, but are generally <0.5 mm. Plagioclase is rare and strongly altered. Lithics cannot be identified with confidence.

Hydrothermal alteration:
Alteration is strong. Groundmass is intensely silicified, with some clay alteration. Possible plagioclase is replaced by calcite and albite. Some calcite appears to be infilling voids alongside quartz, while some may be altered groundmass. Minor pyrite often occurs in clusters and rare Fe-Ti oxides. Coarse, interlocking quartz mosaics are likely infill material. Rare chlorite.

Mineralogy:
Crystals ~10-15%

Primary minerals	Abundance	Secondary minerals	Abundance
Plagioclase	5-10%	Quartz	20-50%
Quartz	~5%	Clay	10-20%
		Calcite	5-10%
		Adularia	1-5%
		Albite	<1%
		Chlorite	<1%
		Fe-Ti oxides	<1%
		Pyrite	<1%

Sample: NM5A, 1700 mRF

Rock type: Tuff/ignimbrite?

Hand Sample Description:
Very pale grey to white in colour with a greenish tinge to some of the grains. Poorly sorted, ranging from very fine sand to fine pebbles almost 1 cm in size. Rare dark grey (lithic?) grains.

Optical Microscope Description:
Grains are mostly white, and appear strongly altered. Phenocrysts are sometimes visible – rarely clear crystals (quartz?) or pinkish crystals (calcite?), but more commonly green (chlorite). Rare dark lithic grains, and possible light rhyolite/dacite lithics. Rare pinkish grains – could be carbonate.

Thin Section Description:
Crystal-poor tuff containing minor plagioclase and rare quartz phenocrysts, with altered, fine-grained lithics set in a fine, altered groundmass. Quartz reaches ~0.7 mm, with rare embayments, although fine angular fragments are more common. Plagioclase consists of rare euhedral to subhedral crystals up to ~0.7 mm, and more common fine crystal fragments. Lithic fragments are also fine-grained with an altered groundmass, and some also have feldspar phenocrysts. Possible altered ferromagnesian minerals.

Hydrothermal alteration:
Alteration is strong to intense. The groundmass of both the tuff and the lithics are altered to fine quartz, clay, calcite, chlorite, Fe-Ti oxides and pyrite. Plagioclase is altered to albite, calcite, adularia and clay. Possible ferromagnesian minerals are completely altered to quartz.

Mineralogy:
Crystals ~10-15%

Primary minerals	Abundance	Secondary minerals	Abundance
Plagioclase	10-15	Quartz	>20%
Quartz	~1%	Clay	>10%
Ferromagnesian minerals?	<1%?	Calcite	10-20%
		Albite	5-10%
		Chlorite	1-5%
		Adularia	~1%
		Fe-Ti oxides	1-5%
		Pyrite	<1%

Sample: NM5, 1750 mRF

Rock type: Tuff/ignimbrite?

Hand Sample Description:
Cuttings are light grey, very coarse to very fine sand size (mostly medium to fine). Larger grains are a mixture of white, light grey and black/dark grey lithic fragments.

Optical Microscope Description:
Grains are mostly white, but felsic crystals are also common. Many crystals have small, dark inclusions. Many of the dark grains appear crystalline, but lithic grains are also present. Minor amount of pyrite and rare chlorite.

Thin Section Description:
Groundmass dominates this rock, but is strongly altered and no primary textures are visible. Quartz is the most common crystal component, with large crystals sometimes >1 mm in size, and sometimes embayed. Plagioclase is rare. Possible rare ferromagnesian minerals are completely altered.

Hydrothermal alteration:
Alteration is strong. Groundmass is strongly quartz and clay altered. Plagioclase is altered to calcite or adularia (possible albite?). Moderate amount of pyrite and Fe-Ti oxides. Minor veins with quartz and calcite infill.

Mineralogy:
Crystals ~15-25%

Primary minerals	Abundance	Secondary minerals	Abundance
Quartz	10-20%	Quartz	>20%
Plagioclase	~5%	Clay	>10%
		Adularia	1-5%
		Calcite	1-5%
		Fe-Ti oxides	1-5%
		Pyrite	1-5%

Sample: NM5A, 1750 mRF

Rock type: Welded ignimbrite?

Hand Sample Description:
Cuttings appear somewhat mixed. The dominant type is a pale grey to greenish rock which contains altered green lithic/pumice clasts in a fine groundmass. Some clasts are white and appear to have no crystals or lithics. Some are white with pale green fragments and rare fine phenocrysts. Rare dark grey lithics may be greywacke.

Optical Microscope Description:
There is a range of rock types, but the most common seems to be pale grey to white in colour with common green patches of altered pumice, lithics or crystals. Some grains have extensive alteration of the groundmass giving the grain a greenish colour. Altered feldspars appear to be the dominant crystal, but rare grains appear to have quartz phenocrysts. These grains sometimes have glass shard shapes and flattened pumice, and they appear more crystal-rich than other grains. The white grains are very crystal-poor and have no visible textures. Rare rhyolite and greywacke fragments.

Thin Section Description:
Many grains are made up of a clay-rich muddy material which seems to glue together many grains. Fragments that can be identified consist of at least 2 distinct rocks – both tuffs? The first is very crystal-poor, with only very rare plagioclase crystals (<5%) – similar to above. The other type is more common, more crystal-rich, containing plagioclase, quartz, and altered ferromagnesian minerals, probably both pyroxene and amphibole. They also contain lithic fragments and vague pumice shapes.

Hydrothermal alteration:
Alteration intensity varies, but is generally strong to intense. The groundmass is altered to fine quartz, clay, chlorite, Fe-Ti oxides, and rare pyrite. Plagioclase is altered to albite, adularia, calcite, clays and Fe-Ti oxides. Ferromagnesian minerals are altered to chlorite.

Mineralogy: (Crystal-rich tuff only)
Crystals ~20-30%

Primary minerals	Abundance	Secondary minerals	Abundance
Plagioclase	15-20%	Quartz	>20%
Quartz	1-5%	Clay	>10%
Pyroxene?	1-5%	Chlorite	5-10%
Amphibole?	1-5%	Calcite	1-5%
		Albite	1-5%
		Adularia	<1%
		Fe-Ti oxides	1-5%
		Pyrite	<1%

Sample: NM5A, 1775 mRF

Rock type: Welded ignimbrite?

Hand Sample Description:
Light grey and fine-grained, mostly ranging from very fine sand size to medium sand size. Minor Fe-staining.

Optical Microscope Description:
Mostly white grains. Some are large enough to contain crystals – both felsic and altered mafic crystals. Minor amount of separate felsic crystals. Minor Fe-staining and chlorite alteration. Rare pyrite.

Thin Section Description:
Most grains are finely crystalline, most likely altered groundmass, but probably also some fine-grained lithics, and altered pumice clasts. Fine-grained clay and carbonate-rich material is also common. Primary quartz is present as generally fine, angular fragments <0.5 mm, although rare grains are larger, with one fragment ~1.5 mm long. Altered plagioclase is also present as mostly angular fragments, but euhedral to subhedral crystals up to 1 mm are also present. Possible completely altered ferromagnesian minerals.

Hydrothermal alteration:
Alteration is strong. The groundmass is commonly altered to quartz, although some grains are clay or calcite-rich. Plagioclase is altered to albite, calcite, and minor adularia. Chlorite is rare. Vein/cavity infill material of quartz and calcite is present.

Mineralogy:
Crystals ~15-25%

Primary minerals	Abundance	Secondary minerals	Abundance
Plagioclase	15-20%	Quartz	>20%
Quartz	1-5%	Clay	>10%
Ferromagnesian minerals?	<1%	Albite	5-10%
		Calcite	5-10%
		Adularia	<1%
		Chlorite	<1%
		Fe-Ti oxides	<1%
		Pyrite	<1%

Sample: NM5, 1800mRF

Rock type: Tuff/ignimbrite?

Hand Sample Description:
Cuttings are light grey, moderately sorted, coarse to very fine sand sized, with rhyolite and greywacke lithics.

Optical Microscope Description:
Cuttings are mostly white with an altered looking coating. Some clear felsic crystals. Rare dark grains may be ferromagnesian minerals. Grey grains are possibly lithics, some appear rounded. Some green (chlorite?) and pale yellow grains. Pyrite is reasonably common. Minor amount of Fe-staining.

Thin Section Description:
Dominated by altered groundmass, though rare spherulitic textures are present in what may be rhyolite lithics. Crystals of quartz are sometimes >1 mm in size and sometimes embayed. Plagioclase is rare and often altered, and very rare possible ferromagnesian minerals are completely altered.

Hydrothermal alteration:
Alteration is strong. Groundmass is commonly altered to a crystalline mosaic of quartz (± albite?), often with disseminated pyrite and Fe-Ti oxides. Sometimes groundmass is clay altered (pumice clasts?). Plagioclase is replaced by adularia, calcite, and albite (with dark inclusions common along cleavage planes). Possible ferromagnesian minerals are altered to chlorite. Rare sericite. Quartz mosaics of infill material are common.

Mineralogy:
Crystals ~10-20%

Primary minerals	Abundance	Secondary minerals	Abundance
Plagioclase	5-10%	Quartz	20-50%
Quartz	5-10%	Albite	5-10%
		Calcite	5-10%
		Chlorite	<1%
		Adularia	<1%
		Sericite?	<1%
		Pyrite	1-5%
		Fe-Ti oxides	1-5%

Sample: NM5A, 1850 mRF

Rock type: Tuff/ignimbrite?

Hand Sample Description:
Cuttings are light grey/greenish. They are well sorted, mostly fine and very fine sand size. Rare rust coloured grains, and larger white grains are up to coarse sand size.

Optical Microscope Description:
Mostly white fragments with a white alteration coating. Minor amount of clean looking felsic crystals. Minor amount of Fe-staining. Rare greenish grains and pyrite.

Thin Section Description:
Consists mostly of fine, altered groundmass material. Lithics are rare, but andesite can be identified. Some grains are carbonate-rich. One larger quartz crystal is ~0.75mm in size, otherwise all crystals/crystal fragments are <0.5 mm. Many appear to be fragments rather than whole crystals.

Hydrothermal alteration:
Alteration is strong. The groundmass is mostly altered to quartz ± albite, although places appear altered to clay. Plagioclase is replaced by albite and calcite. Chlorite is a minor component, possibly as an alteration product of ferromagnesian minerals. Rare pyrite and Fe-Ti oxides. Contains fibrous crystals of zeolites. Possible sericite?

Mineralogy:
Crystals ~10-15%

Primary minerals	Abundance	Secondary minerals	Abundance
Quartz	1-5%	Quartz	20-50%
Plagioclase	5-10%	Albite	>10%
		Calcite	5-10%
		Clay	5-10%
		Chlorite	<5%
		Zeolites?	<1%
		Sericite?	<1%
		Pyrite	<1%
		Fe-Ti oxides	1-5%

Sample: NM5A, 1900 mRF

Rock type: Volcaniclastic?

Hand Sample Description:
Cuttings are light grey with a greenish tinge, moderately-well sorted, and very fine sand to medium sand sized. Minor amount of Fe-staining, and rare dark grains.

Optical Microscope Description:
Most grains are white and are likely altered groundmass material, but green grains are also common (chlorite?). Felsic crystals are a minor. Pyrite is very rare. Dark lithic fragments are extremely rare. Minor Fe-staining.

Thin Section Description:
Dominated by altered groundmass. Quartz is rare and fine, rarely reaching 0.6 mm, and generally <0.3 mm. Plagioclase is more common, but generally strongly altered. Rare andesite lithics. Rare zircons.

Hydrothermal alteration:
Alteration is strong. Groundmass is altered to quartz (± albite?), with minor clay alteration and moderate chloritisation. Plagioclase is altered to albite (which contains common opaque inclusions) and to a lesser degree calcite. Possible ferromagnesian minerals are altered to chlorite. Rare pyrite, Fe-Ti oxides, and possible epidote?

Mineralogy:
Crystals ~15-25%

Primary minerals	Abundance	Secondary minerals	Abundance
Plagioclase	10-20%	Quartz	>20%
Quartz	1-5%	Albite	10-20%
Zircon	<1%	Calcite	5-10%
		Chlorite	5-10%
		Clay	1-5%?
		Fe-Ti oxides	1-5%
		Pyrite	<1%
		Epidote?	<1%

Sample: NM5A, 1950 mRF

Rock type: Volcaniclastic?

Hand Sample Description:
Cuttings are well sorted, light grey/white with a slight greenish tinge, and mostly medium to very fine sand sized. Larger grains up to coarse sand size are mostly white, with subordinate rusty/orange, and rare dark grains.

Optical Microscope Description:
Mostly white fragments with a white alteration coating. Minor amount of clean looking felsic crystals. Minor amount of Fe-staining. Rare greenish grains. Some greywacke and volcanic lithics with visible phenocrysts.

Thin Section Description:
Dominated by altered groundmass and feldspar crystals. Lithics include glassy rhyolite (weakly banded) and andesite (feldspar phenocrysts and microphenocrysts with chlorite-altered ferromagnesian minerals), possible greywacke. Quartz crystals are rare and fine (<0.4mm, mostly <0.3mm). Plagioclase is common, with larger crystals (<75mm).

Hydrothermal alteration:
Alteration is strong. Groundmass is commonly microcrystalline (quartz ± albite?), in places it is clay altered, and rarely forms mosaics of irregularly shaped crystals. Plagioclase is commonly replaced by albite, and rarely calcite and epidote. Chlorite and epidote may also represent replacement of ferromagnesian minerals. Minor pyrite, Fe-Ti oxides and possible acicular clinozoisite, sericite and zeolites (radial aggregate of fibrous crystals).

Mineralogy:
Crystals ~25-35%

Primary minerals	Abundance	Secondary minerals	Abundance
Plagioclase	20-30%	Quartz	>20%
Quartz	1-5%	Albite	>20%
		Epidote/Clinozoisite	1-5%
		Calcite	1-5%
		Chlorite	1-5%
		Clay	1-5%
		Sericite?	<1%
		Zeolites?	<1%
		Fe-Ti oxides	<1%
		Pyrite	<1%

Sample: NM5A, 2000 mRF

Rock type: Volcaniclastic?

Hand Sample Description:
Cuttings are light grey in colour, moderately-well sorted, medium to very fine sand size. Minor amount of Fe-staining. Some grains up to coarse sand size are mostly white or light grey, with very rare dark grains.

Optical Microscope Description:
Most grains are white; probably altered groundmass material. Moderate amount of felsic crystals. Minor amount of green grains are likely chlorite. Moderate amount of yellow crystals (epidote?). Pyrite is very rare.

Thin Section Description:
Dominated by fine-grained groundmass. Quartz is rare and fine (<0.3 mm). Altered plagioclase is common. Rare andesite lithics with common feldspar laths can be identified.

Hydrothermal alteration:
Alteration is strong. Groundmass is strongly quartz (± albite?) altered, with minor clays. Plagioclase is altered to albite with common opaque inclusions, and in places replaced by calcite or epidote. Rare chlorite may have replaced ferromagnesian minerals. Some chlorite appears to be altered groundmass (or pumice?).

Mineralogy:
Crystals ~20-30%

Primary minerals	Abundance	Secondary minerals	Abundance
Plagioclase	15-25%	Quartz	>20%
Quartz	1-5%	Albite	>20%
Ferromagnesian minerals?	<1%	Clay	1-5%
		Epidote	1-5%
		Calcite	1-5%
		Chlorite	1-5%
		Fe-Ti oxides	5-10%
		Pyrite	<1%

Sample: NM5A, 2050mRF

Rock type: Volcaniclastic?

Hand Sample Description:
Cuttings are moderately well sorted, pale grey/green, and mostly medium to very fine sand size. Some larger white flakes and some rusty/orange grains are also present, with minor dark grains.

Optical Microscope Description:
Mostly white fragments with a white alteration coating. Minor amount of clean looking felsic crystals. Moderate amount of Fe-staining. Rare greenish grains. Some appear to have phenocrysts; possibly andesite or rhyolite?

Thin Section Description:
Dominated by groundmass and lithics – crystal-poor. Glass is often dark in ppl, and very fresh – this may be banded rhyolite lithics. Some is mostly dark with a crystalline band, and are possibly organic-rich sediments. Some glass is lighter in ppl and more altered (probably tuff). Greywacke, andesite, and possible argillite lithics are also present. Quartz crystals are rare and fine (<0.4 mm). Plagioclase is mostly altered. Possible relict biotite?

Hydrothermal alteration:
Alteration is moderate. Some grains (rhyolite lithics? mudstone?) remain relatively fresh, but some are completely altered to clay (tuff?). Some is partly altered to quartz/albite/clay. Plagioclase is often altered to albite and sometimes calcite and epidote. Chlorite could represent altered ferromagnesian minerals (possibly amphibole based on shape). Rare pyrite and Fe-Ti oxides.

Mineralogy:
Crystals ~15-25%

Primary minerals	Abundance	Secondary minerals	Abundance
Plagioclase	10-20%	Albite	10-30%
Quartz	1-5%	Quartz	>10%
Amphibole?	<1%	Epidote	5-10%
Biotite?	<1%	Clay	5-10%
		Calcite	1-5%
		Chlorite	1-5%
		Fe-Ti oxides	1-5%
		Pyrite	<1%

Sample: NM5A, 2150 mRF

Rock type: Volcaniclastic?

Hand Sample Description:
Cuttings are well sorted, pale grey, fine to very fine sand size. Some medium and coarse sand sized grains are mostly white or light grey in colour, but rare dark grains are also present.

Optical Microscope Description:
Mostly white fragments with a white alteration coating. Minor amount of clean looking felsic crystals. Minor amount of Fe-staining. Rare green and greenish/grey grains, some quite rounded (lithics?).

Thin Section Description:
Similar to 2050m. Dominated by groundmass or lithic grains. Some of the glass is dark in ppl and relatively fresh (rhyolite lithics? mudstone?). In other places the groundmass is microcrystalline. Rare andesite lithics and possible rhyolite and greywacke. One quartz crystal ~0.75 mm in size, but are generally <0.3 mm.

Hydrothermal alteration:
Alteration is moderate. While some groundmass remains glassy, some appears strongly altered. Plagioclase is commonly altered to albite, calcite and epidote. Chlorite has possibly replaced ferromagnesian minerals.

Mineralogy:
Crystals ~20-25%

Primary minerals	Abundance	Secondary minerals	Abundance
Plagioclase	15-20%	Albite	10-20%
Quartz	1-5%	Quartz	>10%
		Epidote	5-10%
		Chlorite	5-10%
		Calcite	1-5%
		Wairakite?	<1%
		Fe-Ti oxides	1-5%
		Pyrite	<1%

Sample: NM5A, 2250 mRF

Rock type: Volcaniclastic?

Hand Sample Description:
Cuttings are well sorted, pale grey, fine to very fine sand size. Some medium and coarse sand sized grains are mostly white or light grey in colour, but rare dark grains are also present.

Optical Microscope Description:
Mostly white fragments with a white alteration coating. Minor amount of clean looking felsic crystals. Minor greenish and greenish grey grains. Some grains appear to be altered phenocrysts.

Thin Section Description:
Similar to above. Dominated by groundmass, with varying degrees of alteration. Some still quite glassy (rhyolite lithics?), but some devitrified/altered. Very rare quartz crystals are <0.5 mm in size, but are mostly <0.3 mm.

Hydrothermal alteration:
Groundmass is commonly altered to microcrystalline quartz (± albite). Some grains are extensively clay altered. Plagioclase is typically altered to albite, or rarely calcite and epidote. Rare aggregates of clinozoisite. Epidote is not as common as previous. Chlorite is also not as common, and may have replaced ferromagnesian minerals.

Mineralogy:
Crystals ~15-20%

Primary minerals	Abundance	Secondary minerals	Abundance
Plagioclase	10-20%	Albite	>10%
Quartz	<1%	Quartz	>10%
Zircon	Trace	Clay	>10%
		Calcite	1-5%
		Chlorite	1-5%
		Epidote/Clinozoisite	1-5%
		Fe-Ti oxides	1-5%
		Pyrite	<1%

Sample: NM5, 2300 mRF

Rock type: Volcaniclastic?

Hand Sample Description:
Fine-grained cuttings – mostly very fine to medium sand size. Overall the colour is slightly darker than above. Although most grains are light in colour there are common dark grey grains.

Optical Microscope Description:
Most grains are white and appear to be altered groundmass material. The felsic crystal content is minor. Some grains are altered green (chlorite) or yellow (epidote?). The darker grains appear crystalline and may be andesite rather than greywacke? Minor Fe-staining.

Thin Section Description:
Most grains are fine-grained groundmass fragments of a light coloured rock (tuff?), with a moderate component of separate crystals of quartz and plagioclase. There are also common darker grains that are likely andesite. Possible rare greywacke fragments. All crystals are fine, with mostly angular fragments <0.5 mm in size.

Hydrothermal alteration:
Alteration is strong. Groundmass is altered to fine quartz with minor clays. Plagioclase is commonly altered to albite, and rarely calcite or epidote. Chlorite is a minor component, and in part may be altered ferromagnesian minerals, but shape is not distinct enough for confident identification.

Mineralogy:
Crystals ~15-25%

Primary minerals	Abundance	Secondary minerals	Abundance
Plagioclase	15-20%	Quartz	>20%
Quartz	1-5%	Albite	5-10%
Ferromagnesian minerals?	<1%	Clay	1-5%
		Epidote	1-5%
		Calcite	1-5%
		Chlorite	1-5%
		Fe-Ti oxides	1-5%
		Pyrite	<1%

Sample: NM5A, 2350 mRF

Rock type: Volcaniclastic?

Hand Sample Description:
Cuttings are light grey with a slight greenish tinge. Moderately-well sorted, being mostly medium to very fine sand size. Rare larger grains up to coarse sand size are a mix of white, light grey, and dark grey lithologies.

Optical Microscope Description:
Grains are mostly white (altered groundmass?), with a minor amount of felsic crystals. Rare dark grains are probably andesite lithics, but greywacke is also possible. Minor amount of green grains (chlorite?) and yellow crystals (epidote?). Moderate amount of Fe-staining. Rare pyrite.

Thin Section Description:
Dominated by altered groundmass. Quartz is rare and fine (<0.4 mm). Altered plagioclase is common. Andesite lithics with common feldspar laths are minor. Rare fresh hornblende – possibly from downhole mixing.

Hydrothermal alteration:
Alteration is strong. Groundmass is altered to fine quartz with minor clays. Plagioclase is commonly altered to albite, and rarely calcite or epidote. Chlorite is a minor component, and in part may be pseudomorphs after ferromagnesian minerals, but shape is not distinct enough for identification. Possible clinozoisite and sericite.

Mineralogy:
Crystals ~15-25%

Primary minerals	Abundance	Secondary minerals	Abundance
Plagioclase	10-20%	Quartz	20-50%
Quartz	1-5%	Albite	20-50%
		Epidote	5-10%
		Clay	5-10%
		Calcite	1-5%
		Chlorite	1-5%
		Sericite?	<1%
		Clinozoisite?	<1%
		Fe-Ti oxides	1-5%
		Pyrite	<1%

Sample: NM5A, 2450 mRF

Hand Sample Description:
Cuttings are well sorted, light to medium grey, fine to very fine sand sized. Darker than above due to the abundance of dark grains.

Optical Microscope Description:
Mostly white fragments, but a small amount of felsic crystals are visible. Minor mafic minerals are also present. Some grey fragments possibly represent lithic material, but it mostly appears glassy.

Thin Section Description:
Dominated by fine groundmass in varying states of alteration, with some relatively fresh glass, but some fully recrystallised. Rare lithic grains are difficult to distinguish from groundmass. Quartz crystals are rare and fine (<0.3 mm), and are mostly angular fragments. Plagioclase is common. Rare fresh hornblende may be from downhole mixing. Voids rimmed with quartz with chlorite in the centre are also observed.

Hydrothermal alteration:
Alteration is moderate to strong. Plagioclase is commonly altered to albite and calcite. Epidote is common. Chlorite is a minor component. Quartz mosaics are likely vein infill material. Minor Fe-Ti oxides and pyrite.

Mineralogy:
Crystals ~10-20%

Primary minerals	Abundance	Secondary minerals	Abundance
Plagioclase	5-15 %	Albite	10-20%?
Quartz	1-5%	Quartz	10-20%?
Amphibole	<1%	Clay	1-5%
Apatite	<1%	Calcite	1-5%
Zircon	Trace	Chlorite	<1%
		Epidote	1-5%
		Fe-Ti oxides	1-5%
		Pyrite	<1%

Sample: NM6, 1220 mRF

Rock type: Vitric tuff

Hand Sample Description:
Cuttings are poorly sorted ranging from very fine sand to cuttings chips ~0.8 mm in size, although it is mostly fine to very coarse sand size. The most common component is a fine-grained white rock with only very rare felsic crystals visible (tuff?). There are also common lithics of medium grey rock (andesite?) with both dark and light coloured crystals visible. Extensive Fe-staining.

Optical Microscope Description:
The white grains appear to be extensively altered and almost devoid of crystals completely, with crystals only visible in rare grains. The grey grains however are crystal-rich with common felsic crystals and rare fine mafic ones. In places these grains appear to show flow banding (rhyolite?). Dark grains appear to be andesite. Separate crystals are very rare. Rare pyrite.

Thin Section Description:
The main part of the sample, the white tuff grains, are crystal-poor (<10%), although some appear to contain completely altered feldspars. The grey rhyolite grains however are very crystal-rich (35-45%), containing

common plagioclase and quartz. Flow banding is also visible, and these grains may be due to mixing of cuttings with the above unit. Crystals of quartz and plagioclase are also likely from the above unit.

Hydrothermal alteration:
Alteration of the tuff is intense. The groundmass is extensively silicified in places, and sometimes altered to calcite. Clays and Fe-oxides are also common, with rare pyrite. Plagioclase in the tuff is completely altered to calcite. The grains from the overlying lava however are only weakly altered, with relatively fresh plagioclase.

Mineralogy: (of the tuff only)
Crystals <10%

Primary minerals	Abundance	Secondary minerals	Abundance
Plagioclase	<10%	Quartz	>20%
		Calcite	>20%
		Clay	5-10%
		Fe-Ti oxides	5-10%
		Pyrite	<1%

Sample: NM6, 1265 mRF

Rock type: Vitric tuff

Hand Sample Description:
Cuttings are mostly granule size up to small pebbles size (2-8 mm). Grains are mostly white with rare fine crystals. There are also common grey grains, which range from light to dark grey, some with white phenocrysts.

Optical Microscope Description:
The white grains that make up the bulk of the cuttings again appear to be virtually free of crystals, and look strongly altered. The dark grains here mostly have a green colour, probably caused by chlorite alteration. Feldspar phenocrysts are common in these grains, with rare altered ferromagnesian minerals (andesite?). There are some aggregates of euhedral calcite, probably representing vein infill. Minor pyrite.

Thin Section Description:
Grains are mostly of altered, fine-grained, crystal-poor tuff. Altered feldspars are visible, but quartz appears to have been absent in the original rock. One large (4 mm) separate quartz grain is present, possibly due to mixing.

Hydrothermal alteration:
Alteration is intense. The groundmass is altered to an assemblage consisting of quartz, carbonate, clay, Fe-Ti oxides, and rare pyrite. Feldspars are often completely dissolved leaving voids. In other cases the feldspars appear to have been replaced by calcite, clay, or albite. Calcite vein material is also present.

Mineralogy: (of the tuff only)
Crystals <10%

Primary minerals	Abundance	Secondary minerals	Abundance
Plagioclase	<10%	Quartz	>20%
		Calcite	>20%
		Clay	>10%
		Albite	<1%
		Fe-Ti oxides	5-10%
		Pyrite	<5%

Sample: NM6, 1280 mRF

Rock type: Mixed cuttings (Vitric tuff and andesite/dacite/rhyolite lavas)

Hand Sample Description:
Cuttings range from very fine sand size up to chips ~1 cm in size. There is also a mix of lithologies. The most common is white and appears to be very crystal-poor, similar to above. Some are grey/green with visible white crystals. Rare fine-grained, dark grey grains appear to be entirely silicified.

Optical Microscope Description:
The white grains are again crystal-poor, but small, altered feldspars are visible in places. There are at least 2 distinct kinds of dark grains (lavas?) in addition to the silicified grains. One appears less altered, with a grey groundmass and common quartz and feldspar crystals (possibly rhyolite/dacite?). The other often has chlorite alteration, with feldspar phenocrysts and rare small mafic crystals, but no quartz (andesite?).

Thin Section Description:
Most grains in the thin section appear to be from a dark, crystal-poor unit, although many are similar to the altered, crystal-poor tuff described above. Quartz appears to again be absent, although some separate crystals of quartz are present. Feldspars are often completely altered leaving voids, but appear to have been a minor component. The dark rock is also crystal-poor, with altered feldspars. Possible relict ferromagnesian minerals.

Hydrothermal alteration:
Alteration is intense. The groundmass is altered to quartz, clay, Fe-Ti oxides, and pyrite. Feldspars are altered to clay, calcite, albite, and quartz. Ferromagnesian minerals are altered to calcite or chlorite. Rare calcite veins.

Mineralogy:
Crystals 5-10%

Primary minerals	Abundance	Secondary minerals	Abundance
Plagioclase	5-10%	Quartz	>20%
Ferromagnesian minerals?	Rare	Calcite	5-10%
		Clay	>10%
		Chlorite	5-10%
		Albite	<1%
		Fe-Ti oxides	1-5%
		Pyrite	<1%

Sample: NM6, 1300 mRF

Rock type: Andesite breccia?

Hand Sample Description:
Cuttings are a mix of mostly dark grey grains (andesite?) and light grey/white grains (rhyolite/ignimbrite – some have visible crystals). Rarely grains are >5 mm in size, but are mostly fine to very coarse sand size.

Optical Microscope Description:
Dark grains commonly have visible felsic phenocrysts, with rare black or altered green phenocrysts. Banding is rarely visible in the light grains. Rare felsic crystals are present. Chlorite alteration is common, both in the dark and light grains. Pyrite is present, often in aggregates.

Thin Section Description:
Alteration is intense making identification difficult; however, clearly there is a mixture of a dark volcanic rock (probably andesite) and a light volcanic rock (tuff?). Both contain altered plagioclase phenocrysts, while the andesite contains rare possible ferromagnesian minerals – probably pyroxene. At least some of the dark grains may be sedimentary in origin, as weak layering is rarely visible, and some appear to have small rounded (quartz?) grains. Very rare quartz grains reach 0.75 mm in size and are generally rounded.

Hydrothermal alteration:
Alteration is intense. The groundmass is commonly recrystallised to quartz (± albite?), while calcite, chlorite and clay alteration is also prevalent. Plagioclase is altered to calcite, albite, and quartz, possibly clay and chlorite in places? Many crystal shapes are entirely filled with mosaics of secondary quartz. Possible ferromagnesian minerals are completely altered to chlorite.

Mineralogy:
Crystals ~10%

Primary minerals	Abundance	Secondary minerals	Abundance
Plagioclase	5-10%	Quartz	<20%
Quartz	<1%	Chlorite	10-20%
Pyroxene?	<1%	Calcite	5-10%
		Albite	5-10%
		Clay	5-10%
		Fe-oxides	1-5%
		Pyrite	1-5%

Sample: NM6, 1350 mRF

Rock type: Andesite breccia or Ignimbrite?

Hand Sample Description:
Cuttings consist of medium to dark grey chips of a porphyritic volcanic rock. Some chips exceed 1 cm in size, and they are mostly between about 0.5 mm and 1 cm. White phenocrysts are common, and some are >1 mm, while dark phenocrysts are rare. Rare light coloured chips (rhyolite/ignimbrite?).

Optical Microscope Description:
Most chips look like andesite lava, with common plagioclase phenocrysts and altered (to chlorite) ferromagnesian minerals. There are some finely crystalline light coloured chips, and another lithology with a light coloured, altered looking groundmass, and chlorite altered pseudomorphs. Some grains consist of two of these lithologies, or even all 3 in some cases, giving the rock a brecciated look. Minor pyrite.

Thin Section Description:
Cuttings chips are composed mostly of dark, glassy lava or brecciated lava, with some grains having common xenoliths of different lithologies within them. Most common of these is a light, fine-grained, recrystallised rock, sometimes with completely altered feldspar phenocrysts, and in one case a very small quartz crystal. Some appear to be another type of lava, with microphenocrysts of feldspar in the groundmass, and altered plagioclase phenocrysts. The main lithology has a glassy groundmass, with banding commonly visible. There appears to be at least two magma types, with a certain amount of mixing between a lighter and a darker magma type, although both have similar mineralogies. Plagioclase is common, with minor altered ferromagnesian pseudomorphs (pyroxene and possibly hornblende based on shape). Rarely small quartz grains are visible, although this appears to be in brecciated zones between lava clasts or xenoliths. An alternative view is that this is a strongly welded ignimbrite, with rare fiamme-like shapes visible in the brecciated looking zones.

Hydrothermal alteration:

Alteration is moderate. The groundmass is mostly glassy, although the lithic inclusions often appear more strongly altered. Plagioclase is commonly altered to calcite, albite and rarely clay; although in places they seem to be reasonably fresh. Pyroxene is completely replaced by chlorite, and this is often associated with apatite.

Mineralogy:
Crystals ~30-35%

Primary minerals	Abundance	Secondary minerals	Abundance
Plagioclase	25-35%	Calcite	10-20%
Ferromagnesian minerals		Albite	10-20%
Pyroxene ± amphibole?	1-5%	Quartz	1-5%
		Clay	1-5%
		Chlorite	1-5%
		Apatite	<1%
		Fe-Ti oxides	1-5%
		Pyrite	<1%

Sample: NM6, 1380 mRF

Rock type: Volcanic breccia/Vitric tuff

Hand Sample Description:
Cuttings are a mixture of white, crystal-poor tuff clasts and grey andesite clasts. The white tuff appears strongly altered. It has a moderate degree of Fe-staining. The andesitic breccia clasts have common plagioclase crystals visible, with rare dark crystals. It contains common xenoliths that are darker that the host rock, giving a brecciated appearance. They are similar in appearance to the unit above.

Optical Microscope Description:
The white tuff grains appear to be crystal-free, being composed entirely of altered, fine-grained material. Veins are observed in places, often with Fe-staining around the vein. The possible andesite breccia is crystal-rich with common plagioclase and minor altered ferromagnesian minerals. Possible quartz in one grain. Contains xenolith or lithic inclusions, most of which are fine-grained and strongly chlorite altered, although some appear to be silicified.

Thin Section Description:
The white grains are strongly altered, and composed mostly of a fine groundmass with minor plagioclase phenocrysts. Sometimes crystals are completely dissolved leaving voids. One grain contains an original quartz

phenocryst, otherwise only plagioclase can be identified. The possible andesitic clasts are crystal-rich (30-35%), with common altered plagioclase phenocrysts and minor ferromagnesian minerals – probably pyroxene. In places it appears to contain flow banding, and fine-grained xenoliths or lithics are also visible. Composition of the rare fresh plagioclase phenocrysts were estimated using the Michel-Levy method, giving a composition of An≥30.

Hydrothermal alteration:
Alteration intensity is strong. The groundmass is altered to a fine assemblage of quartz, clay, Fe-Ti oxides, and rare pyrite. Feldspars are altered to albite and calcite in the tuff, and also to chlorite and adularia in the andesitic clasts. Possible ferromagnesian minerals are completely altered to chlorite and possibly calcite.

Mineralogy: (of the tuff only)
Crystals ~5-10%

Primary minerals	Abundance	Secondary minerals	Abundance
Plagioclase	5-10%	Quartz	>20%
Quartz	Trace	Clay	>20%
		Calcite	5-10%
		Albite	1-5%
		Fe-Ti oxides	1-5%
		Pyrite	<1%

Sample: NM6, 1400 mRF

Rock type: Crystal-vitric tuff

Hand Sample Description:
This sample contains fewer grey grains than previous, and the few that persist are likely due to mixing. Cuttings are mostly white, many resembling the extremely crystal-poor cuttings described above, but over half of them are distinctly different, having numerous altered crystals and/or lithic grains (often to chlorite). Cuttings are mostly relatively coarse (2 mm – 10 mm).

Optical Microscope Description:
Most grains are more crystal-rich than the tuff above. Very fine flecks altered to chlorite are common, while larger crystals altered to chlorite are also common. Some felsic (probably feldspar) crystals are also visible. The grey grains are similar to above, being crystal-rich and extensively altered to chlorite. Some crystal-poor tuff fragments persist, and appear to have a higher Fe-Ti oxide content.

Thin Section Description:
Tuff grains are more crystal-rich than previous. Quartz is still very rare, but is present in some grains. Feldspar phenocrysts are often completely dissolved leaving voids, but appear to have been reasonably common in the original rock. Possible ferromagnesian minerals are completely altered and shape is not distinctive enough for confident identification. Andesitic grains persist, and are similar to above.

Hydrothermal alteration:
Alteration is moderate to strong. The groundmass is altered to quartz, clay, calcite, chlorite, Fe-Ti oxides, and pyrite. Feldspars are altered to calcite, albite, clay, and possibly chlorite, although in places it appears to be relatively fresh. Possible ferromagnesian minerals are completely altered, mostly to chlorite, or possibly calcite.

Mineralogy:
Crystals ~15-20%

Primary minerals	Abundance	Secondary minerals	Abundance
Plagioclase	10-20%	Quartz	>10%
Quartz	<1%	Clay	>20%
Ferromagnesian minerals	2-3%	Calcite	5-10%
		Chlorite	1-5%
		Albite	1-5%
		Fe-Ti oxides	5-10%
		Pyrite	<1%

Sample: NM6, 1430 mRF

Rock type: Crystal-Vitric tuff

Hand Sample Description:
Cuttings are mostly white/pale grey, although darker grey grains are still present. Mostly coarse sand up to ~8 mm in size. Unlike above, chlorite altered crystals are not obvious, but some crystal shapes are visible.

Optical Microscope Description:
Rare grains of the crystal-rich andesitic rock are still present, as are the very white coloured grains with common small chlorite altered crystals that were common at 1400 mRF. Most grains however are slightly darker than this (pale grey). Chlorite alteration of these grains is less developed than above, but still visible. They appear to have a moderate crystal content, consisting of mainly plagioclase. Minor Fe-staining. Rare pyrite.

Thin Section Description:
Most grains are of an altered tuff. The crystal content is moderate, and appears to be entirely plagioclase, with euhedral-subhedral crystals reaching >1 mm in size and common smaller fragments. The brecciated nature of the andesitic unit above is again observed, with one large medium grey, moderately crystal-rich grain containing two fragments of a dark grey, very crystal-rich rock.

Hydrothermal alteration:
Alteration is moderate to strong. The groundmass is altered to quartz, clay, Fe-Ti oxides, and rare pyrite. Plagioclase is altered to albite, calcite and clay and is sometimes altered completely leaving voids.

Mineralogy:
Crystals ~15-20%

Primary minerals	Abundance	Secondary minerals	Abundance
Plagioclase	15-20%	Clay	>20%
		Quartz	>10%
		Calcite	5-10%
		Albite	5-10%
		Fe-Ti oxides	5-10%
		Pyrite	1-5%

Sample: NM6, 1460 mRF

Rock type: Dacite? or welded ignimbrite? (with common tuff fragments)

Hand Sample Description:
Cuttings range mostly from fine to coarse sand size. There is a mixture of compositions, with dark grey lava (?) grains, some with visible white phenocrysts being the most common. However, white and light grey grains are also common, with some also containing visible phenocrysts, and appear similar to the unit above.

Optical Microscope Description:
The dominant grain type is the medium-dark grey rock. It contains visible crystals, with common large felsic (feldspar) crystals and small mafic crystals. White to pale grey grains are also very common, many of which appear crystal-free, but some also have visible feldspar phenocrysts, and appear similar to the tuff at 1430 mRF. Rarely these grains appear more similar to those at 1400 mRF, with small chlorite altered crystals. Chlorite alteration is reasonably common, with minor Fe-staining. Separate crystals are also present, some of which appear to be quartz. Pyrite is rare.

Thin Section Description:
The cuttings are very mixed, with both the white tuff and the dark grains common. There are rare separate quartz crystals up to ~1 mm in size. The tuff itself is mostly crystal-poor (<10%), containing only plagioclase crystals which are generally small (<0.5 mm), but sometimes reach sizes of up to ~1.5 mm. The tuff appears less crystal-rich than at 1430 mRF. The dark grains here are also crystal-poor, with rare feldspar crystals in a glassy groundmass. One dark grain also contains a quartz phenocryst, while one of the separate quartz crystals has an embayment filled with the darker material, suggesting the quartz is from this unit. This also suggests this unit may be dacite rather than andesite. Alternatively it may be a strongly welded ignimbrite, and vague fiamme-like shapes are sometimes visible. Some of the grains also have xenoliths (or lithics?) of fine-grained rocks. Chlorite, possibly representing altered ferromagnesian minerals is mostly as separate crystals.

Hydrothermal alteration:
Alteration is moderate in the dark rock, but stronger in the tuff, which is similar to above. The groundmass is still mostly glassy. Feldspars are altered to calcite or albite, but in places still appear relatively fresh.

Mineralogy: (of the dark rock only)
Crystals <10%

Primary minerals	Abundance	Secondary minerals	Abundance
Plagioclase	5-10%	Calcite	1-5%
Quartz	<1%	Albite	1-5%
		Quartz	<5%
		Clay	<10%
		Chlorite	<1%
		Fe-Ti oxides	1-5%
		Pyrite	<1%

Sample: NM6, 1510 mRF

Rock type: Andesite/Dacite lava/breccia?

Hand Sample Description:
Cuttings are here very uniform, consisting of dark grey andesite/dacite lava with large feldspar phenocrysts. Size ranges from fine sand to chips >1 cm in size. Xenoliths of lighter grey rock are commonly observed. Small dark crystals are rarely observed.

Optical Microscope Description:
Some of the lighter patches thought to be xenoliths could be alteration around veins, and in some cases veins can be observed. These 'xenoliths' are strongly altered to chlorite, whereas the main rock mass remains dark grey. Large feldspars are the most notable feature, while small mafic crystals are mostly altered to chlorite.

Thin Section Description:
Most of the rock has a dark groundmass that remains mostly glassy. It is crystal-poor, with euhedral to subhedral plagioclase reaching ~1 mm in size being the dominant mineral phase. Altered ferromagnesian minerals are rare, and while the shape suggests they are pyroxene in some cases, they can mostly not be identified with confidence. Rare separate quartz crystals are present, and are assumed to be due to down-hole mixing. Some altered tuff grains are present. The andesite/dacite contains a number of fine-grained inclusions / xenoliths that appear more altered than the host rock. Some of these have altered feldspars.

Hydrothermal alteration:
Alteration intensity is low to moderate. The groundmass of the andesite/dacite remains quite glassy, but the fine-grained fragments appear more strongly altered. Plagioclase is altered to albite, clay and calcite. Ferromagnesian minerals are altered to chlorite.

Mineralogy:
Crystals ~5-10%

Primary minerals	Abundance	Secondary minerals	Abundance
Plagioclase	5-10%	Quartz	<10%
Pyroxene?	<1%	Clay	<20%
		Albite	1-5%
		Calcite	1-5%
		Chlorite	<1%
		Fe-Ti oxides	1-5%
		Pyrite	<1%

Sample: NM6, 1560 mRF

Rock type: Dacite/Rhyolite breccia or tuff?

Hand Sample Description:
The cuttings are a mix of the dark grey cuttings as above, but also have common lighter fragments. Cuttings are mostly fine to coarse sand, but do contain some coarser chips >0.5 mm.

Optical Microscope Description:
Cuttings here are mixed in composition. While the dark grains from above are still present, the majority of grains are either light grey or white. The light grey grains have a higher crystal content than the dark grey grains, and banding is sometimes visible. Small, altered ferromagnesian minerals can be seen, and these chips are possibly dacite or rhyolite. The white grains are crystal-poor, possibly altered tuff. Chlorite alteration appears common. Pyrite is rare.

Thin Section Description:
Most grains are crystal-poor lava or tuff. The large, light grey (dacite?) chips are more crystal-rich than the darker chips above but have a similar mineralogy, consisting of mostly plagioclase and rare ferromagnesian minerals. They have the same brecciated appearance as above, with altered inclusions of different composition again visible. Crystal-poor tuff, some grains with well preserved vitriclastic textures, is also common. Separate quartz crystals are again present in small quantities

Hydrothermal alteration:
Alteration is moderate. The groundmass is glassy in some grains, but commonly altered to fine quartz, clay, chlorite, Fe-Ti oxides and pyrite. The tuff grains are more strongly altered. Plagioclase is altered to albite, calcite, and clay, although it rarely remains relatively fresh. Ferromagnesian minerals are altered to chlorite.

Mineralogy: (of the dacite? only)
Crystals ~10-15%

Primary minerals	Abundance	Secondary minerals	Abundance
Plagioclase	10-15%	Quartz	10-20%
Ferromagnesian minerals (pyroxene)	1-2%	Clay	>10%
		Calcite	1-5%
		Albite	1-5%
		Chlorite	1-5%
		Fe-Ti oxides	1-5%
		Pyrite	<1%

Sample: NM6, 1610 mRF

Rock type: Dacite breccia?

Hand Sample Description:
The cuttings appear slightly darker here, with the dark grey andesitic chips more common than at 1560 mRF. It again appears brecciated, with inclusions of lighter coloured rock. Light to medium grey grains dominate, and white grains are also present. Grain size is mostly fine to coarse sand size, with rare chips >0.5 mm.

Optical Microscope Description:
Cuttings are mostly medium grey, with a moderate crystal content consisting of plagioclase and altered ferromagnesian minerals. They appear more similar to 1560 mRF than 1510 mRF, but the dark grey grains common at 1510 mRF are also common here. Crystal-poor white grains are also present.

Thin Section Description:
Appears similar to 1560 mRF, with tuff fragments being less common here. Dark, andesite chips appear similar to those above, being crystal-poor with plagioclase and small, altered ferromagnesian minerals. The dacite has a similar mineralogy, but appear slightly more crystal-rich.

Hydrothermal alteration:
Alteration is moderate. The groundmass is altered to fine quartz, clay, chlorite, Fe-Ti oxides and pyrite. The tuff grains generally appear more strongly altered. Plagioclase is altered to albite, calcite, and clay. Ferromagnesian minerals are completely altered to chlorite, and rarely quartz.

Mineralogy:
Crystals ~10-20%

Primary minerals	Abundance	Secondary minerals	Abundance
Plagioclase	10-20%	Quartz	10-20%
Ferromagnesian minerals	<1%	Clay	>20%
		Calcite	1-5%
		Albite	1-5%
		Chlorite	1-5%
		Fe-Ti oxides	1-5%
		Pyrite	<1%

Samples: NM6, 1645 mRF (cuttings) & 1650 mRF (GNS thin section)

Rock type: Crystal-vitric tuff/ignimbrite

Hand Sample Description:
Cuttings are mostly light grey, although some of the dark grey grains from above are present. Cuttings are mostly fine to coarse sand size, with rare chips up to ~1 cm in size.

Optical Microscope Description:
Cuttings are mixed, with some resembling both the dacite and andesite above. Pale grey to white grains that appear to have a low crystal content dominate. Fine crystals are visible in some of these grains, and weak banding is rarely visible. Some larger felsic crystals are also present within these grains, and as separate crystals.

Thin Section Description: (1650 mRF)
Most of the cuttings chips appear to be of a highly altered ignimbrite. In places banding is visible, and rarely glass shard shapes are visible. Lithic grains are commonly visible within the ignimbrite, most being fine-grained with a recrystallised groundmass, although some have visible phenocrysts. Crystals are almost entirely plagioclase, with only very rare quartz in what are likely lithic fragments. Rare completely altered ferromagnesian minerals.

Hydrothermal alteration:
Alteration is strong. The groundmass is altered to quartz, clay, chlorite, calcite, and Fe-Ti oxides. Plagioclase is altered to calcite, albite, adularia, and clay. Ferromagnesian minerals are altered to chlorite and quartz.

Mineralogy:
Crystals ~15-25%

Primary minerals	Abundance	Secondary minerals	Abundance
Plagioclase	15-25%	Quartz	>20%
Ferromagnesian minerals	<1%	Clay	10-20%
Quartz	<1%	Calcite	1-10%
Zircon	Trace	Chlorite	1-10%
		Albite	1-5%
		Adularia	1-5%
		Fe-Ti oxides	1-5%
		Pyrite	<1%

Sample: NM6, 1670 mRF

Rock type: Crystal-lithic ignimbrite

Hand Sample Description:
Cuttings are uniformly light grey with a greenish tinge, although rare lighter and darker grains exist. Grain size ranges from fine sand to chips >1 cm in size.

Optical Microscope Description:
The cuttings appear to be of a moderately crystal- and lithic-rich ignimbrite. Flattened pumice shapes are commonly visible indicating a degree of welding. Lithics are common, although often appear highly altered making identification difficult. They range in colour from white to dark grey and some have altered crystals within them. Crystals within the ignimbrite appear to be mostly feldspar and altered ferromagnesian minerals.

Thin Section Description:
The ignimbrite contains common altered plagioclase crystals and rare altered ferromagnesian minerals in a glassy groundmass. Quartz phenocrysts are very rare. Dark patches of Fe-oxide-rich material are abundant within the groundmass. Flattened, altered pumice clasts are sometimes visible, while lithic clasts are common. Lithics are mostly fine-grained and altered (tuff and/or sediments?), but some have feldspars, and in very rare cases quartz phenocrysts. In places the groundmass shows welding textures.

Hydrothermal alteration:
Alteration is moderate. The groundmass remains glassy in places, otherwise it is altered to fine quartz, clay, and chlorite. Pumice clasts are altered mostly to clay and chlorite. Plagioclase is altered to albite, calcite, clay, and possibly chlorite in rare cases. Possible ferromagnesian minerals are altered to chlorite and quartz.

Mineralogy:
Crystals ~15-25%

Primary minerals	Abundance	Secondary minerals	Abundance
Plagioclase	15-25%	Quartz	5-10%
Quartz	<1%	Clay	>10%
Ferromagnesian minerals	1-2%	Chlorite	5-10%
		Albite	5-10%
		Calcite	1-5%
		Fe-Ti oxides	10-20%
		Pyrite	<1%

Sample: NM6, 1700 mRF

Rock type: Ignimbrite

Hand Sample Description:
Cuttings are much lighter than above, being mostly white with common pale grey to greenish lithics. Rare dark grey lithics from above are still present. The ignimbrite contains a moderate crystal content and common lithics. Most of the cuttings are coarse sand to granule size, with some chips >1 cm in size.

Optical Microscope Description:
Appears to be a different unit than above. It is much lighter in colour, and flattened pumice (altered to chlorite) are more common. Glass shard shapes are also visible. Fine-grained lithics are also visible, some with plagioclase phenocrysts. Plagioclase phenocrysts are present in the ignimbrite, as well as rare ferromagnesian minerals.

Thin Section Description:
Again appears lighter in colour than the above unit, with more common flattened pumice indicating welding. Crystals are predominantly plagioclase, with euhedral-subhedral crystals and common crystal fragments. Completely altered ferromagnesian minerals are also present, although shape is not distinctive enough for confident identification. Altered fine-grained lithics are common.

Hydrothermal alteration:
Alteration is strong. The groundmass is altered to fine quartz, clay, chlorite, and Fe-Ti oxides. Plagioclase is altered to albite, calcite, rare adularia, and clay. Ferromagnesian minerals are altered to chlorite and calcite. Pumice is altered to clay and chlorite.

Mineralogy:
Crystals ~15-20%

Primary minerals	Abundance	Secondary minerals	Abundance
Plagioclase	15-20%	Clay	>10%
Ferromagnesian minerals	~1%	Quartz	>10%
		Calcite	1-5%
		Albite	1-5%
		Chlorite	1-5%
		Adularia	<1%
		Fe-Ti oxides	1-5%
		Pyrite	<1%

Sample: NM6, 1750 mRF (cuttings sample) & 1760 mRF (GNS thin section)

Rock type: Crystal-lithic ignimbrite

Hand Sample Description: (1750 mRF)
Cuttings are poorly sorted, ranging in size from fine sand to chips >1 cm in size. It is mostly light grey/white in colour, but rare medium or dark grey grains are present (andesite?). The bulk of the rock appears to be a lithic-rich tuff/ignimbrite in a fine groundmass. Medium grey chips are more common and appear to have a mixture of lithics and crystals in a fine groundmass.

Optical Microscope Description: (1750 mRF)
Most grains appear to be from a partially welded ignimbrite. Chlorite altered patches are common, with many probably being pumice clasts. While some flattening of these clasts has occurred, many appear un-flattened. Felsic crystals are dominantly plagioclase, and altered ferromagnesian crystals are also visible. Lithics are often visible in the ignimbrite, with possible rhyolite/dacite. Rare grains appear to be a crystal-rich volcanic rock with feldspar, quartz, and minor altered ferromagnesian phenocrysts (rhyolite?).

Thin Section Description: (1760 mRF)
Similar to above. Most of the cuttings chips appear to be a moderately crystal-poor ignimbrite, and in some cases fine-grained lithics are visible within the ignimbrite. Some of the cuttings (~5%) are rhyolite chips with altered phenocrysts of plagioclase and rare ferromagnesian minerals (pyroxene?) and flow banding and spherulites visible in the groundmass. Crystals in the ignimbrite are mostly plagioclase, with rare altered ferromagnesian minerals (pyroxene?). One quartz phenocryst was observed. Flattened pumice shapes are rare, and where observed are altered to a clay, quartz, or chlorite. Glass shard shapes are often visible.

Hydrothermal alteration: (1760 mRF)
Alteration is strong to intense. The groundmass and fine-grained lithic clasts are altered to finely crystalline quartz, clay, chlorite, pyrite and Fe-Ti oxides. Plagioclase is completely altered to albite, calcite, and adularia. Ferromagnesian minerals (possibly pyroxene?) are completely altered to chlorite.

Mineralogy:
Crystals ~15-20%

Primary minerals	Abundance	Secondary minerals	Abundance
Plagioclase	15-20%	Quartz	>20%
Ferromagnesian minerals	<1%	Clay	>10%
Quartz	<1%	Calcite	5-10%
		Albite	5-10%
		Chlorite	5-10%
		Adularia	1-5%
		Pyrite	<1%
		Fe-Ti oxides	<1%

Sample: NM6, 1800 mRF

Rock type: Mixed cuttings (mostly crystal-lithic tuff)

Hand Sample Description:
Cuttings are mostly fine to coarse sand in size and medium grey in colour. Some of the larger chips (up to ~3 mm) are white with visible green patches, similar to the unit above. Most grains however are a medium grey colour, sometimes with fine crystals. There are also rare dark grey grains, possibly andesite or greywacke.

Optical Microscope Description:
Cuttings appear to be mixed here. Most grains are white (or greenish) with no visible crystals, however many grains also have common small green (chlorite) patches (crystals and/or pumice/lithics). Many grains appear to be a lithology not seen above, containing common quartz and feldspar phenocrysts in a pinkish coloured matrix. Large separate quartz crystals are also more common than previous. The dark grains appear to be andesite.

Thin Section Description:
The most common lithology is a crystal-lithic tuff similar to above, with mostly plagioclase phenocrysts, flattened pumice shards, and fine-grained lithic fragments (some with feldspar phenocrysts). However some tuff fragments appear to have common quartz phenocrysts. These are possibly the pinkish grains noted above. Separate quartz crystals are also common here, reaching sizes of up to ~1 mm, and they are commonly rounded and sometimes embayed. Andesite and greywacke fragments are also present.

Hydrothermal alteration:
Alteration is moderate to strong. The groundmass is altered to fine quartz, clay, chlorite, Fe-Ti oxides and rare pyrite. Pumice is altered to clay and chlorite. Plagioclase is altered to albite, calcite, and adularia, although in places it remains relatively fresh. Possible ferromagnesian minerals are altered to chlorite.

Mineralogy:
Crystals ~20-30%

Primary minerals	Abundance	Secondary minerals	Abundance
Plagioclase	15-25%	Quartz	>10%
Quartz	1-5%	Clay	>10%
Ferromagnesian minerals	~1%	Albite	5-10%
		Chlorite	1-5%
		Calcite	1-5%
		Adularia	<1%
		Fe-Ti oxides	1-5%
		Pyrite	<1%

Sample: NM6, 1850 mRF

Rock type: Crystal tuff/ignimbrite

Hand Sample Description:
The cuttings appear more uniform than above. Size of the cuttings range from fine sand to chips >1 cm in size. They are darker than the tuff at 1750 mRF, being light grey in colour. Lithics are also not as prominent as above, but can still be seen in some grains. White crystals are visible in most grains.

Optical Microscope Description:
Most grains have a fine, light grey (but commonly altered to chlorite) groundmass, with common feldspar phenocrysts and rarer altered ferromagnesians and possible quartz. Small black crystals are also present.

Thin Section Description:
This is very different to1750 mRF. It is more crystal-rich, it contains common quartz crystals, and only rare lithics and pumice shards. Quartz is common as fine fragments, but there are also common large, embayed phenocrysts up to ~1.5 cm in size. Mostly subhedral plagioclase phenocrysts are up to ~2.5 cm in size, but are mostly >1 mm. Fine crystal fragments are common. Lithics appear to be predominantly fine-grained tuff. Completely altered ferromagnesian minerals are difficult to identify, but some shapes suggest amphibole.

Hydrothermal alteration:
Alteration is moderate to strong. The groundmass is altered to quartz, clay, chlorite and calcite. Plagioclase is altered to calcite, albite, clay and adularia. Ferromagnesian minerals are altered to chlorite, quartz, and calcite.

Mineralogy:
Crystals ~25-35%

Primary minerals	Abundance	Secondary minerals	Abundance
Plagioclase	20-30%	Quartz	>10%
Quartz	~5%	Clay	>10%
Ferromagnesian minerals (amphibole?)	~1%	Albite	10-20%
		Calcite	5-10%
Apatite	Trace	Chlorite	1-5%
Zircon	Trace	Adularia	<1%
		Fe-Ti oxides	1-5%
		Pyrite	<1%

Sample: NM6, 1890 mRF

Rock type: Mixed cuttings

Hand Sample Description:
Cuttings are mixed, with white/light grey and pale green grains dominant, with common medium grey, and rare dark grey grains. Size varies from fine sand up to ~1 cm, with most being coarse sand to granule size. Phenocrysts are visible in many grains of all colours, with both white and altered green crystals.

Optical Microscope Description:
Most grains are white with common chlorite patches or crystals. Felsic crystals are also visible. Lithics of greywacke are present, as well as a medium grey volcanic rock with quartz, feldspar and ferromagnesian phenocrysts. Rare finely crystalline red grains with felsic phenocrysts.

Thin Section Description: (GNS thin section)
Similar to above, but with slightly more mixing of lithologies. Most grains appear to be a tuff/ignimbrite containing quartz and plagioclase phenocrysts. Lithic grains are sometimes observed in the ignimbrite, but most of the other lithologies occur as separate grains in the cuttings. Crystal-poor tuff grains are minor compared to the crystal-rich tuffs. Possible rhyolite lithics contain plagioclase, quartz and completely altered ferromagnesian minerals. Greywacke and andesite are minor components. Quartz in the tuff is commonly large (>1 mm) and sometimes embayed. Plagioclase reaches >2 mm in size. Some chlorite altered pumice shapes are observed.

Hydrothermal alteration:
Alteration is strong to intense. The groundmass is altered to quartz, clay, pyrite, and Fe-Ti oxides with chlorite common in places. Plagioclase is completely altered to calcite, albite, and rarely adularia. Ferromagnesian minerals are completely altered to chlorite.

Mineralogy:
Crystals ~25-35%

Primary minerals	Abundance	Secondary minerals	Abundance
Plagioclase	20-30%	Quartz	>10%
Quartz	1-5%	Calcite	>10%
Ferromagnesian minerals	<1%	Clay	>10%
Apatite	Trace	Chlorite	1-10%
Zircon	Trace	Albite	1-10%
		Adularia	<1%
		Pyrite	<1%
		Fe-Ti oxides	<1%

Sample: NM6, 1950 mRF

Rock type: Crystal tuff

Hand Sample Description:
Cuttings are finer grained than above, being very fine sand to coarse sand size. Overall the cuttings have a light grey to greenish colour. Individual grains range from white to dark grey, with minor Fe-staining.

Optical Microscope Description:
Most grains are white, some of which contain visible phenocrysts – mostly altered green (chlorite?) crystals but some contain felsic crystals. Some of the darker grains appear similar to the unit above, with felsic and mafic phenocrysts in a fine grey groundmass. Some of the dark grey grains appear to be greywacke. Separate crystals appear to be both quartz and feldspar. Rare pyrite.

Thin Section Description:
Crystal content, particularly the quartz content seems to be lower in this section. While the size of the cuttings makes comparison difficult, it also appears lighter in colour than above. Quartz here reaches only ~0.5 mm in size and is commonly fragments of crystals. Plagioclase also only reaches ~0.75 mm, but crystal size could, at least in part be due to drilling recovery (drilling with water). Ferromagnesian minerals are minor and cannot be distinguished based on shape. Fe-staining is common.

Hydrothermal alteration:
Alteration is strong. The groundmass is altered to fine quartz, clay, chlorite, calcite, Fe-Ti oxides, and pyrite. Plagioclase is altered to albite, calcite and adularia. Ferromagnesian minerals are altered to chlorite. Calcite and quartz vein material is also present.

Mineralogy:
Crystals ~15-25%

Primary minerals	Abundance	Secondary minerals	Abundance
Plagioclase	15-20%	Quartz	>10%
Quartz	1-2%	Clay	>10%
Ferromagnesian minerals	~1%	Albite	5-10%
		Calcite	5-10%
		Chlorite	5-10%
		Adularia	1-5%
		Fe-Ti oxides	1-5%
		Pyrite	<1%

Sample: NM6, 2000 mRF

Rock type: Crystal tuff

Hand Sample Description:
Finer grained than above, being mostly very fine sand to medium sand size. Overall the colour is light grey-greenish, but some white grains and rusty coloured grains are visible.

Optical Microscope Description:
Cuttings are mostly pale grey to white in colour, and these are often altered to chlorite and have a green colour. Separate crystals are rare. Dark grains are rare and identification is difficult. Fe-staining is minor.

Thin Section Description:
Slightly more crystal-rich than above, but it is probably the same unit as at 1950 mRF, and quartz is still very minor compared to plagioclase. Quartz reaches ~0.5 mm in size, and is mostly sub-angular. Plagioclase reaches

~1 mm in size, but is mostly present as fragments <0.5 mm. Possible ferromagnesian minerals are rare and completely altered. Minor Fe-staining.

Hydrothermal alteration:
Alteration intensity is strong. The groundmass is altered to quartz, clay, calcite, and chlorite. Plagioclase is altered to albite, calcite, and adularia. Ferromagnesian minerals are altered to chlorite and possibly calcite. Quartz and calcite vein material is also present. Possible epidote.

Mineralogy:
Crystals ~25-35%

Primary minerals	Abundance	Secondary minerals	Abundance
Plagioclase	20-30%	Quartz	>10%
Quartz	1-2%	Clay	>10%
Ferromagnesian minerals	1-2%	Albite	10-20%
		Calcite	5-10%
		Adularia	1-5%
		Chlorite	1-5%
		Fe-Ti oxides	1-5%
		Epidote?	Trace

Sample: NM6, 2050 mRF

Rock type: Crystal tuff

Hand Sample Description:
Slightly coarser than above, being mostly fine to coarse sand size. It is pale grey, with some dark grey and white grains. Minor amount of Fe-staining.

Optical Microscope Description:
Most grains are white to pale grey, often with visible phenocrysts. Chlorite alteration is moderate, and some grains contain what appears to be flattened pumice altered to chlorite. Separate crystals are relatively common. Rare dark grains are possibly andesite or greywacke. Rare pyrite.

Thin Section Description:
Similar to above. The most notable difference is that wispy shapes resembling flattened pumice are more common here, indicating a degree of welding. Quartz is minor compared to plagioclase, reaching ~0.5 mm in size, it is mostly sub-angular in shape. Plagioclase reaches ~1.5 mm in size, but is mostly present as fragments <0.5 mm. Possible ferromagnesian minerals are rare and completely altered. Minor Fe-staining.

Hydrothermal alteration:
Alteration intensity is strong. The groundmass is altered to quartz, clay, calcite, and chlorite. Pumice is altered to clay and chlorite. Plagioclase is altered to albite, calcite, and adularia. Ferromagnesian minerals are altered to chlorite and possibly calcite. Quartz and calcite vein material is also present.

Mineralogy:
Crystals ~20-30%

Primary minerals	Abundance	Secondary minerals	Abundance
Plagioclase	15-25%	Quartz	>10%
Quartz	1-2%	Clay	>10%
Ferromagnesian minerals	1-2%	Calcite	5-10%
		Albite	5-10%
		Chlorite	5-10%
		Adularia	1-5%
		Fe-Ti oxides	1-5%
		Pyrite	<1%

Sample: NM6, 2100 mRF

Rock type: Crystal tuff

Hand Sample Description:
Very fine-grained cuttings are mostly very fine to fine sand size. Overall it is light grey-greenish in colour.

Optical Microscope Description:
Most grains are white, although many are altered to a green colour (chlorite). Separate crystals are moderate and seem to consist of both plagioclase and quartz. Rare dark grains. Minor Fe-staining and rare pyrite.

Thin Section Description:
Cuttings are finer than previous, but appear to be similar in composition. Quartz is rare and found as fine crystal fragments <0.3 mm. Plagioclase rarely exceeds 0.5 mm, and is also often broken, although euhedral crystals can also be seen. Possible ferromagnesian minerals. Rare andesite lithics can be identified.

Hydrothermal alteration:
Alteration is strong. The groundmass is altered to quartz, clay, calcite, and chlorite. Plagioclase is altered to albite, calcite, and adularia. Ferromagnesian minerals are altered to chlorite and possibly calcite. Quartz and calcite vein material is also present. Rare pyrite.

Mineralogy:
Crystals ~20-30%

Primary minerals	Abundance	Secondary minerals	Abundance
Plagioclase	20-30%	Quartz	>10%
Quartz	<1%	Clay	>10%
Ferromagnesian minerals	<1%	Albite	10-20%
		Calcite	1-5%
		Chlorite	1-5%
		Adularia	1-5%
		Fe-Ti oxides	1-5%
		Pyrite	<1%

Sample: NM6, 2150 mRF

Rock type: Crystal tuff

Hand Sample Description:
Similar to above, being mostly very fine to medium sand size. Light grey with a green tinge. Rare Fe-staining.

Optical Microscope Description:
Most grains are white and look like altered groundmass material; however, felsic crystals are also present. Minor amount of Fe staining and chlorite alteration. Rare pyrite.

Thin Section Description:
Similar to above. Quartz is minor compared to plagioclase, and is again present as fine angular fragments <0.3 mm in size. Plagioclase reaches ~0.75 mm in size, and euhedral crystals are present, although plagioclase is mostly present as broken fragments. Rare possible ferromagnesian minerals.

Hydrothermal alteration:
Alteration is strong. The groundmass is altered to quartz, clay, calcite, and chlorite. Plagioclase is altered to albite, calcite, and adularia. Ferromagnesian minerals are altered to chlorite. Rare pyrite.

Mineralogy:
Crystals ~15-25%

Primary minerals	Abundance	Secondary minerals	Abundance
Plagioclase	15-25%	Quartz	>10%
Quartz	<1%	Clay	>10%
Ferromagnesian minerals	<1%	Albite	5-10%
		Calcite	1-5%
		Chlorite	1-5%
		Adularia	1-5%
		Fe-Ti oxides	1-5%
		Pyrite	<1%

Sample: NM6, 2200 mRF

Rock type: Crystal tuff

Hand Sample Description:
Similar to above. Mostly very fine sand to medium sand sized grains and light grey-green in colour.

Optical Microscope Description:
Again, most grains are white and look like fine altered tuff fragments, with minor felsic crystals. Minor chlorite alteration and a moderate amount of Fe-staining.

Thin Section Description:
Similar to above, with the fine grain size and alteration making identification difficult. Most grains appear to be altered tuff fragments, but many may be altered lithic fragments. The crystal content is moderate to high, and mostly consists of plagioclase fragments. Quartz fragments are rare, small (<0.3 mm), and angular. Possible ferromagnesian minerals are also rare.

Hydrothermal alteration:
Alteration is strong to intense. The groundmass is altered to fine quartz, clay, chlorite, and calcite. Plagioclase is altered to albite, calcite, adularia, and clay. Possible ferromagnesian minerals are altered to chlorite and possibly calcite. Calcite is common here compared to above, and some of it may be vein infill.

Mineralogy:
Crystals ~20-30%

Primary minerals	Abundance	Secondary minerals	Abundance
Plagioclase	20-30%	Quartz	>10%
Quartz	<1%	Clay	>10%
Ferromagnesian minerals?	<1%	Calcite	10-20%
		Albite	10-20%
		Adularia	1-5%
		Chlorite	1-5%
		Fe-Ti oxides	1-5%
		Pyrite	<1%

Appendix 2: Summary of the Tahorakuri Formation in NM5 and NM6

The following summarises the different lithologies observed from optical and petrographical examination of the drill cuttings from NM5/NM5A and NM6. Mineral percentages given are estimates. Ignimbrite is used to describe primary deposits inferred to have been emplaced by pyroclastic density currents. Tuff is used to describe deposits inferred to be primary volcanic deposits, where the mode of emplacement is unknown.

NM5/NM5A

NM5 and NM5A were drilled in 2008 and the stratigraphy was described by *Ramirez and Rae* (2009). NM5 was drilled to a depth of 1803 mRF (metres below the drilling rig floor), with NM5A sidetracked from 1130 mRF and drilled to a depth of 2997 mRF. NM5 cuttings were examined from 1050 mRF to 1800 mRF, and NM5A cuttings were examined from 1700 mRF to 2450 mRF. The cuttings are generally very fine-grained, and therefore do not provide as much information as those from NM6. Crystals are generally separate, rather than as phenocrysts within in a rock, and rock fragments are small. The stratigraphy is described below and is summarised in Figure 1.

1080-1230 mRF: Tuff

This interval consists of altered volcanic tuff. Towards the top of the unit the cuttings are mixed, with a larger than usual grain-size making identification possible. At 1100 mRF there are common rhyolite lithics from the unit above, tuff grains, crystals, and sedimentary lithics. The sediments are fine-grained, with small quartz and feldspar fragments, and weak banding is visible in places. There is possibly a small amount of sediment between the overlying rhyolite and the pyroclastic deposits. This interval may also represent a sequence of tuffs, with a number of lithic-rich horizons, as a small amount of dark lithics persist throughout. At 1100 mRF it has a moderate crystal content, with a similar amount of quartz and altered plagioclase, and rare ferromagnesian minerals. Quartz phenocrysts are often large (up to ~1.5 mm) and embayed. Below 1100 mRF the cuttings are very fine-grained, with altered tuff fragments appearing to dominate, and a minor amount of crystals and lithic fragments. Crystals are dominantly quartz, with only very rare plagioclase recognised, possibly due to the destruction of the clay altered plagioclase during drilling. There are abundant Fe-oxides and iron staining at the top of this unit, progressively decreasing with depth. This may indicate a break in time between deposition of the tuff and rhyolite, with the possible sediments or soil being baked by the rhyolite.

1230-1385 mRF: Tuff/rhyolite breccia?

This interval was described by *Ramirez and Rae* (2009) as a rhyolite breccia with crystal-poor rhyolite clasts in a glassy matrix. The grain-size of the cuttings makes it difficult to determine the nature of the unit. Overall they are lighter in colour than above, with a slightly lower crystal content. Most grains appear to be strongly altered groundmass from a tuff rather than rhyolite, as the rhyolites encountered here often have a fresher, often glassy groundmass. However, slightly darker and less altered grains are also present and could be rhyolite.

~1385-1700 mRF: Tuffs/ignimbrites

As above, the grainsize makes identification of rock within this interval difficult. It appears to be dominated by fine-grained, altered, crystal-poor volcanic rocks. Lithics are reasonably common, with light (rhyolite?) and dark (andesite, greywacke?) lithics present. The crystal content is moderate to low, with plagioclase dominating over quartz, which is present as small (<0.5 mm), mostly broken fragments.

~1700-1825 mRF: Quartz-bearing welded ignimbrite

This unit corresponds to core that was drilled from NM5 at 1775-78 mRF. There it is a light grey to pale green, crystal-rich, welded ignimbrite. It has a strongly eutaxitic texture defined by the common altered (to clay, chlorite, and quartz) pumice fiamme, and also contains a minor amount of angular lithics. Crystals are dominated by plagioclase, with often large (>2 mm) euhedral to subhedral phenocrysts as well as smaller crystal fragments. However, quartz is also relatively common in this unit, with large (>1 mm), often embayed phenocrysts being a distinctive feature. Ferromagnesian minerals are completely altered, but based on their shapes it appears that amphibole is probably more common than pyroxene.

The distinctive feature of the cuttings in this interval is the abundance large, often embayed quartz phenocrysts. These appear to be more common in the cuttings than core, whereas the ferromagnesian minerals, completely altered to chlorite, are rare in the cuttings. The process of drilling likely destroys softer alteration minerals such as chlorite and clays, but not quartz.

This ignimbrite is present at least from 1750-1800 mRF; however, it is unclear how thick it is. The cuttings from NM5 indicate the top could be as high as 1690 mRF, whereas in NM5A it is likely somewhere between 1700 mRF and 1750 mRF. However, the lower contact of this unit is uncertain due to the size of the cuttings. Below 1800 mRF the cuttings become extremely fine-grained making identification difficult.

~1825->2467 mRF: Tuffs/ignimbrites with lithic-rich horizons

Most grains in this interval appear to be fragments of altered tuff or ignimbrite groundmass, with a moderate amount of plagioclase, and rare quartz crystal fragments. Altered pumice and lithics are also likely present. Near the bottom of this interval lithic-rich horizons containing dark grey lithics are visible, most notably at 2100 mRF, 2300 mRF, and 2450 mRF.

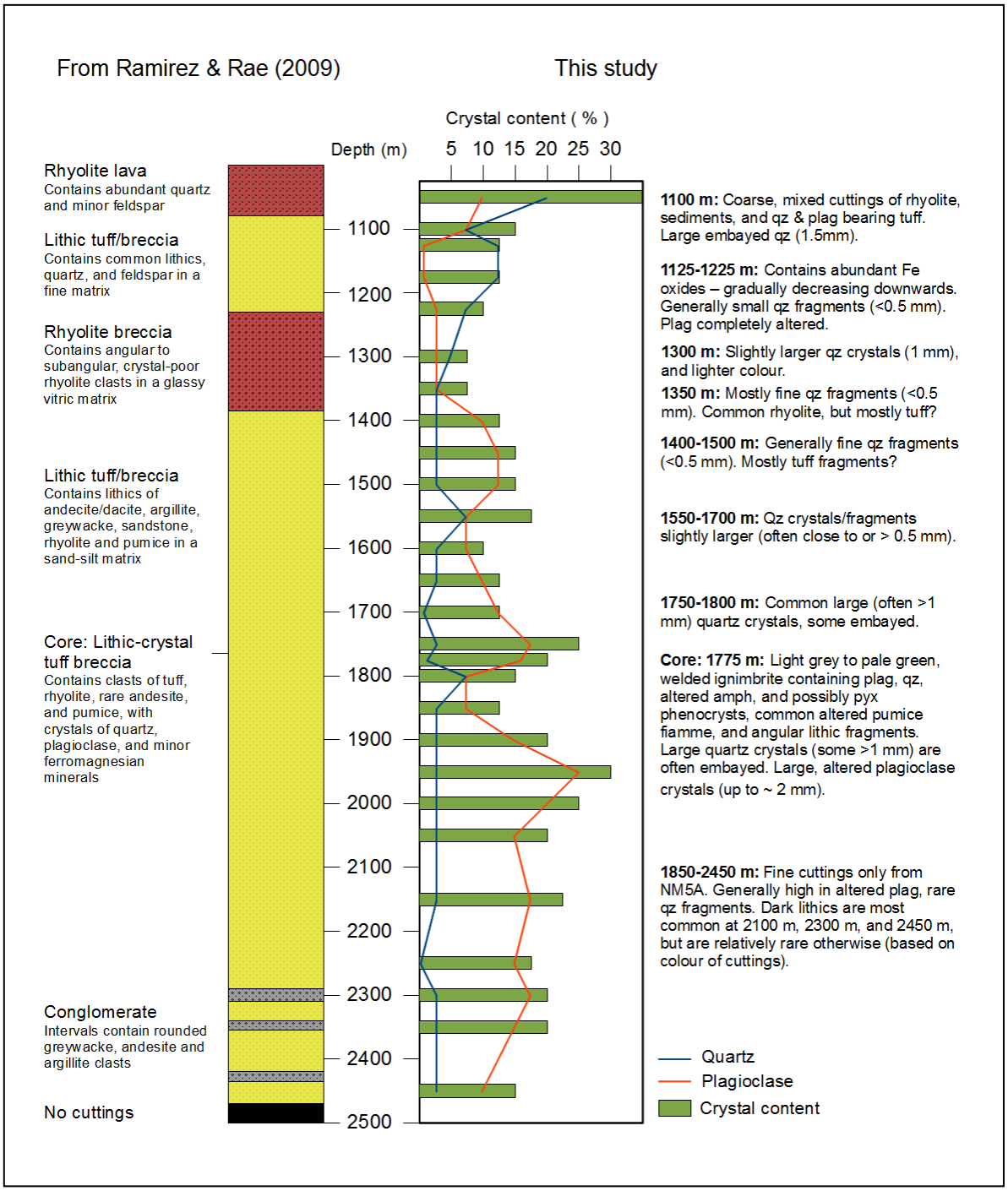

Figure 1: Summary of the lithologies encountered in NM5. The stratigraphy as described by *Ramirez and Rae* (2009) is shown on the left, while the plagioclase, quartz and overall crystal contents of the cuttings as observed here are also shown.

NM6

NM6 was drilled in 2009 to a depth of 3398 mRF, and the stratigraphy was described by *Rae et al.* (2009). Observations made here generally agree with this stratigraphy but additional information on the nature of the Tahorakuri Formation is provided. In contrast to NM5, the drill cuttings are often of sufficient size to enable the rock type to be identified, and it is clear that there is significant variation in lithology within the Tahorakuri Formation in this well. The stratigraphy is described below and is summarised in Figure 2.

1215-1280 mRF: Tuffs

Below the rhyolite is a unit consisting of intensely altered, crystal-poor tuffs. Although there is some mixing with cuttings from the above unit, as well as rare dark grey lithic fragments, most of the cuttings observed in this interval are from a white tuff. The tuff is crystal-poor, with <10% of the rock being composed of entirely altered crystals. It is likely that most were originally plagioclase, but ferromagnesian minerals may have also been present. Quartz was not observed. No textures are preserved due to the intense hydrothermal alteration.

1280-1360 mRF: Volcanic breccia/ignimbrite?

This unit was described by *Rae et al.* (2009) as porphyritic andesite lava and breccia. However, a re-examination of this interval by *Lewis et al.* (2012) concluded it is most likely a welded ignimbrite. It is a medium to dark grey rock with common feldspar phenocrysts and lithic fragments in a glassy groundmass. The crystal content increases markedly from 1300 mRF to 1350 mRF indicating more than one lithology may be present. Both the crystal-rich and crystal-poor varieties contain common rock fragments within the rock, with multiple lithologies. These could be xenoliths within lava, but their abundance gives the rock a very brecciated appearance. They may also be lithics within a welded ignimbrite, although no welding textures were observed here. Some of the cuttings chips appear to be sedimentary, with weak layering visible. Crystals are dominantly plagioclase, with minor altered ferromagnesian minerals. Quartz grains are very rare, but appear to be present in brecciated zones between lithic grains. Some of these dark volcanic chips persist to 1380 mRF where some of the feldspars were fresh enough to estimate a composition of An≥30 based on extinction angles of albite twins. This is more similar to the silicic rocks of the Tahorakuri Formation than andesite, for which compositions of An54-82 were reported by *Anderson* (2011). Together with the quartz grains this suggests this rock is more evolved than andesite, consistent with it being a welded ignimbrite or possibly dacite breccia.

1360-1460 mRF: Tuffs

There is considerable variation in the tuffs within this interval. At 1380 mRF the cuttings are dominated by a light grey to pinkish, crystal-poor tuff, with a minor amount of altered plagioclase phenocrysts and very rare quartz in a strongly altered groundmass. At 1400 mRF the cuttings are dominated by white tuff with a moderate crystal content consisting of plagioclase, ferromagnesian minerals, and rare quartz. Plagioclase is often dissolved leaving behind voids, while the ferromagnesian minerals are altered to chlorite giving the rock a speckled appearance, which distinguishes it from the other tuffs in NM6. At 1430 mRF the cuttings are dominated by grey tuff with a moderate crystal content consisting entirely of plagioclase.

1460-1640 mRF: Andesite-dacite breccia/ignimbrite?

This unit was described by *Rae et al.* (2009) as andesite or dacite lava and breccia; however, *Lewis et al.* (2012) also concluded this interval is most likely a welded ignimbrite. In hand sample it appears similar to andesite, with common white phenocrysts in a dark groundmass, but under the microscope much of it appears brecciated. Lithic fragments or xenoliths are common at most intervals observed, again with a variety of mostly fine-grained lithologies. The unit varies in colour from medium to dark grey, with feldspar phenocrysts throughout. At 1460 mRF it is crystal-poor with dominantly plagioclase phenocrysts, however rare grains also contain quartz phenocrysts. At 1510 mRF the cuttings chips are mostly darker than above or below, with minor plagioclase and rare altered ferromagnesian minerals. No quartz was observed. The cuttings at 1560 mRF are lighter in colour that at 1510 mRF, and also have a higher crystal content, again consisting of mostly plagioclase with rare altered ferromagnesian minerals. At 1640 mRF the cuttings appear to be mixed. It is clear there is a variation in lithology, and if they are extrusive rocks, both andesite and dacite may be present, although they would best be described as andesite/dacite breccia. However, as with the unit from 1280-1360 mRF, the common lithic fragments (and possibly pumice) may suggest it is simply a welded ignimbrite.

1640-1695 mRF: Light grey welded ignimbrite

The Tahorakuri Formation from 1640-2220 mRF was described by *Rae et al.* (2009) as a partially welded ignimbrite containing abundant partially flattened pumice clasts, rhyolite, andesite, and silicified tuff lithics, and crystals of quartz, plagioclase, amphibole, and possibly pyroxene. Here, this is divided into at least 3 separate sheets. Whether these sheets are

genetically related is not clear, but the first 2 are mineralogically very similar, and the top sheet may be a more strongly welded part of the underlying sheet.

The unit from 1640-1695 mRF is a light grey, moderately crystal and lithic-rich, welded ignimbrite. Flattened pumice clasts are sometimes visible. The groundmass remains relatively glassy, particularly near the bottom of the unit, but in places vitriclastic textures are observed. Banding is also seen in places. Lithics are common, with a variety of lithologies, although most are fine-grained. Crystals are dominantly plagioclase, with a minor amount of completely altered ferromagnesian minerals, and very rare quartz.

1695-1775 mRF: White, partially welded ignimbrite

This unit is a partially welded ignimbrite, with common altered pumice clasts more common than above, but not showing the same degree of flattening. Vitriclastic textures are commonly seen in the groundmass, and fine-grained lithics are again common. The groundmass is lighter in colour than above, while pumice and possibly some lithics are altered to chlorite giving the rock a white and pale green appearance. It has a slightly lower crystal content than above, which is again dominated by plagioclase, with minor completely altered ferromagnesian minerals. Quartz is extremely rare, with only one phenocryst observed.

~1775-1890 mRF: Quartz-bearing welded ignimbrite

This unit is distinct from all other units within the Tahorakuri Formation in NM6. Most notable is the presence of large, often embayed quartz phenocrysts. Whereas the pyroclastic units above had no, or very rare (<<1%) quartz fragments, the presence of large (often >1 mm) quartz crystals at up to ~5 % of the rock by volume is distinctive. This unit is also more crystal-rich than the other pyroclastic units, with abundant plagioclase often as fine crystal fragments, although large (up to ~2.5 mm) euhedral crystals are also common. A minor amount of completely altered ferromagnesian minerals are also present, with shapes resembling both amphibole and pyroxene. Pumice and lithic clasts are less abundant than above, but flattened pumice fiamme are present, indicating welding. This unit is similar to that cored from NM5 at 1775 mRF and recognised in the cuttings from ~1700-1825 mRF.

~1900-2220 mRF: Welded ignimbrite?

The cuttings from 1900 mRF to the bottom of the Tahorakuri Formation are extremely fine-grained, making identification of the rock type difficult. It is therefore uncertain whether the crystal-rich ignimbrite continues into this interval or not. The cuttings are still generally

crystal-rich, with common plagioclase and minor quartz, and the overall green-grey colour of the altered rock chips are consistent with it being the same ignimbrite as above. On the other hand, there is no evidence of the large embayed quartz phenocrysts common above, although this may have more to do with the drilling parameters. Small fiamme like shapes were most commonly observed at 2050 mRF, and dark lithics become slightly more common towards the bottom of this section.

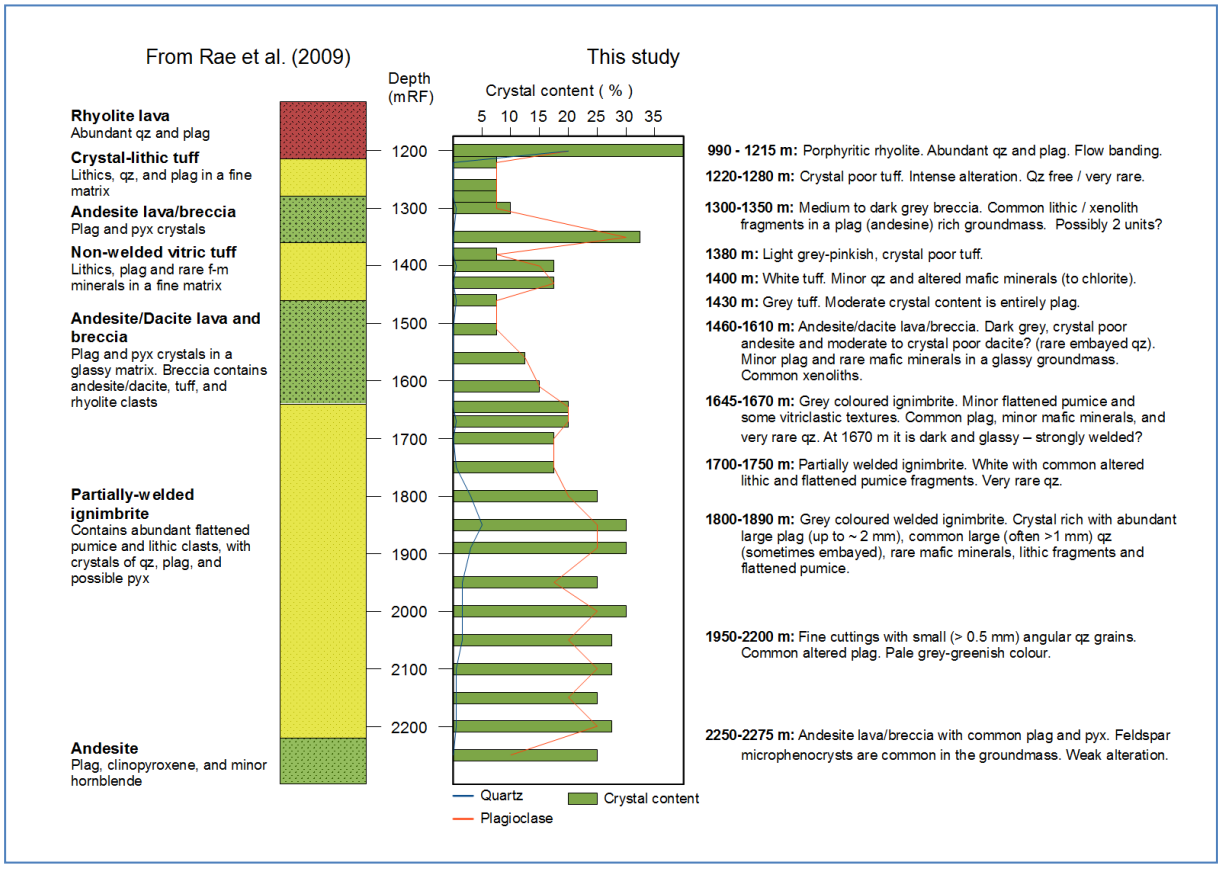

Figure 2: Summary of the lithologies encountered in NM6. The stratigraphy as described by *Rae et al.* (2009) is shown on the left, while the plagioclase, quartz and overall crystal contents of the cuttings as observed here are also shown.

References

Anderson, L. C. A. (2011), A comparison of buried andesites at Ngatamariki and Rotokawa geothermal fields, Taupo, M.Sc. thesis, University of Waikato, Hamilton, New Zealand.

Lewis, B., I. Chambefort, A. J. Rae, and F. Sanders (2012), Geology of Injection Well NM10, Ngatamariki Geothermal Field, *GNS Science consultancy report 2012/231*.

Rae, A. J., L. E. Ramirez, and C. Bardsley (2009), Geology of Exploration Well NM6, Ngatamariki Geothermal Field, *GNS Science consultancy report 2009/130*, 68p.

Ramirez, L. E., and A. J. Rae (2009), Geology of Injection Well NM5, NM5A, Ngatamariki Geothermal Field, *GNS Science consultancy report 2009/41*, 29p.

Appendix 3: Electron microprobe results

Sample:	SB-2028a	SB-2028b	SB-2028c	SB-2028d	FB11-OD8a	FB11-OD8b	FB11-OD8c	FB11-OD8d	NM5-1125a
Type:	Sanidine	Sanidine	Sanidine	Sanidine	Adularia	Adularia	Adularia	Adularia	Adularia
SiO_2	64.16	62.63	63.15	62.56	63.11	64.60	63.82	64.05	63.43
Al_2O_3	18.45	17.94	18.53	18.21	17.57	18.28	17.76	18.07	18.07
FeO	0.00	0.14	0.06	0.00	0.00	0.00	0.00	0.00	0.00
MgO	0.00	0.00	0.00	0.00	0.00	0.00	0.00	0.00	0.00
CaO	0.09	0.11	0.14	0.12	0.00	0.00	0.00	0.00	0.00
Na_2O	3.25	3.30	3.15	3.13	0.07	0.08	0.09	0.11	0.25
K_2O	11.45	11.59	11.35	11.42	16.91	16.69	16.70	16.84	16.63
BaO	0.47	0.40	0.78	0.69	0.02	0.00	0.02	0.01	0.09
Total	97.87	96.11	97.16	96.13	97.68	99.65	98.39	99.08	98.47
An	0.46	0.55	0.72	0.62	0.00	0.00	0.00	0.00	0.00
Ab	30.00	30.04	29.45	29.22	0.63	0.72	0.81	0.98	2.23
Or	69.54	69.41	69.82	70.16	99.38	99.28	99.19	99.02	97.77

Sample:	NM5-1125b	NM5-1125c	NM5-1125d	NM5-1300a	NM5-1300b/1	NM5-1300b/2	NM5-1450a	NM5-1450b	NM5-1450d
Type:	Adularia	Adularia	Adularia	Adularia	Adularia	Illite?	Adularia	Adularia	Adularia
SiO_2	64.08	63.37	63.62	64.45	64.17	51.07	64.23	64.16	64.19
Al_2O_3	18.33	18.29	18.14	18.30	18.12	30.82	18.41	18.52	17.99
FeO	0.05	0.00	0.03	0.00	0.13	1.24	0.00	0.00	0.00
MgO	0.00	0.00	0.00	0.00	0.00	1.83	0.00	0.00	0.00
CaO	0.00	0.00	0.00	0.00	0.00	0.13	0.00	0.00	0.00
Na_2O	0.16	0.29	0.21	0.28	0.11	0.07	0.28	0.26	0.17
K_2O	16.37	16.50	16.63	16.42	16.70	8.70	16.53	16.43	16.54
BaO	0.24	0.06	0.03	0.01	0.04	0.00	0.02	0.03	0.00
Total	99.23	98.51	98.66	99.46	99.27	93.86	99.47	99.40	98.89
An	0.00	0.00	0.00	0.00	0.00		0.00	0.00	0.00
Ab	1.46	2.60	1.88	2.53	0.99		2.51	2.35	1.54
Or	98.54	97.40	98.12	97.47	99.01		97.49	97.65	98.46

Sample:	NM5-1450g	NM5-1500c	NM5-1500g	NM5-1600b/1	NM5-1600b/2	NM5-1600d/1	NM5-1600d/2	NM5-1600e
Type:	Adularia	Adularia	Adularia	Adularia	Albite	Adularia	Albite	Adularia
SiO_2	63.72	63.57	63.83	64.20	67.37	63.73	67.67	63.91
Al_2O_3	18.21	17.95	18.16	18.28	19.51	18.29	19.41	18.11
FeO	0.00	0.00	0.00	0.00	0.00	0.11	0.00	0.00
MgO	0.00	0.00	0.00	0.00	0.00	0.00	0.00	0.00
CaO	0.00	0.00	0.00	0.00	0.08	0.00	0.13	0.00
Na_2O	0.34	0.47	0.45	0.41	10.98	0.51	11.03	0.40
K_2O	16.41	16.43	16.26	16.32	0.24	16.24	0.17	16.34
BaO	0.07	0.05	0.02	0.03	0.00	0.05	0.00	0.00
Total	98.75	98.47	98.72	99.24	98.18	98.93	98.41	98.76
An	0.00	0.00	0.00	0.00	0.40	0.00	0.64	0.00
Ab	3.05	4.17	4.04	3.68	98.19	4.56	98.36	3.59
Or	96.95	95.83	95.96	96.32	1.41	95.45	1.00	96.41

Sample:	NM5-1600f/1	NM5-1600f/2	NM5-1600g/1	NM5-1600g/2	NM5-1600g/3	NM5-1700e	NM5-1700f	NM5-1700g
Type:	Adularia	Calcite?	Adularia	Albite	Ankerite?	Adularia	Adularia	Adularia
SiO_2	63.17	0.00	62.53	66.40	1.57	64.02	63.66	64.34
Al_2O_3	18.00	0.00	17.71	18.92	1.21	18.15	18.22	18.31
FeO	0.11	1.26	0.00	0.00	15.42	0.00	0.07	0.00
MgO	0.00	0.25	0.00	0.00	8.39	0.00	0.00	0.00
CaO	0.00	54.42	0.00	0.07	29.37	0.00	0.00	0.00
Na_2O	0.35	0.00	0.45	9.78	0.00	0.29	0.59	0.46
K_2O	16.40	0.02	16.33	2.36	0.43	16.66	16.09	16.35
BaO	0.08	0.00	0.02	0.04	0.02	0.03	0.05	0.04
Total	98.11	55.95	97.04	97.57	56.41	99.15	98.68	99.50
An	0.00		0.00	0.34		0.00	0.00	0.00
Ab	3.14		4.02	86.01		2.58	5.28	4.10
Or	96.86		95.98	13.66		97.42	94.72	95.90

Appendix 4: SIMS data

Note: Highlighted samples were not used due to high proportions of ^{206}Pb attributable to common Pb or low U contents.

Sample: NM2-01 Well: NM2 Depth: 2254.7-2255.2 mRF

Spot Name	ppm U	ppm Th	% comm 206	7corr $^{206}Pb/^{238}U$	1 sigma error	207 Corrected $^{206}Pb/^{238}U$ Age, Ma	1 sigma error	^{230}Th-Corrected 206/238 Age, Ma	2 sigma error
~~NM2_01_05.1~~	~~767~~	~~502~~	~~31.64~~	~~2.4E-4~~	~~2.0E-05~~	~~1.6~~	~~0.4~~	~~1.666~~	~~0.813~~
~~NM2_01_24.1~~	~~696~~	~~557~~	~~22.25~~	~~2.5E-4~~	~~6.8E-06~~	~~1.6~~	~~0.1~~	~~1.687~~	~~0.276~~
NM2_01_06.1	397	205	5.16	2.5E-4	2.5E-06	1.6	0.05	**1.718**	0.102
NM2_01_03.1	411	255	10.27	2.7E-4	2.2E-06	1.7	0.04	**1.806**	0.087
NM2_01_23.1	581	357	14.41	2.7E-4	4.5E-06	1.7	0.09	**1.819**	0.183
NM2_01_11.1	312	145	9.18	2.7E-4	5.4E-06	1.7	0.1	**1.833**	0.217
NM2_01_30.1	393	221	9.45	2.7E-4	4.5E-06	1.7	0.09	**1.842**	0.182
NM2_01_19.1	654	353	5.87	2.8E-4	2.6E-06	1.8	0.05	**1.888**	0.104
NM2_01_32.1	833	607	2.37	2.8E-4	1.7E-06	1.8	0.03	**1.889**	0.067
NM2_01_26.1	544	323	3.96	2.8E-4	1.8E-06	1.8	0.04	**1.896**	0.072
NM2_01_17.1	700	536	5.21	2.8E-4	3.2E-06	1.8	0.06	**1.898**	0.128
NM2_01_15.1	846	771	2.98	2.8E-4	3.9E-06	1.8	0.08	**1.899**	0.159
NM2_01_21.1	1919	2816	2.61	2.8E-4	2.6E-06	1.8	0.05	**1.901**	0.105
NM2_01_14.1	250	111	11.45	2.8E-4	3.7E-06	1.8	0.07	**1.908**	0.150
NM2_01_20.1	417	289	6.77	2.8E-4	2.9E-06	1.8	0.06	**1.911**	0.116
NM2_01_08.1	1204	1276	2.43	2.8E-4	2.6E-06	1.8	0.05	**1.914**	0.103
NM2_01_10.1	521	364	2.45	2.8E-4	6.4E-06	1.8	0.1	**1.916**	0.258
NM2_01_18.1	1084	1128	2.74	2.9E-4	2.0E-06	1.9	0.04	**1.937**	0.079
NM2_01_25.1	1641	2626	5.14	2.9E-4	2.8E-06	1.9	0.06	**1.956**	0.112
NM2_01_28.1	1165	1363	1.35	2.9E-4	2.5E-06	1.9	0.05	**1.962**	0.099
NM2_01_02.1	545	410	6.65	2.9E-4	2.7E-06	1.9	0.05	**1.963**	0.109
NM2_01_09.1	2833	2667	1.28	2.9E-4	1.8E-06	1.9	0.04	**1.965**	0.072
NM2_01_27.1	581	435	6.03	2.9E-4	3.5E-06	1.9	0.07	**1.984**	0.142
NM2_01_22.1	428	272	6.43	2.9E-4	5.0E-06	1.9	0.1	**1.991**	0.202
NM2_01_13.1	1198	1158	0.50	3.0E-4	2.9E-06	1.9	0.06	**1.992**	0.116
NM2_01_04.1	712	509	3.09	2.9E-4	3.7E-06	1.9	0.08	**1.992**	0.151
~~NM2_01_29.1~~	~~181~~	~~98~~	~~39.54~~	~~3.0E-4~~	~~1.2E-05~~	~~1.9~~	~~0.2~~	~~2.002~~	~~0.468~~
NM2_01_33.1	386	278	3.95	3.0E-4	3.6E-06	1.9	0.07	**2.003**	0.144
NM2_01_34.1	576	451	0.68	3.0E-4	2.3E-06	1.9	0.05	**2.020**	0.092
NM2_01_16.1	859	756	0.23	3.0E-4	2.7E-06	1.9	0.05	**2.021**	0.110
NM2_01_07.1	884	672	0.98	3.0E-4	3.2E-06	1.9	0.06	**2.023**	0.129
NM2_01_12.1	527	382	2.62	3.1E-4	2.9E-06	2.0	0.06	**2.075**	0.118
NM2_01_31.1	1199	1065	0.80	3.1E-4	2.1E-06	2.0	0.04	**2.077**	0.087

Sample: NM3-01 Well: NM3 Depth: 1495.7-1497.7 mRF

Spot Name	ppm U	ppm Th	% comm 206	7corr $^{206}Pb/^{238}U$	1 sigma error	207 Corrected $^{206}Pb/^{238}U$ Age, Ma	1 sigma error	^{230}Th-Corrected 206/238 Age, Ma	2 sigma error
NM3_01_26.1	1135	1614	6.80	1.1E-4	1.4E-06	0.7	0.03	**0.786**	0.057
NM3_01_24.1	352	166	14.72	1.1E-4	2.5E-06	0.7	0.05	**0.798**	0.100
NM3_01_03.1	1132	1465	12.18	1.1E-4	1.2E-06	0.7	0.02	**0.809**	0.047
NM3_01_06.1	565	710	25.47	1.2E-4	2.4E-06	0.8	0.05	**0.854**	0.098
NM3_01_22.1	588	688	13.69	1.3E-4	2.1E-06	0.9	0.04	**0.947**	0.086
NM3_01_33.1	754	855	5.67	1.4E-4	2.8E-06	0.9	0.06	**0.956**	0.113
NM3_01_21.1	332	288	21.21	1.4E-4	3.2E-06	0.9	0.06	**0.960**	0.130
NM3_01_28.1	521	581	11.02	1.4E-4	2.9E-06	0.9	0.06	**0.969**	0.117
NM3_01_14.1	4965	3690	2.61	1.4E-4	8.2E-07	0.9	0.02	**0.990**	0.033
NM3_01_29.1	300	246	15.12	1.4E-4	3.3E-06	0.9	0.07	**1.015**	0.132
NM3_01_27.1	494	450	11.71	1.4E-4	2.8E-06	0.9	0.06	**1.016**	0.112
NM3_01_11.1	403	346	17.98	1.4E-4	2.2E-06	0.9	0.05	**1.016**	0.091
NM3_01_08.1	259	155	17.50	1.4E-4	4.6E-06	0.9	0.09	**1.026**	0.188
NM3_01_20.1	251	190	17.74	1.5E-4	4.5E-06	0.9	0.09	**1.036**	0.182
NM3_01_18.1	1166	1486	6.18	1.5E-4	2.2E-06	1.0	0.04	**1.053**	0.087
NM3_01_31.1	992	1057	3.81	1.5E-4	1.7E-06	1.0	0.03	**1.056**	0.070
NM3_01_36.1	140	84	24.44	1.5E-4	6.0E-06	1.0	0.1	**1.058**	0.241
NM3_01_15.1	1918	3724	3.04	1.5E-4	1.3E-06	1.0	0.03	**1.059**	0.051
NM3_01_10.1	4216	9144	3.12	1.6E-4	1.1E-06	1.0	0.02	**1.068**	0.045
NM3_01_37.1	289	183	10.77	1.5E-4	3.8E-06	1.0	0.08	**1.084**	0.153
NM3_01_38.1	137	76	28.68	1.5E-4	4.2E-06	1.0	0.09	**1.094**	0.172
NM3_01_04.1	3954	4768	3.95	1.6E-4	1.4E-06	1.0	0.03	**1.117**	0.055
NM3_01_02.1	214	107	24.34	1.6E-4	4.7E-06	1.1	0.10	**1.148**	0.191
~~NM3_01_25.1~~	~~924~~	~~1006~~	~~36.21~~	~~1.7E-4~~	~~2.1E-06~~	~~1.1~~	~~0.04~~	~~**1.166**~~	~~0.085~~
NM3_01_01.1	518	502	6.38	1.7E-4	3.2E-06	1.1	0.07	**1.171**	0.131
NM3_01_35.1	337	234	10.06	1.7E-4	3.6E-06	1.1	0.07	**1.199**	0.144
NM3_01_32.1	691	594	7.38	1.8E-4	2.5E-06	1.2	0.05	**1.243**	0.099
NM3_01_23.1	183	108	15.64	1.9E-4	7.2E-06	1.2	0.1	**1.299**	0.291
NM3_01_30.1	505	300	7.43	2.0E-4	3.0E-06	1.3	0.06	**1.362**	0.123
NM3_01_07.1	592	369	7.16	2.5E-4	4.4E-06	1.6	0.09	**1.713**	0.176
NM3_01_05.1	350	234	13.84	2.5E-4	5.9E-06	1.6	0.1	**1.716**	0.238
NM3_01_34.1	209	83	15.14	2.6E-4	3.8E-06	1.7	0.08	**1.802**	0.154
NM3_01_17.1	517	408	9.36	2.8E-4	3.4E-06	1.8	0.07	**1.885**	0.136
NM3_01_13.1	284	154	10.76	2.8E-4	3.5E-06	1.8	0.07	**1.918**	0.143
NM3_01_19.1	340	214	14.22	3.0E-4	5.6E-06	1.9	0.1	**2.025**	0.225
NM3_01_12.1	609	341	4.81	3.0E-4	4.6E-06	1.9	0.09	**2.044**	0.186
NM3_01_09.1	321	177	5.93	3.2E-4	4.7E-06	2.1	0.09	**2.186**	0.190

Sample: NM3-02 Well: NM3 Depth: 1246-1248 mRF

Spot Name	ppm U	ppm Th	% comm 206	7corr $^{206}Pb/^{238}U$	1 sigma error	207 Corrected $^{206}Pb/^{238}U$ Age, Ma	1 sigma error	^{230}Th-Corrected 206/238 Age, Ma	2 sigma error
~~NM3_02_02.1~~	~~282~~	~~190~~	~~50.64~~	~~3.9E-5~~	~~3.2E-06~~	~~0.253~~	~~0.065~~	~~**0.341**~~	~~0.130~~
NM3_02_26.1	467	446	10.04	5.1E-5	2.2E-06	0.327	0.044	**0.410**	0.088
NM3_02_23.1	113	97	18.59	7.4E-5	4.3E-06	0.480	0.086	**0.567**	0.172
NM3_02_09.1	278	317	27.40	8.2E-5	4.1E-06	0.528	0.082	**0.609**	0.165
NM3_02_13.1	259	163	28.96	8.8E-5	3.1E-06	0.568	0.062	**0.661**	0.124
NM3_02_06.2	223	204	17.44	9.0E-5	2.9E-06	0.580	0.058	**0.666**	0.116
NM3_02_08.1	291	346	34.76	9.4E-5	3.1E-06	0.607	0.062	**0.686**	0.124
NM3_02_14.1	272	318	34.46	9.5E-5	3.9E-06	0.612	0.079	**0.692**	0.157
NM3_02_17.2	401	642	5.05	9.8E-5	2.3E-06	0.630	0.046	**0.700**	0.092
NM3_02_05.1	718	1083	13.41	9.9E-5	3.4E-06	0.637	0.068	**0.708**	0.136
NM3_02_10.1	244	296	21.27	1.0E-4	4.1E-06	0.672	0.082	**0.751**	0.164
NM3_02_21.2	192	120	3.43	1.0E-4	4.7E-06	0.676	0.096	**0.770**	0.191
NM3_02_18.1	229	225	35.56	1.2E-4	4.7E-06	0.758	0.095	**0.843**	0.191
NM3_02_22.1	318	509	24.59	1.2E-4	3.7E-06	0.776	0.074	**0.846**	0.148
NM3_02_16.1	152	100	40.50	1.5E-4	1.3E-05	0.984	0.269	**1.077**	0.537
NM3_02_01.1	179	92	29.60	1.5E-4	8.6E-06	0.984	0.174	**1.081**	0.349
NM3_02_15.1	172	127	21.91	1.6E-4	4.3E-06	1.015	0.088	**1.105**	0.175
NM3_02_07.1	187	110	22.25	1.7E-4	8.0E-06	1.086	0.161	**1.180**	0.322
NM3_02_24.1	238	188	-0.40	1.7E-4	3.6E-06	1.111	0.072	**1.200**	0.144
NM3_02_11.1	500	123	13.32	1.9E-4	4.0E-06	1.215	0.082	**1.318**	0.163

Sample: NM5-01 Well: NM5 Depth: 1775-1778 mRF

Spot Name	ppm U	ppm Th	% comm 206	7corr $^{206}Pb/^{238}U$	1 sigma error	207 Corrected $^{206}Pb/^{238}U$ Age, Ma	1 sigma error	^{230}Th-Corrected 206/238 Age, Ma	2 sigma error
NM5_01_12.1	277	213	37.92	1.1E-4	3.33E-06	0.7	0.07	**0.809**	0.135
NM5_01_26.1	437	563	11.74	1.3E-4	3.54E-06	0.8	0.07	**0.888**	0.143
NM5_01_13.1	123	62	38.96	1.3E-4	6.49E-06	0.8	0.1	**0.914**	0.262
NM5_01_02.1	169	83	34.61	1.3E-4	4.92E-06	0.8	0.10	**0.915**	0.199
NM5_01_15.1	283	191	16.23	1.3E-4	4.50E-06	0.8	0.09	**0.929**	0.182
~~NM5_01_38.1~~	~~198~~	~~153~~	~~61.56~~	~~1.3E-4~~	~~6.64E-06~~	~~0.9~~	~~0.1~~	~~**0.955**~~	~~0.268~~
NM5_01_03.1	232	131	26.06	1.3E-4	3.49E-06	0.9	0.07	**0.962**	0.141
NM5_01_27.1	785	622	11.20	1.4E-4	2.59E-06	0.9	0.05	**0.963**	0.105
NM5_01_07.1	155	75	25.38	1.4E-4	4.48E-06	0.9	0.09	**1.003**	0.181
NM5_01_34.1	189	114	25.60	1.5E-4	4.17E-06	0.9	0.08	**1.035**	0.169
NM5_01_05.1	215	123	21.71	1.5E-4	3.65E-06	0.9	0.07	**1.036**	0.148
NM5_01_01.1	197	91	10.76	1.5E-4	3.77E-06	1.0	0.08	**1.049**	0.152
NM5_01_33.1	283	198	26.08	1.5E-4	3.24E-06	1.0	0.07	**1.054**	0.131
NM5_01_11.1	152	79	34.62	1.5E-4	7.16E-06	1.0	0.1	**1.062**	0.289
NM5_01_16.1	172	104	21.66	1.5E-4	4.94E-06	1.0	0.10	**1.066**	0.200
NM5_01_32.1	1920	3626	2.37	1.6E-4	8.33E-07	1.0	0.02	**1.069**	0.034
NM5_01_28.1	196	135	14.11	1.5E-4	5.94E-06	1.0	0.1	**1.080**	0.240
NM5_01_30.1	227	115	11.67	1.5E-4	5.96E-06	1.0	0.1	**1.085**	0.241
NM5_01_06.1	159	83	32.07	1.5E-4	4.51E-06	1.0	0.09	**1.088**	0.182
NM5_01_04.1	360	210	14.50	1.5E-4	4.53E-06	1.0	0.09	**1.091**	0.183
NM5_01_35.1	229	146	19.00	1.6E-4	4.57E-06	1.0	0.09	**1.094**	0.185
NM5_01_09.1	530	570	9.44	1.6E-4	2.39E-06	1.0	0.05	**1.110**	0.097
NM5_01_10.1	320	220	19.19	1.6E-4	5.94E-06	1.0	0.1	**1.117**	0.240
NM5_01_14.1	511	575	10.05	1.6E-4	2.34E-06	1.1	0.05	**1.136**	0.095
NM5_01_23.1	626	764	12.09	1.6E-4	3.39E-06	1.1	0.07	**1.137**	0.137
NM5_01_24.1	159	85	16.76	1.6E-4	5.66E-06	1.1	0.1	**1.159**	0.229
NM5_01_29.1	187	131	17.65	1.7E-4	4.22E-06	1.1	0.09	**1.160**	0.171
NM5_01_17.1	372	305	9.15	1.7E-4	2.44E-06	1.1	0.05	**1.181**	0.099
NM5_01_22.1	282	208	25.08	1.7E-4	3.43E-06	1.1	0.07	**1.182**	0.139
NM5_01_21.1	225	180	27.59	1.7E-4	3.85E-06	1.1	0.08	**1.186**	0.156
NM5_01_19.1	276	163	14.80	1.9E-4	4.28E-06	1.2	0.09	**1.319**	0.173

Sample: NM11-01 Well: NM11 Depth: 2083-2089.9 mRF

Spot Name	ppm U	ppm Th	% comm 206	7corr $^{206}Pb/^{238}U$	1 sigma error	207 Corrected $^{206}Pb/^{238}U$ Age, Ma	1 sigma error	^{230}Th-Corrected 206/238 Age, Ma	2 sigma error
~~NM11_01_28.1~~	~~168~~	~~138~~	~~71.85~~	~~4.5E-5~~	~~7.7E-06~~	~~0.291~~	~~0.157~~	~~**0.377**~~	~~0.313~~
~~NM11_01_04.2~~	~~126~~	~~64~~	~~14.28~~	~~6.9E-5~~	~~3.0E-06~~	~~0.444~~	~~0.060~~	~~**0.539**~~	~~0.121~~
~~NM11_01_10.1~~	~~206~~	~~194~~	~~34.96~~	~~7.3E-5~~	~~5.0E-06~~	~~0.471~~	~~0.101~~	~~**0.557**~~	~~0.202~~
~~NM11_01_23.1~~	~~297~~	~~179~~	~~43.38~~	~~7.9E-5~~	~~4.7E-06~~	~~0.510~~	~~0.095~~	~~**0.604**~~	~~0.189~~
~~NM11_01_30.1~~	~~309~~	~~267~~	~~41.23~~	~~8.4E-5~~	~~4.7E-06~~	~~0.544~~	~~0.096~~	~~**0.632**~~	~~0.192~~
~~NM11_01_26.1~~	~~165~~	~~134~~	~~58.24~~	~~8.8E-5~~	~~9.4E-06~~	~~0.570~~	~~0.189~~	~~**0.659**~~	~~0.379~~
NM11_01_36.1	280	213	5.29	9.7E-5	3.1E-06	0.628	0.063	**0.718**	0.127
~~NM11_01_19.1~~	~~41~~	~~34~~	~~64.38~~	~~9.8E-5~~	~~1.9E-05~~	~~0.635~~	~~0.386~~	~~**0.723**~~	~~0.772~~
~~NM11_01_22.1~~	~~128~~	~~82~~	~~46.71~~	~~9.9E-5~~	~~8.8E-06~~	~~0.640~~	~~0.179~~	~~**0.733**~~	~~0.357~~
~~NM11_01_37.1~~	~~149~~	~~127~~	~~40.29~~	~~1.0E-4~~	~~5.4E-06~~	~~0.672~~	~~0.109~~	~~**0.760**~~	~~0.217~~
~~NM11_01_18.1~~	~~77~~	~~41~~	~~38.59~~	~~1.0E-4~~	~~9.6E-06~~	~~0.666~~	~~0.195~~	~~**0.762**~~	~~0.389~~
~~NM11_01_12.1~~	~~82~~	~~69~~	~~60.38~~	~~1.1E-4~~	~~1.4E-05~~	~~0.684~~	~~0.279~~	~~**0.772**~~	~~0.558~~
NM11_01_41.1	298	147	6.08	1.1E-4	3.5E-06	0.686	0.070	**0.783**	0.140
~~NM11_01_17.1~~	~~81~~	~~50~~	~~54.24~~	~~1.1E-4~~	~~1.3E-05~~	~~0.715~~	~~0.267~~	~~**0.809**~~	~~0.534~~
NM11_01_01.2	338	193	3.19	1.1E-4	1.5E-06	0.740	0.031	**0.835**	0.063
NM11_01_33.1	243	170	6.70	1.2E-4	2.4E-06	0.745	0.048	**0.837**	0.096
~~NM11_01_29.1~~	~~195~~	~~98~~	~~39.76~~	~~1.1E-4~~	~~5.9E-06~~	~~0.741~~	~~0.119~~	~~**0.838**~~	~~0.237~~
~~NM11_01_15.1~~	~~198~~	~~101~~	~~44.83~~	~~1.2E-4~~	~~7.0E-06~~	~~0.743~~	~~0.141~~	~~**0.839**~~	~~0.283~~
NM11_01_38.1	350	238	1.58	1.2E-4	1.8E-06	0.789	0.037	**0.881**	0.074
NM11_01_39.1	601	586	-0.70	1.2E-4	2.2E-06	0.800	0.045	**0.885**	0.090
NM11_01_42.1	417	311	2.71	1.3E-4	2.3E-06	0.814	0.046	**0.905**	0.093
~~NM11_01_14.1~~	~~154~~	~~86~~	~~34.57~~	~~1.3E-4~~	~~5.7E-06~~	~~0.823~~	~~0.116~~	~~**0.919**~~	~~0.232~~
NM11_01_35.1	313	194	12.28	1.3E-4	4.0E-06	0.832	0.081	**0.926**	0.162
NM11_01_20.2	258	176	9.41	1.3E-4	3.1E-06	0.837	0.064	**0.929**	0.127
~~NM11_01_34.1~~	~~163~~	~~105~~	~~10.01~~	~~1.3E-4~~	~~3.3E-06~~	~~0.845~~	~~0.066~~	~~**0.938**~~	~~0.132~~
NM11_01_32.1	289	193	3.60	1.4E-4	3.1E-06	0.875	0.063	**0.968**	0.126
~~NM11_01_16.1~~	~~79~~	~~69~~	~~41.47~~	~~1.4E-4~~	~~1.9E-05~~	~~0.928~~	~~0.383~~	~~**1.016**~~	~~0.766~~
NM11_01_08.2	273	220	4.51	1.5E-4	2.9E-06	0.950	0.059	**1.039**	0.117
NM11_01_11.2	348	210	7.48	1.5E-4	2.2E-06	0.948	0.045	**1.043**	0.089
NM11_01_05.2	213	194	1.24	1.5E-4	2.9E-06	0.960	0.059	**1.046**	0.119
~~NM11_01_09.1~~	~~140~~	~~82~~	~~56.27~~	~~1.5E-4~~	~~1.2E-05~~	~~0.953~~	~~0.250~~	~~**1.047**~~	~~0.500~~
~~NM11_01_13.1~~	~~181~~	~~96~~	~~27.36~~	~~1.5E-4~~	~~9.6E-06~~	~~0.960~~	~~0.193~~	~~**1.056**~~	~~0.386~~
NM11_01_07.1	339	355	22.79	1.5E-4	6.2E-06	0.998	0.124	**1.081**	0.249
NM11_01_06.2	187	121	3.34	1.6E-4	3.7E-06	1.009	0.075	**1.102**	0.151
NM11_01_02.1	383	274	13.85	1.9E-4	4.5E-06	1.251	0.090	**1.343**	0.180
NM11_01_21.1	280	196	12.14	2.0E-4	5.9E-06	1.263	0.118	**1.355**	0.237
NM11_01_24.1	436	388	10.32	2.6E-4	5.6E-06	1.659	0.113	**1.746**	0.225
~~NM11_01_27.1~~	~~88~~	~~50~~	~~36.98~~	~~2.7E-4~~	~~1.7E-05~~	~~1.734~~	~~0.340~~	~~**1.829**~~	~~0.681~~
NM11_01_40.1	1588	1175	0.12	2.9E-4	2.8E-06	1.855	0.058	**1.946**	0.115
NM11_01_31.1	290	336	28.83	2.9E-4	4.4E-05	1.887	0.895	**1.968**	1.789
NM11_01_03.1	457	281	9.05	3.1E-4	5.5E-06	1.974	0.111	**2.068**	0.222

Sample: RK6-01 Well: RK6 Depth: 1612-1614 mRF

Spot Name	ppm U	ppm Th	% comm 206	7corr $^{206}Pb/^{238}U$	1 sigma error	207 Corrected $^{206}Pb/^{238}U$ Age, Ma	1 sigma error	^{230}Th-Corrected 206/238 Age, Ma	2 sigma error
~~RK6_01_08.1~~	~~132~~	~~56~~	~~15.86~~	~~2.4E-4~~	~~9.52E-06~~	~~1.576~~	~~0.192~~	~~1.675~~	~~0.385~~
~~RK6_01_07.1~~	~~133~~	~~58~~	~~15.09~~	~~2.5E-4~~	~~9.90E-06~~	~~1.631~~	~~0.200~~	~~1.729~~	~~0.400~~
~~RK6_01_23.1~~	~~274~~	~~141~~	~~16.26~~	~~2.6E-4~~	~~9.16E-06~~	~~1.686~~	~~0.185~~	~~1.782~~	~~0.370~~
RK6_01_35.1	392	272	1.04	2.7E-4	2.88E-06	1.723	0.058	**1.815**	0.116
RK6_01_26.1	2631	3811	1.52	2.7E-4	1.34E-06	1.764	0.027	**1.838**	0.054
RK6_01_37.1	2012	2050	-0.10	2.7E-4	2.72E-06	1.759	0.055	**1.842**	0.110
RK6_01_14.1	329	201	4.94	2.8E-4	2.38E-06	1.778	0.048	**1.872**	0.096
~~RK6_01_17.1~~	~~347~~	~~209~~	~~12.49~~	~~2.8E-4~~	~~5.56E-06~~	~~1.798~~	~~0.112~~	~~1.892~~	~~0.225~~
RK6_01_36.1	1106	1139	0.28	2.8E-4	1.75E-06	1.812	0.035	**1.896**	0.071
RK6_01_06.1	4601	8809	1.27	2.9E-4	1.10E-06	1.839	0.022	**1.901**	0.044
RK6_01_05.1	285	179	4.91	2.8E-4	6.87E-06	1.813	0.139	**1.906**	0.277
RK6_01_27.1	1298	966	6.38	2.8E-4	3.50E-06	1.819	0.071	**1.909**	0.141
RK6_01_15.1	852	926	2.99	2.8E-4	3.42E-06	1.832	0.069	**1.914**	0.138
RK6_01_34.1	2114	1782	-0.70	2.8E-4	1.70E-06	1.829	0.034	**1.917**	0.069
RK6_01_33.1	1002	1359	1.62	2.9E-4	3.19E-06	1.849	0.064	**1.925**	0.129
RK6_01_19.1	435	275	8.70	2.9E-4	5.70E-06	1.841	0.115	**1.934**	0.230
RK6_01_25.1	1769	2561	2.98	2.9E-4	2.10E-06	1.877	0.042	**1.950**	0.085
RK6_01_32.1	2014	3831	0.70	2.9E-4	2.05E-06	1.895	0.041	**1.957**	0.083
RK6_01_30.1	1757	1996	2.39	2.9E-4	2.49E-06	1.887	0.050	**1.968**	0.101
RK6_01_11.1	638	403	2.49	2.9E-4	3.20E-06	1.878	0.065	**1.972**	0.129
RK6_01_20.1	370	218	8.99	2.9E-4	3.52E-06	1.880	0.071	**1.975**	0.142
RK6_01_10.1	228	111	9.37	2.9E-4	7.80E-06	1.884	0.158	**1.981**	0.315
RK6_01_21.1	1043	1326	0.96	3.0E-4	2.06E-06	1.908	0.042	**1.985**	0.083
RK6_01_02.1	4597	10033	1.15	3.0E-4	1.31E-06	1.933	0.026	**1.988**	0.053
RK6_01_16.2	421	386	3.46	3.0E-4	4.58E-06	1.902	0.093	**1.989**	0.185
RK6_01_12.1	774	583	7.06	3.0E-4	2.20E-06	1.908	0.045	**1.999**	0.089
RK6_01_04.1	9688	13739	1.83	3.0E-4	9.13E-07	1.926	0.018	**2.000**	0.037
RK6_01_29.1	1363	1223	1.74	3.0E-4	2.93E-06	1.922	0.059	**2.009**	0.118
~~RK6_01_22.1~~	~~1508~~	~~1569~~	~~21.53~~	~~3.0E-4~~	~~3.47E-06~~	~~1.933~~	~~0.070~~	~~2.017~~	~~0.140~~
RK6_01_28.1	11510	20701	1.00	3.1E-4	1.27E-06	2.008	0.026	**2.072**	0.051
RK6_01_09.1	318	172	4.77	3.1E-4	4.45E-06	1.984	0.090	**2.080**	0.180
~~RK6_01_18.1~~	~~554~~	~~388~~	~~28.14~~	~~3.1E-4~~	~~5.16E-06~~	~~2.019~~	~~0.104~~	~~2.111~~	~~0.208~~
RK6_01_24.1	719	664	7.84	3.2E-4	5.22E-06	2.033	0.105	**2.119**	0.211

Appendix 5: List of samples

Sample	Depth (mRF)	Core/Cuttings description?	Thin section?	Raman analysis?	EMP analysis?	SIMS analysis
NM1 1305	1305.5-1307.7	Core	LW	-	-	-
NM2 1155	1155.5-1157.5	Core	AE	-	-	-
NM2 1354	1354.2-1356.2	Core	LW	-	-	-
NM2 1415	1415-1417	Core	AE	-	-	-
NM2 1582	1582-1586	Core	AE	-	-	-
NM2 2255	2254.7-2255.2	Core	AE	-	-	Yes
NM3 1246	1246-1248	Core	LW	-	-	Yes
NM3 1496	1495.7-1497.7	Core	AE	-	-	Yes
NM3 1743	1743-1745	Core	AE	-	-	-
NM4 1225	1225-1226	Core	LW	-	-	-
NM4 1475	1475.2-1477.2	Core	GNS	-	-	-
NM5 1775	1775-1778	Core	LW	-	-	Yes
NM8A	2525.0-2526.8	Core	LW	-	-	-
NM11 2083	2083.0-2089.1	Core	LW	-	-	Yes
RK6 1612	1612-1614	Core	AE	-	-	Yes
NM5 1100	1100	Cuttings	AE	-	-	-
NM5 1125	1125	Cuttings	AE	Yes	Yes	-
NM5 1175	1175	Cuttings	AE	Yes	-	-
NM5 1225	1225	Cuttings	AE	Yes	-	-
NM5 1300	1300	Cuttings	AE	Yes	Yes	-
NM5 1350	1350	Cuttings	AE	Yes	-	-
NM5 1400	1400	Cuttings	AE	Yes	-	-
NM5 1450	1450	Cuttings	AE	Yes	Yes	-
NM5 1500	1500	Cuttings	AE	Yes	Yes	-
NM5 1550	1550	Cuttings	AE	Yes	-	-
NM5 1600	1600	Cuttings	AE	Yes	Yes	-
NM5 1650	1650	Cuttings	AE	Yes	-	-
NM5 1700	1700	Cuttings	AE	Yes	Yes	-
NM5A	1700	Cuttings	AE	-	-	-
NM5 1750	1750	Cuttings	AE	Yes	-	-
NM5A	1750	Cuttings	AE	-	-	-
NM5A	1775	Cuttings	AE	-	-	-
NM5 1800	1800	Cuttings	AE	Yes	-	-
NM5A	1850	Cuttings	AE	-	-	-
NM5A	1900	Cuttings	AE	-	-	-
NM5A	1950	Cuttings	AE	-	-	-
NM5A	2000	Cuttings	AE	-	-	-
NM5A	2050	Cuttings	AE	-	-	-
NM5A	2150	Cuttings	AE	-	-	-
NM5A	2250	Cuttings	AE	-	-	-
NM5A	2300	Cuttings	AE	-	-	-
NM5A	2350	Cuttings	AE	-	-	-
NM5A	2450	Cuttings	AE	-	-	-
NM6 1220	1220	Cuttings	AE	-	-	-
NM6 1265	1265	Cuttings	AE	-	-	-
NM6 1280	1280	Cuttings	AE	-	-	-
NM6 1300	1300	Cuttings	AE	-	-	-
NM6 1350	1350	Cuttings	AE	-	-	-
NM6 1380	1380	Cuttings	AE	-	-	-
NM6 1400	1400	Cuttings	AE	-	-	-
NM6 1430	1430	Cuttings	AE	-	-	-
NM6 1460	1460	Cuttings	AE	-	-	-
NM6 1510	1510	Cuttings	AE	-	-	-
NM6 1560	1560	Cuttings	AE	-	-	-
NM6 1610	1610	Cuttings	AE	-	-	-

Sample	Depth (mRF)	Core/Cuttings description?	Thin section?	Raman analysis?	EMP analysis?	SIMS analysis
NM6 1645	1645	Cuttings	AE	-	-	-
NM6 1650	1650	-	GNS	-	-	-
NM6 1670	1670	Cuttings	AE	-	-	-
NM6 1700	1700	Cuttings	AE	-	-	-
NM6 1750	1750	Cuttings	AE	-	-	-
NM6 1760	1760	-	GNS	-	-	-
NM6 1800	1800	Cuttings	AE	-	-	-
NM6 1850	1850	Cuttings	AE	-	-	-
NM6 1890	1890	Cuttings	AE	-	-	-
NM6 1950	1950	Cuttings	AE	-	-	-
NM6 2000	2000	Cuttings	AE	-	-	-
NM6 2050	2050	Cuttings	AE	-	-	-
NM6 2100	2100	Cuttings	AE	-	-	-
NM6 2150	2150	Cuttings	AE	-	-	-
NM6 2200	2200	Cuttings	AE	-	-	-

Note: The first part of the sample name refers to the well number; the second part refers to the depth in metres below the drilling rig floor (mRF). With core samples this refers to the whole number closest to the start of the core interval. Thin sections are labelled as follows: AE – samples were obtained from Mighty River Power Ltd. and thin sections were made for the purposes of this study; LW – samples were obtained from Mighty River Power Ltd. and thin sections were made for the purposes of research by Latasha Wyering; GNS – existing GNS thin sections were used.